~~CONFIDENTIAL~~

MASTER

NYO-3434-7
C-93b
AEC RESEARCH AND
DEVELOPMENT REPORT

[illegible]

THERMO ELECTRON CORPORATION

SUMMARY OF DESIGN, FABRICATION, PROTOTYPE TESTING, IN-PILE TESTING AND HOT CELL EXAMINATION OF SD-4 THERMIONIC DIODE

June 25, 1964 - June 30, 1968

DISTRIBUTION OF THIS DOCUMENT IS [illegible]

This document contains
~~CONFIDENTIAL RESTRICTED DATA~~
relating to civilian applications
of atomic energy.

~~RESTRICTED DATA~~

This document contains restricted data as defined in the Atomic Energy Act of 1954. Its transmittal or disclosure of its contents in any manner to an unauthorized person is prohibited.

DISTRIBUTION OF THIS DOCUMENT UNLIMIT

~~CONFIDENTIAL~~

~~DISTRIBUTION OF THIS DOCUMENT IS LIMITED
to Government Agencies and Their Contractors~~ GAE

DISCLAIMER

This report was prepared as an account of work sponsored by an agency of the United States Government. Neither the United States Government nor any agency Thereof, nor any of their employees, makes any warranty, express or implied, or assumes any legal liability or responsibility for the accuracy, completeness, or usefulness of any information, apparatus, product, or process disclosed, or represents that its use would not infringe privately owned rights. Reference herein to any specific commercial product, process, or service by trade name, trademark, manufacturer, or otherwise does not necessarily constitute or imply its endorsement, recommendation, or favoring by the United States Government or any agency thereof. The views and opinions of authors expressed herein do not necessarily state or reflect those of the United States Government or any agency thereof.

DISCLAIMER

Portions of this document may be illegible in electronic image products. Images are produced from the best available original document.

LEGAL NOTICE

This report was prepared as an account of Government-sponsored work. Neither the United States, nor the Commission, nor any person acting on behalf of the Commission:

A. Makes any warranty or representation, expressed or implied, with respect to the accuracy, completeness, or usefulness of the information contained in this report, or that the use of any information, apparatus, method, or process disclosed in this report may not infringe privately owned rights; or

B. Assumes any liabilities with respect to the use of, or for damages resulting from the use of any information, apparatus, method, or process disclosed in this report.

As used in the above, "person acting on behalf of the Commission" includes any employee or contractor of the Commission, or employee of such contractor, to the extent that such employee or contractor of the Commission or employee of such contractor prepares, disseminates, or provides access to, any information, pursuant to his employment or contract with the Commission, or his employment with such contractor.

Printed in the U.S.A. Charge $3.45. Available from the U.S. Atomic Energy Commission, Division of Technical Information Extension, P.O. Box 1001, Oak Ridge, Tennessee. Please direct to the same address inquiries covering the procurement of other classified AEC reports.

~~CONFIDENTIAL~~

SPECIAL REREVIEW FINAL DETERMINATION
Class: U
Reviewers Class. Date
TR U 2-23-82

This report contsins 165 pages
NYO-3434-7
C-93b (M-3679
Report No. TE4042-186-68

NOTICE
This report was prepared as an account of work sponsored by the United States Government. Neither the United States nor the United States Energy Research and Development Administration, nor any of their employees, nor any of their contractors, subcontractors, or their employees, makes any warranty, express or implied, or assumes any legal liability or responsibility for the accuracy, completeness or usefulness of any information, apparatus, product or process disclosed, or represents that its use would not infringe privately owned rights.

THERMO ELECTRON CORPORATION

SUMMARY OF DESIGN, FABRICATION, PROTOTYPE TESTING, IN-PILE TESTING, AND HOT CELL EXAMINATION OF SD-4 THERMIONIC DIODE

UNCLASSIFIED

June 1964 - June 1968

~~GROUP 1~~
Excluded from Automatic Downgrading and Declassification

Classification cancelled or changed to
by authority of DOC
by K.J.C. TIC, date AUG 31 1973

by

R. C. Howard, J. B. Dunlay, T. O. P. Speidel
Thermo Electron Corporation

E. O. Speidel, J. H. Saling, V. W. Storhok
Battelle Memorial Institute

Contract AT(30-1)-3434
U.S. Atomic Energy Commission

Work Performed by

R. C. Howard, J. B. Dunlay, T. Speidel, J. Kalajian, V. Poirier
H. Hardister, F. Campagna
Thermo Electron Corporation

and

E. O. Speidel, J. H. Saling, V. W. Storhok, W. A Carbiener, J. Allgeier
Battelle Memorial Institute

~~RESTRICTED DATA~~
This document contains restricted data as defined in the Atomic Energy Act of 1954. Its transmittal or the disclosure of its contents in any manner to an unauthorized person is prohibited.

~~CONFIDENTIAL~~

DISTRIBUTION OF THIS DOCUMENT UNLIMITED
DISTRIBUTION OF THIS DOCUMENT IS LIMITED
To Government Agencies and Their Contractors

TABLE OF CONTENTS

ACKNOWLEDGMENTS		8
Chapter		Page
1	INTRODUCTION (U)	9
2	DIODE DESIGN AND FABRICATION (U)	10
3	IN-PILE CAPSULE DESIGN AND FABRICATION (U)	26
	A. DESIGN	26
	B. ASSEMBLY	30
	C. HAZARDS ANALYSIS	37
	D. COOLANT SYSTEM	38
4	DIODE TESTING (U)	40
	A. SUMMARY	40
	B. DETAILED DESCRIPTION OF TEST PERIODS	40
5	HOT CELL EXAMINATION SUMMARY (C)	58
	A. INTRODUCTION	58
	B. SUMMARY OF FINDINGS	58
	C. CONCLUSIONS	72
6	ELECTRICAL TESTING OF SD-2 PROTOTYPE DIODE (U)	75
	A. INTRODUCTION	75
	B. ASSEMBLY AND PROCESSING	75
	C. TESTING	78
	D. SIGNIFICANCE	86
APPENDIX A.	FUELED EMITTER FABRICATION (C)	90
	B. POSTIRRADIATION EVALUATION OF THERMO ELECTRON CORPORATION'S SD-4 DIODE (C)	106

LIST OF ILLUSTRATIONS

Figure		Page
2.1	Design of Converter SD-4	11
2.2	Collector	15
2.3	Heat Choke Fins	16
2.4	Water Coolant Jacket	17
2.5	Outer Coolant Container	18
2.6	Assembly of Diode Components	19
2.7	Outer Coolant Assembly	20
2.8	Main Diode Insulator Assembly	21
2.9	Electron Bombardment Heater	22
2.10	Final Subassembly of Diode SD-4	23
2.11	Final Subassembly of Diode SD-4	24
2.12	Final Assembled Converter	25
3.1	In-Pile Tube Section	28
3.2	In-Pile Lead Section	29
3.3	In-Pile End of Lower Section of In-Pile Capsule	31
3.4	Connection between Upper and Lower Sections of the In-Pile Capsule	32
3.5	Connection between Upper and Lower Sections of the In-Pile Capsule	33
3.6	In-Pile End of Lower Section of In-Pile Capsule	35
3.7	In-Pile End of Lower Section of In-Pile Capsule	36
3.8	Schematic of In-Pile Coolant System	39
4.1	Performance Summary	41
4.2	Comparison of I-V Sweep Data at Controlled Reference Points During Out-of-Pile and In-Pile Operation	43
4.3	I-V Sweep Data During Emitter Temperature Transient	52

Figure		Page
5.1	Microstructures of Fuel in Irradiated SD-4 and Unirradiated SD-2 Diodes	60
5.2	Microstructures of Fuel in Irradiated SD-4 and Unirradiated SD-2 Diodes	61
5.3	Compositie Photographs of Longitudinal Section through Top Half of Emitter	62
5.4	Composite Photographs of Transverse Section near Axial Center of Emitter	63
5.5	Apparent Hot Spot in Fuel near Inner Clad-Core Interface	64
5.6	Representative Microstructures of the Rhenium Clad (Emitter) - Polarized Light	66
5.7	Vapor-Deposited Layer of Molybdenum on the Niobium Collector Surface	67
5.8	Microstructures of Representative Areas of the Heat Exchanger	69
5.9	Comparison of Ceramic Insulation used in Out-of-Pile and In-Pile Diodes	70
6.1	SD-2 Electrically Heated Diode	76
6.2	Diode SD-2 in Test Stand	77
6.3	Typical Performance Data for Diode SD-2	79
6.4	Filament Used in Diode SD-2	81
6.5	Dummy Emitter Test Set-up	81
6.6	SD-2 Life Testing to 1250 Hours	87
6.7	Out-of-Pile Life Test of SD-2	89

LIST OF TABLES

Table		Page
2.1	SUMMARY OF SD-4 DESIGN PARAMETERS	12
4.1	SUMMARY OF SD-4 OPERATING CHARACTERISTICS	45
4.2	TYPICAL OPERATING CONDITIONS FOR SD-4 DURING OUT-OF-PILE TESTS	46
4.3	SUMMARY OF SD-4 REPRODUCIBILITY TESTS . . .	48
5.1	KNOOP MICROHARDNESS MEASUREMENTS ON THE CERAMIC INSULATORS FROM SD-2 AND SD-4	71
5.2	BURN-UPS OBTAINED FROM ISOTOPIC ANALYSIS	73
6.1	COMPARISON OF OPERATING CONDITIONS DURING LIFE TEST OF SD-2	83

ACKNOWLEDGMENTS

This report, which summarizes the design, fabrication, testing, and hot cell examination of the SD-4 diode experiment, is compiled from portions of the quarterly reports submitted under Contract AT(30-1)-3434, from "Converter SD-4 Design and Summary of Test Results" by R. C. Howard and J. B. Dunlay of Thermo Electron, presented at the Second International Conference on Thermionic Electric Power Generation, Stresa, Italy, 1968, and from "Post Irradiation Examination of SD-4 In-Pile Diode" by T. Speidel and R. C. Howard of Thermo Electron and E. O. Speidel and J. H. Saling of Battelle Memorial Institute, presented at the 1968 Thermionics Specialists Conference, Natick, Massachusetts. It includes the complete Battelle Memorial Institute hot cell examination report as an appendix (Appendix B).

Many people from Thermo Electron and Battelle Memorial Institute contributed to this experiment. The authors would like to acknowledge in particular the efforts of Jack Kalajian, Victor Poirier, Frank Campagna, and Harold Hardister of Thermo Electron, who performed the detailed design and fabrication of the diode and the in-pile capsule. The major contributors from Battelle Memorial Institute include W. Carbienier, and J. Allgeier, who were responsible for the in-pile testing.

CHAPTER 1

INTRODUCTION

Thermo Electron Corporation, in the performance of Contract AT(30-1)-3434, "Evaluation of Cermet Fuels with Rhenium Emitters," sponsored by the Atomic Energy Commission, carried out an in-pile test of a thermionic diode, SD-4.

Thermo Electron Corporation designed and fabricated the thermionic diode and the in-pile capsule. Battelle Memorial Institute, as a subcontractor, fabricated the fueled emitter, carried out the in-pile testing, and performed the hot cell examination.

The test consisted of a cylindrical thermionic converter with a rhenium emitter fueled with a cermet of UO_2-W. The external environment of the converter was a static vacuum formed by an initial pump-out and seal-off of a stainless steel housing. The test operated in-pile for 8125 hours over a period of about two years. More than 80 cycles between shutdown and full power occurred during this period. The average electrode power density throughout the test lifetime was 7.8 watts/cm^2. For fixed reference levels of reactor power, cesium pressure, and collector temperature, the diode performance was stable throughout the life of the test. The test was terminated when difficulties occurred in auxiliary heaters and coolant systems causing a loss of control of the cesium reservoir temperature. A complete hot cell examination of the diode was performed following the in-pile test.

UNCLASSIFIED

CHAPTER 2.
DIODE DESIGN AND FABRICATION

The diode design used in the in-pile program (Figure 2.1) permits either out-of-pile testing with electrical heating or in-pile testing with fission heating. The basic design philosophy is to allow complete testing of the diode out-of-pile with only minor modifications necessary for testing in-pile. The design includes provisions for independent control of emitter, collector, and cesium reservoir temperatures. In addition, the collector cooling arrangement permits an accurate calorimetric measurement to be made of total heat rejected. Thus a reliable estimate of converter efficiency can be obtained during both out-of-pile and in-pile testing. In Table 2.1, a summary of the converter design parameters is presented.

The cermet fuel is in a hollow, cylindrical shape and is clad internally with tungsten and externally with rhenium. Fabrication of the fuel emitter performed by BMI is fully described in Appendix A. The purpose of the internal clad is to suppress evaporation of the uranium contained in the cermet. By preventing this evaporation, loss of fuel is minimized and the stability of electron bombardment heating is greatly improved. Thermocouple holes at three axial locations in the fuel annulus are provided to obtain an axial temperature profile of the fueled emitter during out-of-pile testing. The rhenium external clad on the fuel also acts as the emitter. This clad has an extension approximately 0.4 inch longer than the fueled length, which serves as the "optimized lead." The extension is joined to a molybdenum support ring which, in turn, is joined to one of the niobium seal flanges. The other end of the rhenium emitter has a small diameter pin which fits into an insulated hole in the collector bottom. This pin provides additional support and alignment for operation and for any shock

UNCLASSIFIED

E-67-53

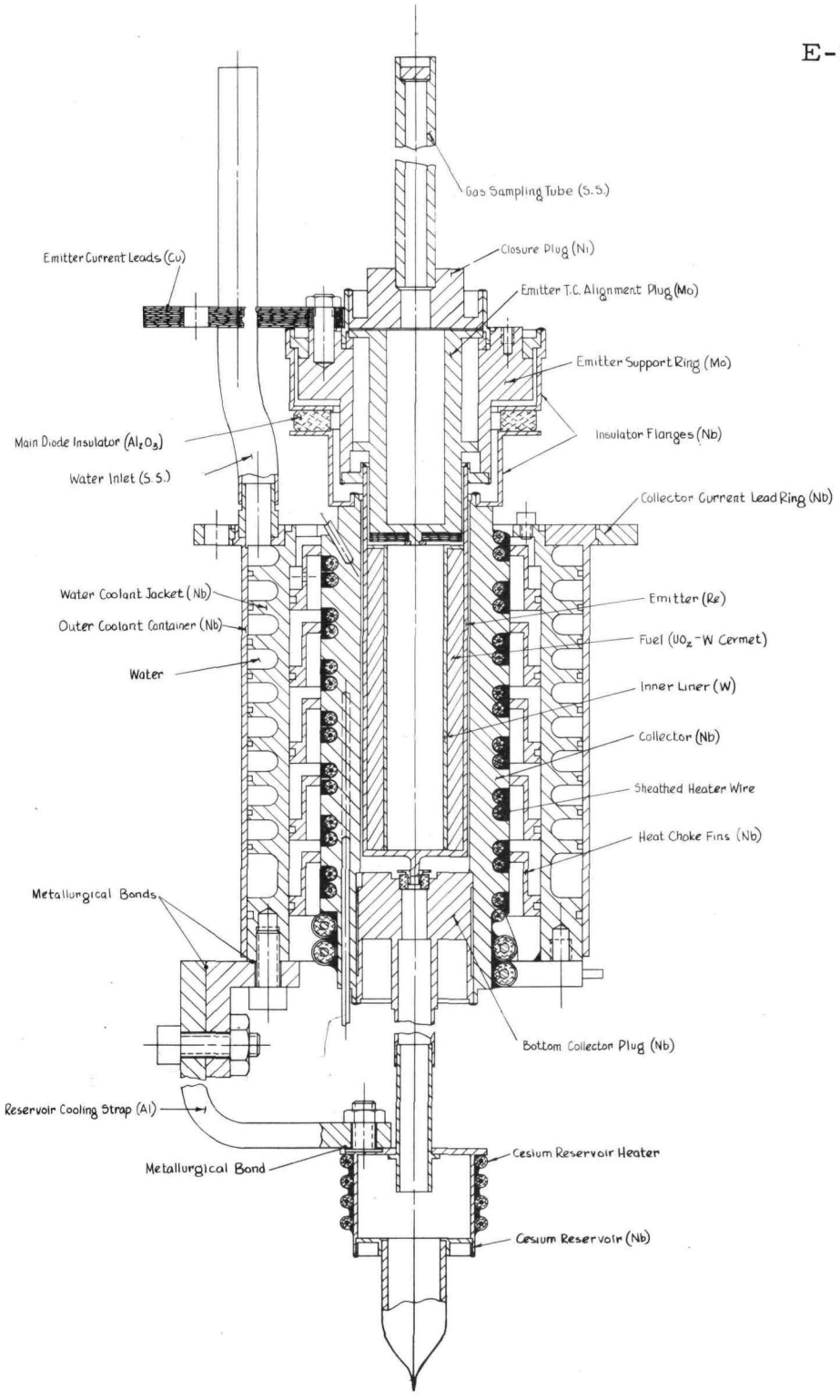

Figure 2.1 SD-4 Diode

TABLE 2.1

SUMMARY OF SD-4 DESIGN PARAMETERS

Fuel Form:	
Type	Cermet
Fuel	UO_2
Diluent	W
Loading, vol. % UO_2	80
Density, %	95
Geometry	Annular
Thickness, inches	0.080
Inner Clad	W
Emitter:	
Material	Rhenium
Thickness, inches	0.018
Surface Condition	Treated
Diameter, inches	0.500
Length, inches	1.500
Area, cm^2	15
Diode Structure:	
Insulator	Al_2O_3
Flanges	Nb
Collector	Nb (Mo coated)
Cesium Reservoir	Ni
Emitter Support	Mo
Exterior Environment	Vacuum ($\sim$10 microns)

and vibration which might occur during shipping and handling.

Inside the inner tungsten liner of the fuel is a cavity to permit electron-bombardment heating of the fueled emitter. The electron-bombardment gun which occupies this cavity during out-of-pile testing consists of a helical filament attached to a massive central rod for alignment. The gun includes electrical insulators and its own radiator to dissipate heat conducted out of the cavity. After electrical testing is completed, the gun is removed and the "closure plug" is welded as shown in Figure 2.1. In making this weld, no other part of the diode structure is heated, thus eliminating any temperature effect on the rest of the structure. This is a key aspect of the design because it insures that a valid comparison can be made of in-pile to out-of-pile diode behavior. If the converter were thermally cycled or otherwise affected during this operation, the cause of any change in behavior could not be reliably determined.

At a radial gap of about 0.010 inch from the emitter, there is a cylindrical collector made of massive niobium. The collector is joined at one end to one of the niobium seal flanges and, at the other end, to the bottom collector plug. Sheathed heaters are imbedded in the outside surface of the collector. A niobium tube covers these heater wires and provides a smooth surface for the "heat choke" fins, which maintain the difference between the collector temperature and the water coolant temperature. These fins are made of niobium and are joined on their outside surface to a water-cooling jacket also made of niobium. The combinations of the heater wires with the heat choke fins constitutes the collector temperature control scheme. Since this entire structure is brazed together, accurate prediction and control of collector temperature is possible. The thickness of the collector was selected as a

compromise between the space available in the in-pile test hole (2.75 inches) and the temperature uniformity of the collector. Three holes are provided in the collector walls for sheathed thermocouples to obtain a measurement of the axial temperature variation.

The cesium reservoir tubulation is joined to the bottom collector plug and communicates with the diode through slanted holes in the bottom plug. At the other end of the tubulation, there is a cesium reservoir chamber. The design of this chamber prevents liquid cesium from spilling into the diode regardless of its inclination. Thus, during disassembly in the hot cell, all cesium can be removed from the converter by cutting off the cesium reservoir; therefore, no contamination of the diode interior with cesium oxide need occur. Sheathed heater wire is brazed to the reservoir, and copper straps are connected from the reservoir to the water cooling jacket surrounding the collector. This combination of heater wire and cooling straps permits control of the cesium reservoir temperature despite the uncertainties in gamma heating rates.

The main diode insulator seal is of the "SET" type of construction and consists of niobium flanges brazed to alumina rings. The emitter current leads are connected to the emitter support ring with threaded screws. The collector current leads are connected to a flange on the outside coolant jacket with threaded rods held by nuts. Inlet and outlet water tubes are brazed at the top end of the coolant jacket, which contains a double thread for water flow.

Figures 2.1 through 2.12 show photographs of the diode during various stages of construction.

UNCLASSIFIED

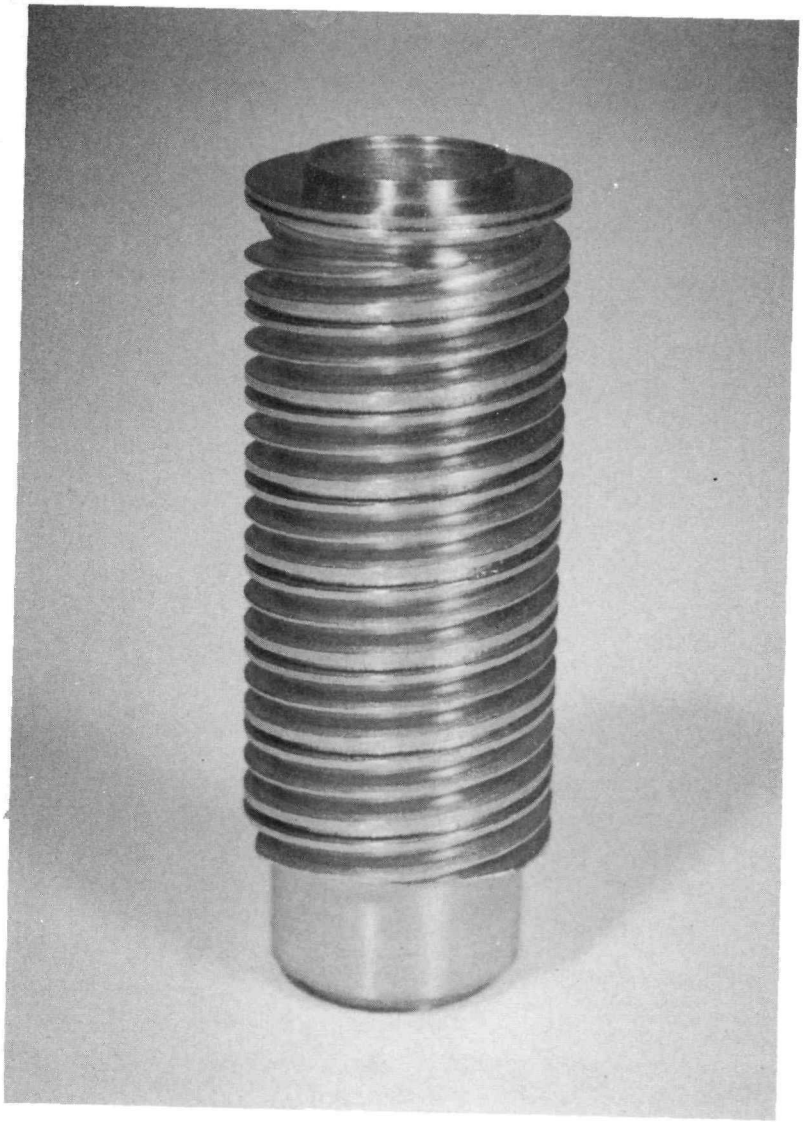

Figure 2.2. Collector

UNCLASSIFIED

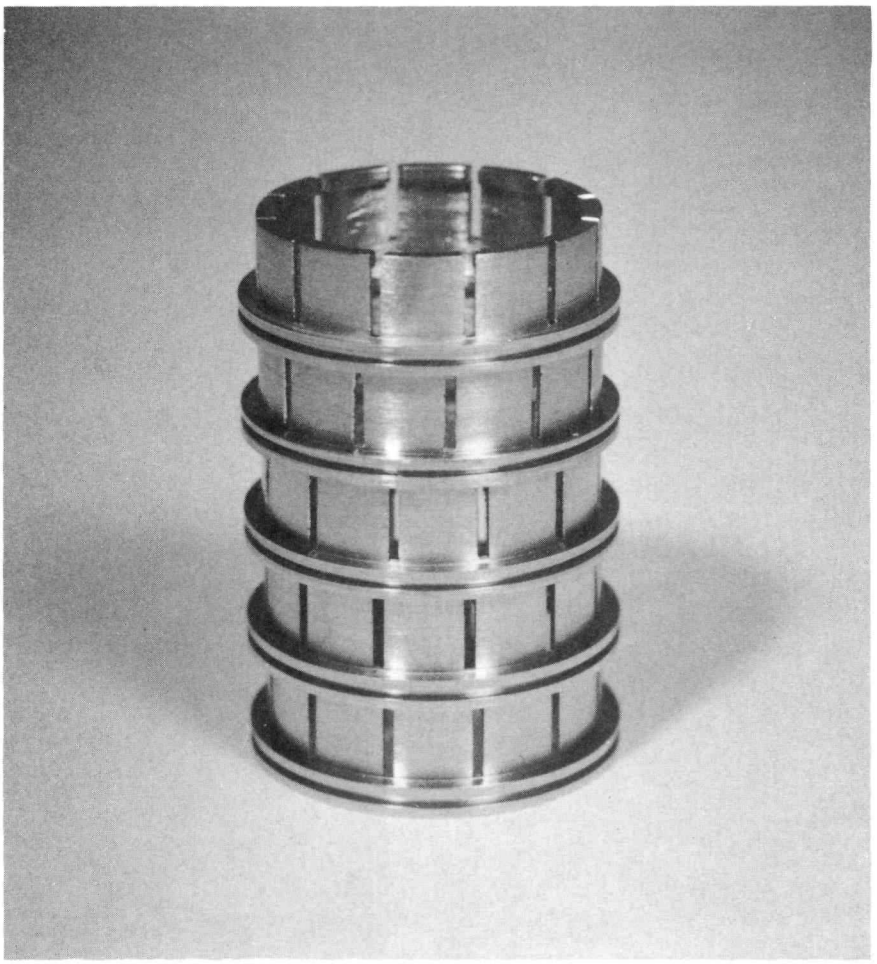

Figure 2.3. Heat Choke Fins

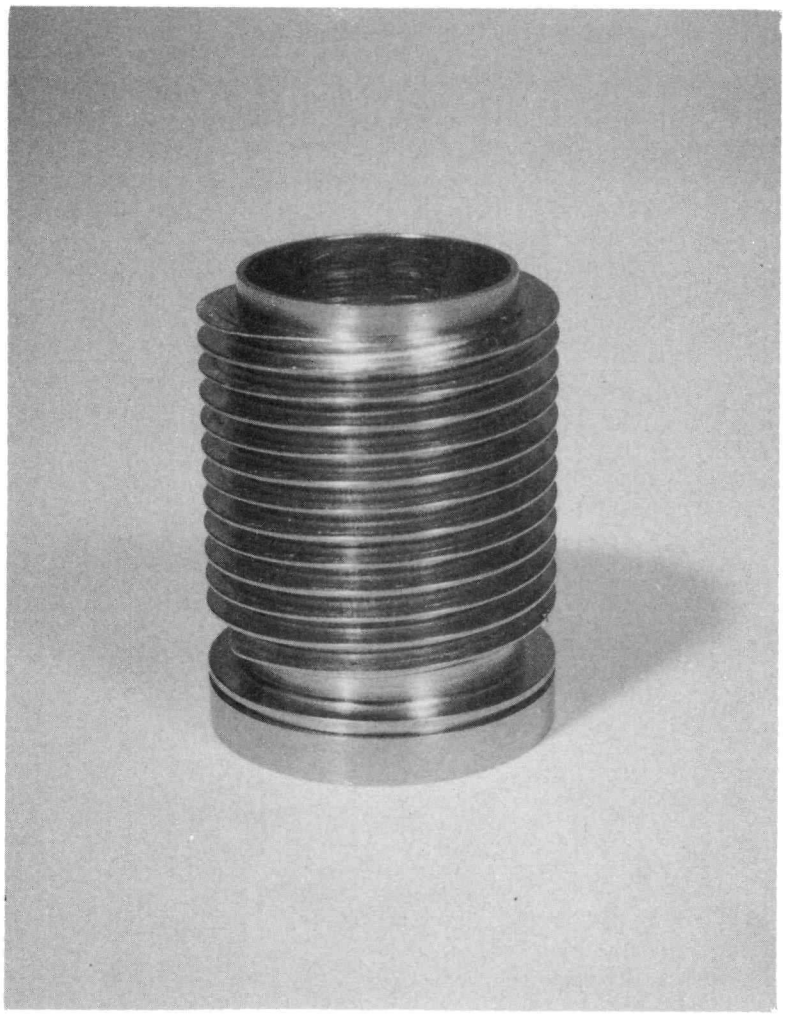

Figure 2.4. Water Coolant Jacket

UNCLASSIFIED

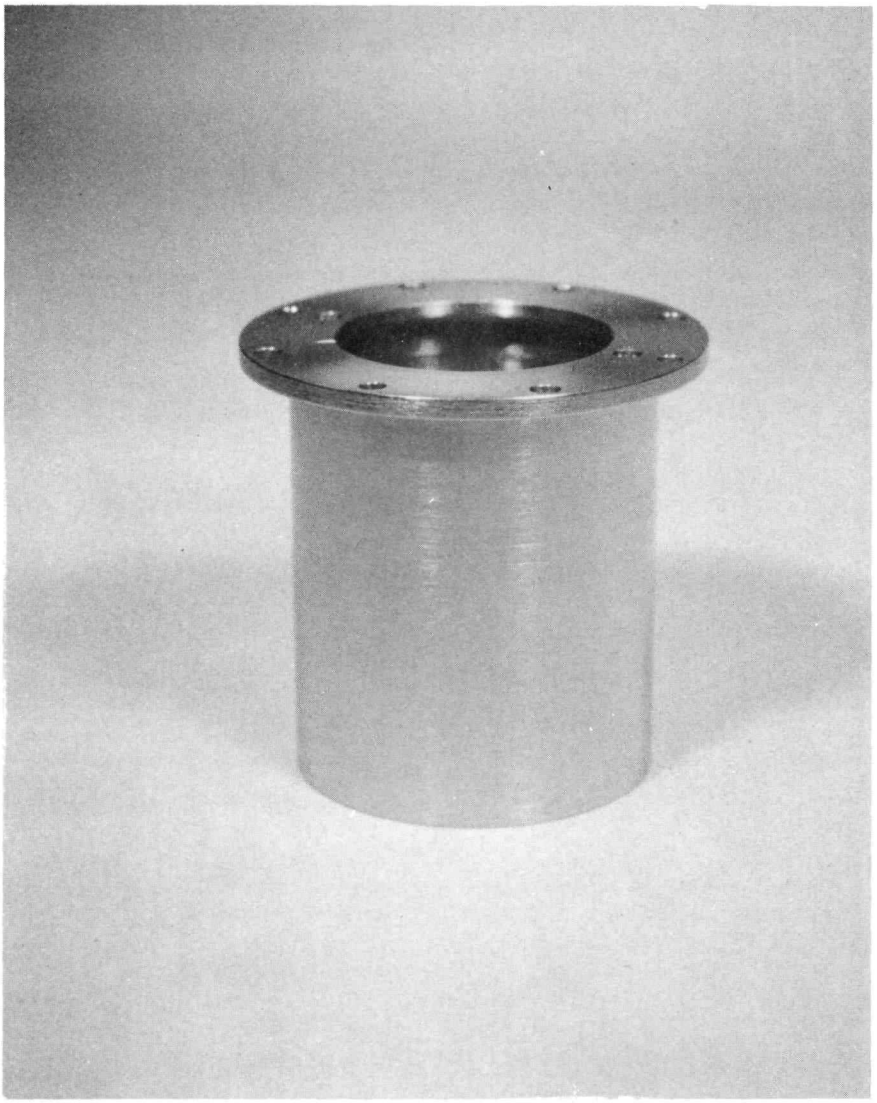

Figure 2.5. Outer Coolant Container

UNCLASSIFIED

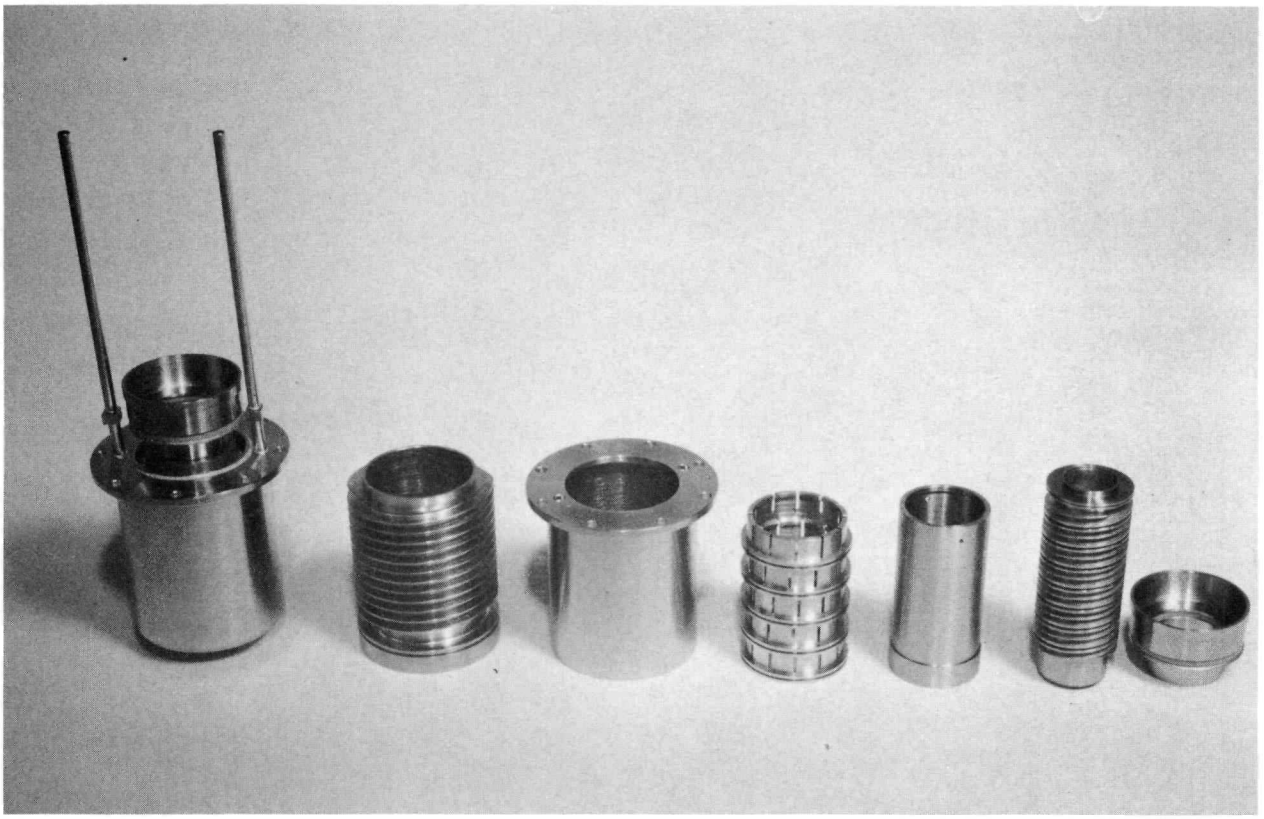

Figure 2.6. Assembly of Diode Components

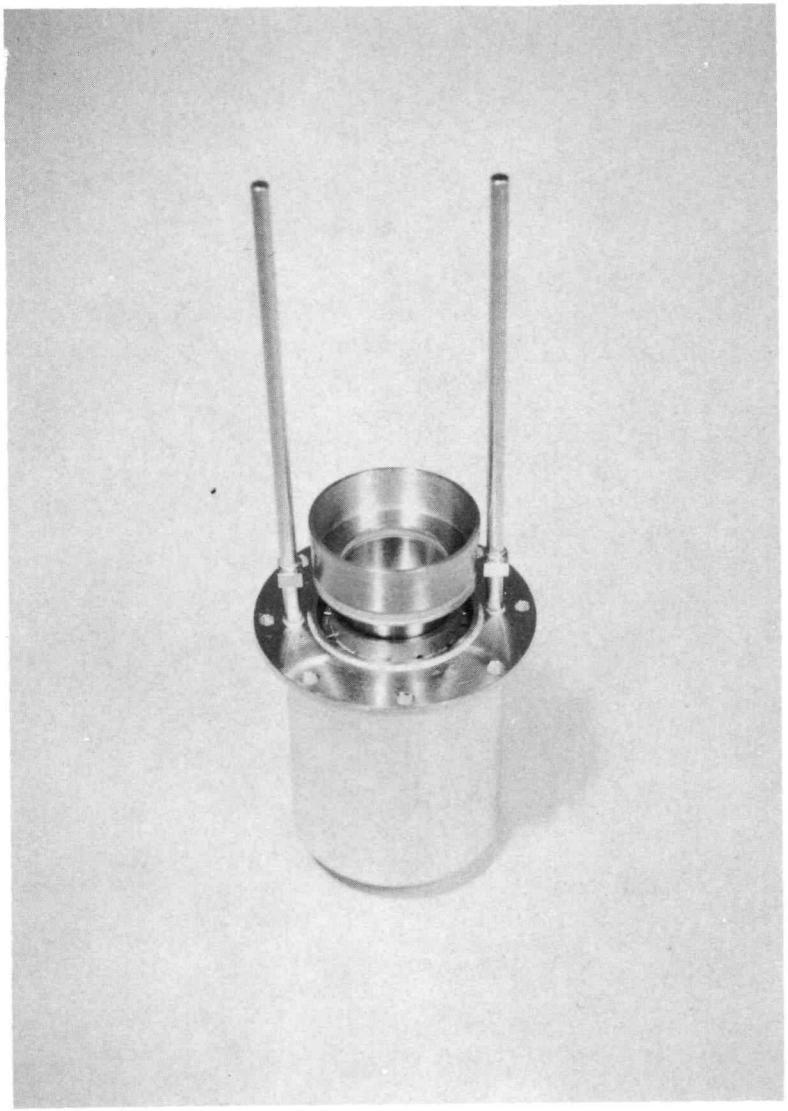

Figure 2.7. Outer Coolant Assembly

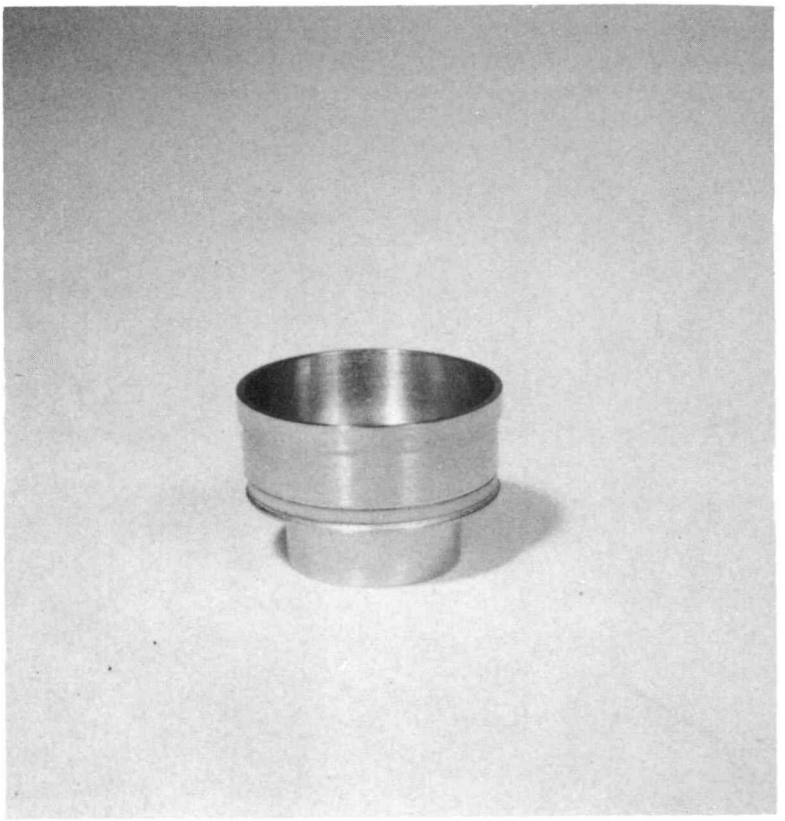

Figure 2.8 Main Diode Insulator Assembly

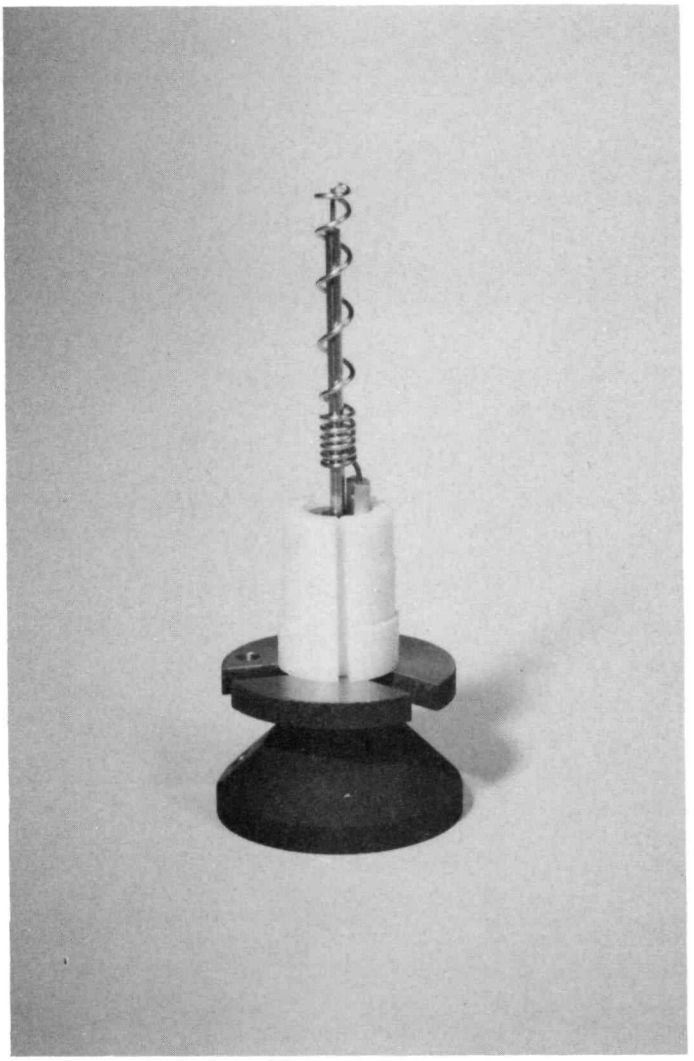

Figure 2.9. Electron Bombardment Heater

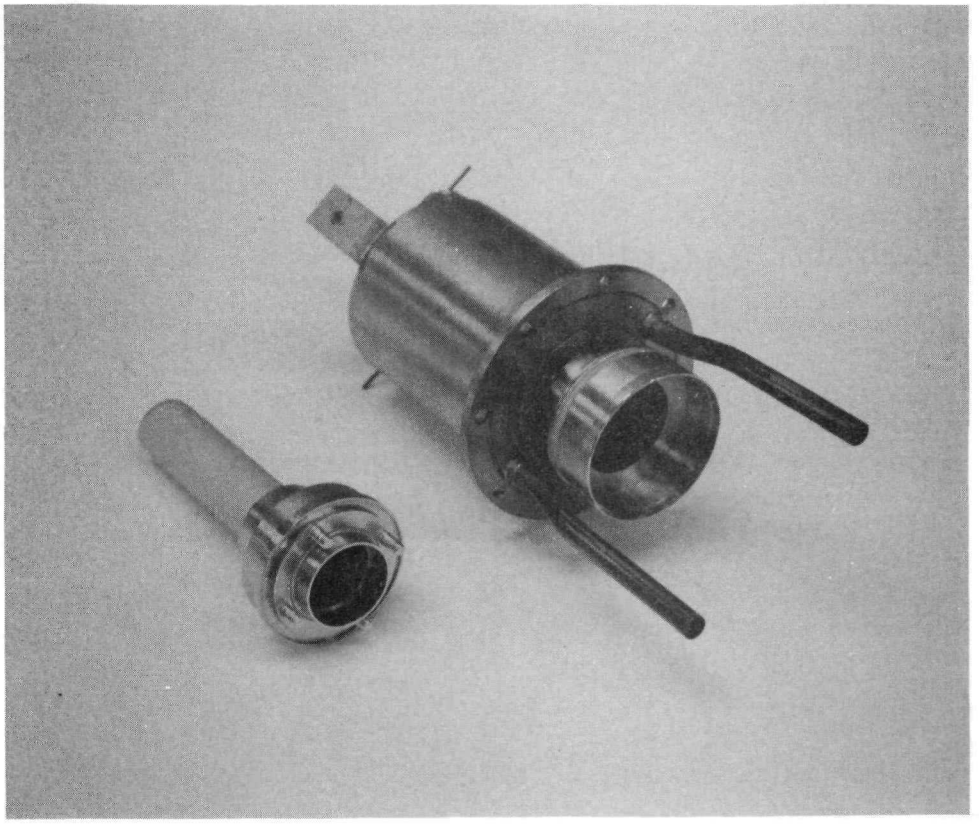

Figure 2.10. Final Subassembly of Diode SD-4

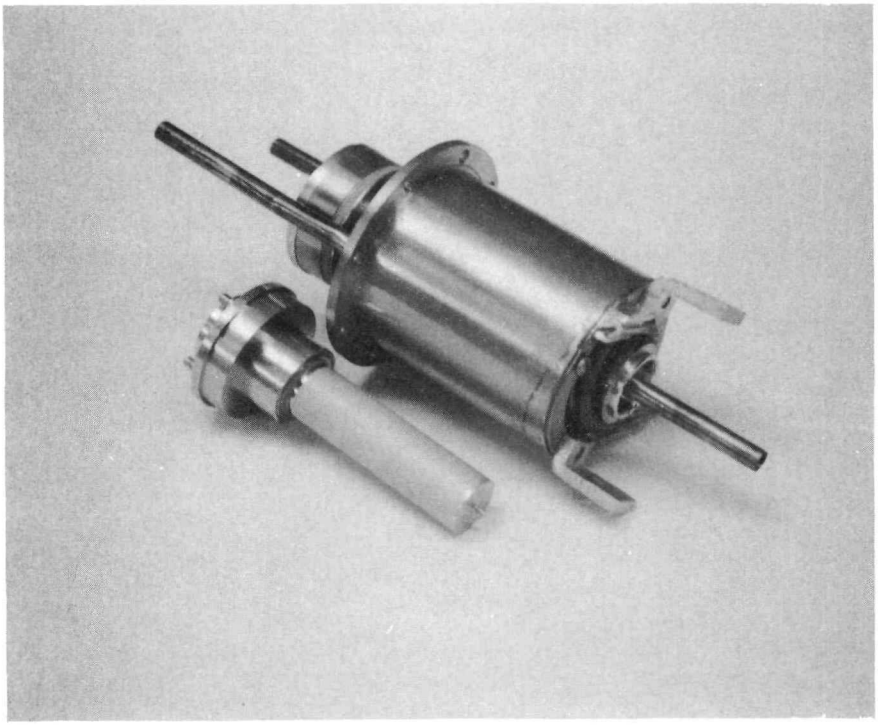

Figure 2.11. Final Subassembly of Diode SD-4

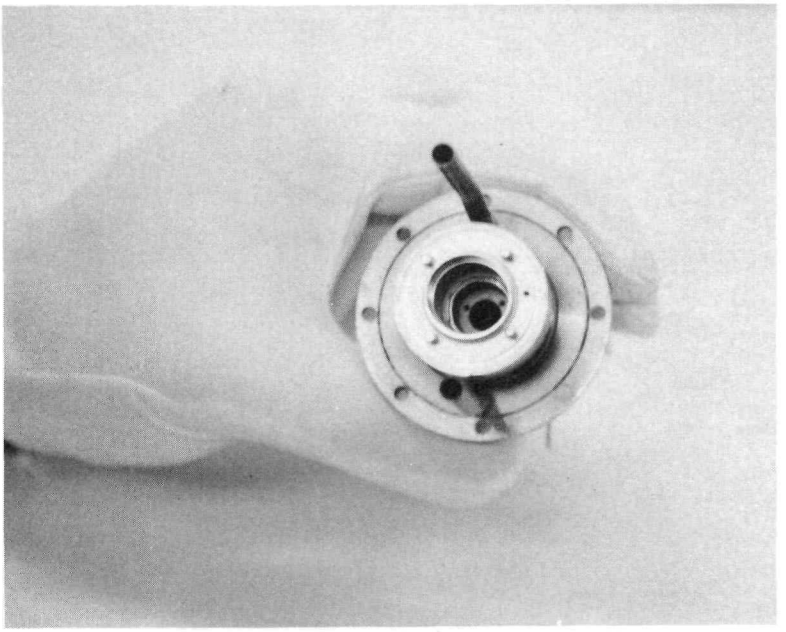

Figure 2.12. Final Assembled Converter

CHAPTER 3.
IN-PILE CAPSULE DESIGN AND FABRICATION

A. DESIGN

The detailed design of the capsule assembly is shown in Figures 3.1 and 3.2. The diode was inside a stainless steel "housing tube" which was evacuated and sealed off after assembly. The vacuum environment protected the exposed refractory metals from oxidation during high temperature operation and provided the insulating effect necessary for accurate calorimetric measurements of diode efficiency. The diode was positioned radially within the tube by a "ceramic spacer disk" which was bolted to the collector current flange. Axial positioning was maintained by the two solid cylindrical collector current leads, also attached to the collector current flange. These leads extended upward for about three inches and were joined at that point to a thicker single rod. This rod extended upward about six feet more and was brazed into the vacuum seal plate. Thus, the diode was axially supported from the vacuum seal plate through the collector current leads.

The emitter current leads were cables flexibly attached to the emitter plug on the diode. The emitter leads were coaxial sheathed wire. The sheath was electrically insulated by compacted MGO, but was swaged in close thermal contact with the emitter lead. Lead cooling (to within approximately 2 inches of the emitter lead connection to the diode) was provided by attaching the collector water lines directly to the sheath. The temperature difference between the diode connection and the water-cooled lead was established along flexible copper straps. These straps provided thermal stree relief for the differential expansion of the collector and emitter leads.

Auxiliary heater leads and thermocouple leads were also made through swaged sheath leads to simplify assembly procedures and to reduce the operating temperature of the leads. These leads were heated primarily by gamma heating. The gamma heat was radiated from the surface of the sheaths to the water-cooled capsule wall. The required radiating temperature of the sheaths was reduced by increasing the emissivity of the sheath surface. High surface emissivities were obtained by establishing a thin oxide coating on the sheaths prior to installation in the capsule assembly. Since each lead was electrically insulated from its surrounding sheath, the need for the ceramic spacer disks was eliminated. The numerous heater and thermocouple leads were positioned within the capsule by stainless steel spacers.

After passing through the top spacer disk, the leads penetrated the vacuum seal plate which was the final closure of the evacuated housing tube. This plate contained leadthroughs for the emitter current and voltage leads, for the heater leads, and for all thermocouple leads. Since the collector was maintained at ground potential, the collector leads and water coolant lines were brazed directly to the vacuum seal plate.

A gamma-heated zirconium getter located at the bottom of the capsule was designed to consume the outgas expected to occur from all heated components within the capsule. The bottom of the getter was brazed to the bottom of the capsule to provide adequate cooling for the getter. Gamma heat in the getter was transferred along the length of getter, through the bottom of the capsule, and into the surrounding water. The top of the getter was designed to operate at about 900° C,

OSTI #0401013361 N40-3434-7

REV	DESCRIPTION	DATE	BY	APPR
A	SEE OBS L.O. (3-22-65)	9-8-65	V.P.	

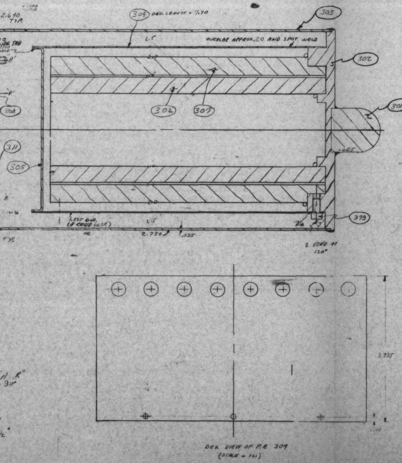

309 DEV. LENGTH = 7.90
303
2.640 TYP.
+.000 -.010
2.5
OVERLAP APPROX. .20 AND SPOT WELD
SIDE TAB SPOT WELD
302
2.0
1.0
306
307
301
308
311
305
.625
1.395 DIA. (8 REQ'D EQ. SP.)
2.750
.035
.125 DIA.
"J"
379
3 REQ'D AT 120°
TYP.
3.375
DEV. VIEW OF P.N. 309 (SCALE = 1x1)

UNCLASSIFIED

P.N.	SIZE	REV	REQ'D	MAT'L	NOTES
379	A		1	SS.	
375	ND		1	—	# R385 VALVE (VEECO)
376	ND		16	—	# C-320 SEAL (ALITE)
377	ND		2	—	5/16 O.D. x 3/16 CU COND. (PYRO)
378	A		4	Al_2O_3	
379	ND		3	SS	#2-56 x 3/16 L.G. H.S.C.S.

PART	SIZE	REQ			NOTES
LAYOUT & SUB-ASSEM					
1050	D	1	P.N. 353, 356, 359, 357, 358, 360, 366, 367, 368, 372, 379, 3		

PART	SIZE	REV	REQ	MAT'L	NOTES
373	A		2	SS	
372	B		2	CU-Zn	
371	A		2	CU	#4 WELDING CABLE ([illegible])
370	A		4	Ni	
369	A		2	CU-Zn	
368	A		2	—	#C-625 SEAL (ALITE)
367	ND		4	—	#CA-8005 (EIMAC)
366	A		4	SS	
365	B		2	CU-Zn	
364	A		2	CU-Zn	
363	ND		2	SS	# 6-32 x 3/16 L.G. H.S.C.S.
362	A		20	CU	.010 THK
361	ND		4	SS	# 6-32 x 1/4 L.G. H.S.C.S.
360	D		1	SS	
359	ND		1	—	DISCHARGE GAUGE #GPH-100A (CVC
358	A		1	SS	
357	B		1	SS	
356	C		1	SS	
355	B		8	SS	
359	ND		16	SS	# 10-32 x 1.0 L.G. H.S.C.S.
353	C		1	SS	
352	D		1	SS	
351	C		1	CU	3/4 x 3/8 RECT.
350	B		6	SS	
349	ND		6	SS	#4-40 x 1/4 L.G. H.S.C.S.
348	ND		6	SS	# 4-40 x 3/16 L.G. H.S.C.S.
347	C		3	SS	
346	A		2	SS	MAKE FROM # 10-32 NUT
345	A		32	SS	
344	ND		13	—	.125 O.D. T.C. - C+A
343	ND		3	—	.125 O.D. T.C. - W-Re
342	A		32	SS	
341	ND		16	—	1/4 O.D. SHT. x .080 CU WIRE - PYRO
340	C		1	CU-Zn	
339	ND		1	SS	# 1/4-20 NUT
338	A		1	CU-Zn	
337	ND		6	SS	#6 WASHER
336	A		3	Al_2O_3	JAN #1009
335	ND		1	SS	# 4-40 x 1 1/8 L.G. H.S.C.S.
334	ND		6	SS	# 6-32 x .188 L.G. H.S.C.S.
332	A		4	SS	
331	A		32	Al_2O_3	
330	A		32	SS	
329	A		32	Al_2O_3	MADE FROM .125 O.D. [illegible] TUBE
328	A		32	SS	
327	A		2	CU	
326	ND		2	SS	#4-40 x .188 L.G. H.S.C.S.
325	ND		2	SS	#4-40 x .312 L.G. H.S.C.S.
324	ND		AS REQ'D	CU	5/16 O.D. TUBE
322	ND		2	CU	5/16 - 3/16 REDUCER
321	B		2	CU-Zn	
320	ND		2	SS	#4-40 x .500 L.G. H.S.C.S.
319	C		1	SS	
318	ND		5	SS	.050 DIA. WIRE
317	A		2	CU	
316	A		2	CU	
315	A		3	SS	
314	ND		12	SS	#4-40 HEX NUT
313	C		1	SS	
312	A		22	Al_2O_3	
311	A		22	Al_2O_3	
310	ND		66	SS	#2 WASHER
309	ND		22	SS	#2-56 NUT
308	ND		22	SS	#2-56 x 7/16 L.G. S.H.C.S.
307	B		1	Zr	
306	B		1	Zr	
305	B		1	Nb	.010 THK
304	B		1	Nb	.010 THK
303	B		1	SS	
302	B		1	SS	
301	A		1	SS	

7 SEE FIXTURE LAYOUTS (3090, 3190 ETC.) FOR FIXTURE INFORMATION.
6 UNK = UNKNOWN N.D. = NO DRAWING, PROCURE FROM THIS L.O.
5 DOTTED LINES INDICATE ROUGH OR PRELIMINARY MACHINING.
4 ALL MATING CORNERS & FILLETS ARE .015 X 45° CHFR. AND .010 R. RES.
3 MAX. PERMISSABLE TAP DRILL DEPTH AND MIN. PERMISSABLE FULL THREAD DEPTHS ARE SHOWN.
2 SECTION LOCATIONS DEFINED BY LETTER LOCATION AT END VIEW.
1 NOTES 2 THRU 7 APPLY UNLESS OTHERWISE SPECIFIED.

NOTES

DESIGN FINALIZED	DATE	INIT.	DATE	INIT.	DATE	INIT.	DATE	INIT.

	A	B	C	D	E	F	G	H	J	K	L	M	N	P	R	S	T	U	V	W	Y	Z	J
1		✓	✓		✓		✓	✓	✓	✓	✓				✓	✓						✓	
2	✓	✓	✓	✓	✓																		
V	✓	✓	✓	✓		✓	✓		✓														
∥																							
⊥																							
⊙																							

UNLESS OTHERWISE SPECIFIED
DECIMAL: .X ±.03, .XX ±.01, .XXX ±.005
FILLET RADIUS: .010 MAXIMUN
THREADS: CLASS 2
✱DIA. CONC. WITHIN ___ T.I.R.
ALL OTHER DIA. CONC. WITHIN .005 ___ T.I.R.
SURFACES TO BE PERP. WITHIN .005 ___ T.I.R.
SURFACES TO BE PAR. WITHIN .005 ___ T.I.R.
HOLE ANGULAR TOL. 0-2.0 RAD. ±0° 9'
2.0-4.0 RAD. ±0° 5'
ALL OTHER ANGULAR TOL. TO BE ±0° 30'
REMOVE ALL BURRS AND EDGES

SCALE: 2 x 1
FINISH: —
509-1000 SHT 4
NEXT ASSY.
SIMILAR TO

THERMO ELECTRON
ENGINEERING CORPORATION
85 FIRST AVENUE · WALTHAM, MASS. 02154

DRAWN	CHECKED	ENGINEER
VP 9-6-65		

TITLE:
Figure 3.1

SIZE	DRAWING NUMBER	SHEET	REV
H	509-1000	3	A

UNCLASSIFIED

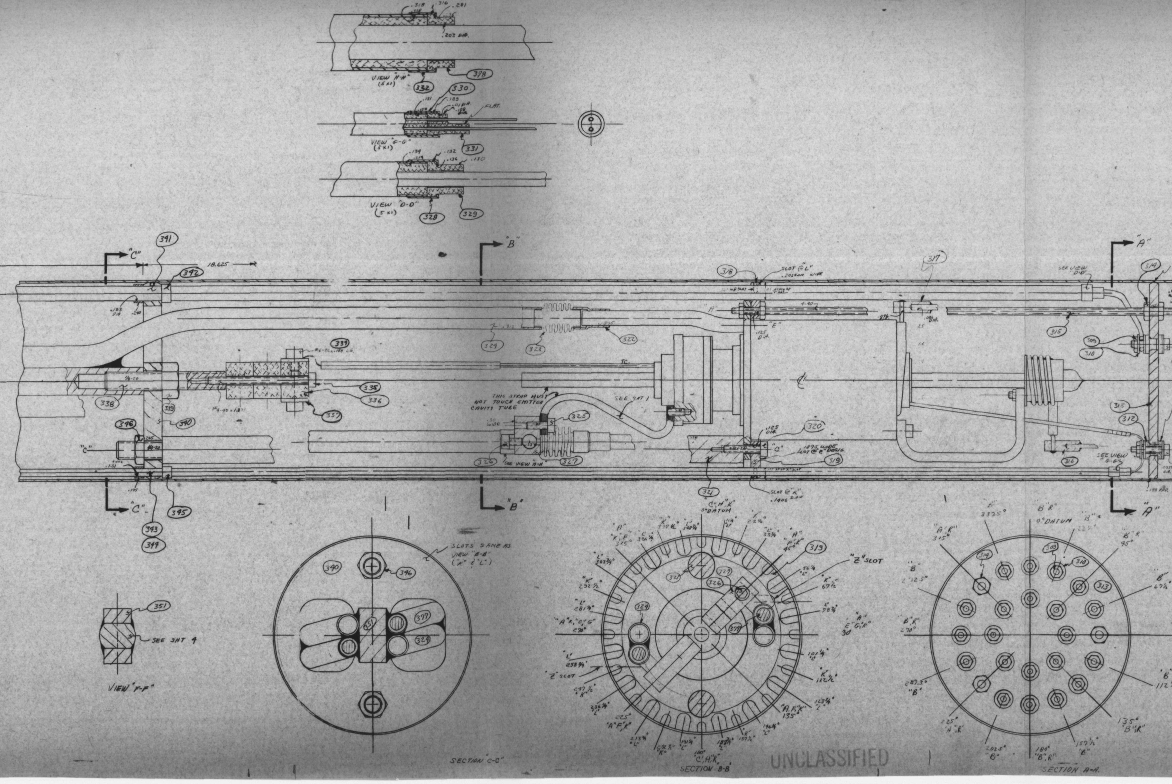
VIEW "H-H" (5×1)
VIEW "G-G" (5×1)
VIEW "D-D" (5×1)
FLAT
.203 DIA.
"A"
"B"
"C"
18.625
SLOT @ "L" .2036 WIDE
SLOT @ "K" .1406
.1875 WIDE SLOT @ "E" DEGS.
"E"
.125 DIA.
SEE VIEW D-D
SEE VIEW G-G
THIS STRAP MUST NOT TOUCH EMITTER CAVITY TUBE
SEE SHT 1
SEE VIEW "H-H"
TC.
1/4-20
SEE SHT 4
VIEW "F-F"
SECTION "C-C"
SLOTS SAME AS VIEW "B-B" ("K" & "L")
SECTION "B-B"
"C","H","K" 0° DATUM
"Z" SLOT
SECTION A-A
"B","R" 0° DATUM
309
310
312
313
314
315
316
317
318
319
320
321
322
323
325
326
327
328
329
330
331
332
335
336
337
338
339
340
351
377
378
390
391
392
393
395
396
399

UNCLASSIFIED

UNCLASSIFIED

UNCLASSIFIED

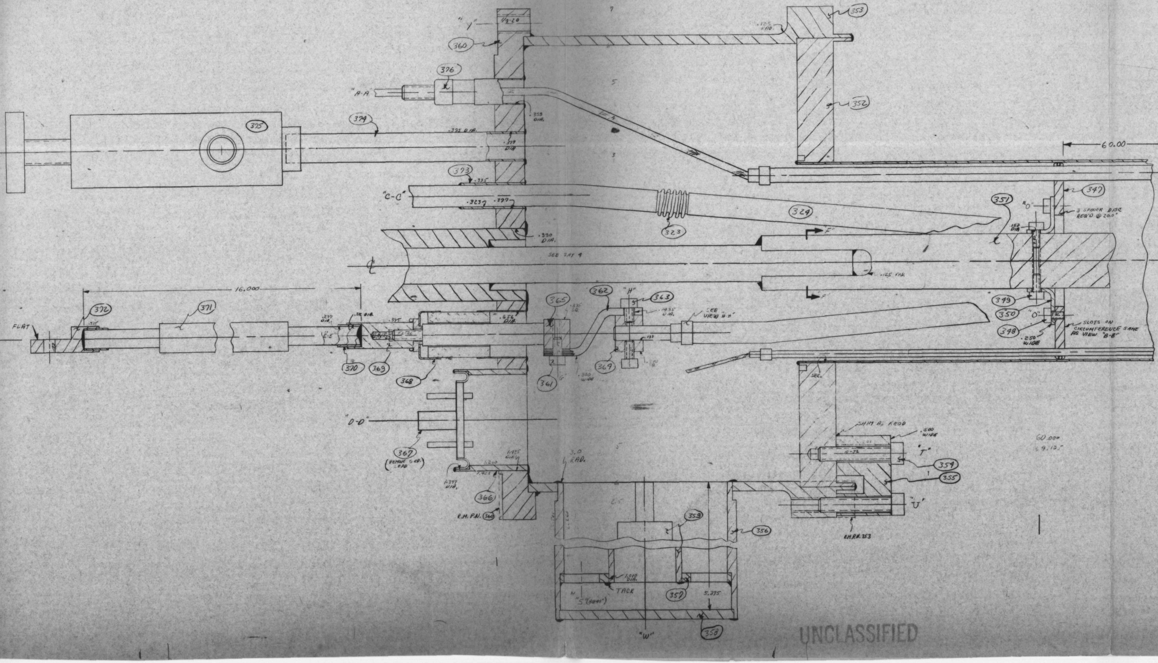
"Y"
1/4-20
360
353
.125 RAD.
376
"A-A"
352
.359 DIA.
374
375
.375 DIA.
.379 DIA
"B"
60.00
373
.375
"C-C"
.323
.377
324
323
347
351
"O"
3 SPIDER DISC REQ'D @ 20.0"
.152 DIA
"F"
.990 DIA.
SEE SHT 4
℄
.125 RAD.
"F"
16.000
372
371
FLAT
.315
.277 DIA.
.312 DIA.
"E-E"
.375
370
369
368
.656 DIA.
365
.375 SQ.
361
"G"
.300 WIDE
362
"H"
363
.1495 DIA.
.137
369
SEE VIEW "H-H"
349
350
"O"
348
.250 WIDE
SLOTS ON CIRCUMFERENCE SAME AS VIEW "B-B"
SEL.
"D-D"
367
(REMOVE G.RD. LEAD)
1.425 DIA.
1.260
1.423
1.397 DIA.
366
R.M. P.N. 360
3.0 RAD.
SHIM AS REQD
.500 WIDE
10-32
"T"
354
355
"U"
R.M.P.N. 353
60.000
49.125
359
356
1.010 DIA.
TACK
"S" (BASE)
357
5.375
358
"W"

UNCLASSIFIED

UNCLASSIFIED

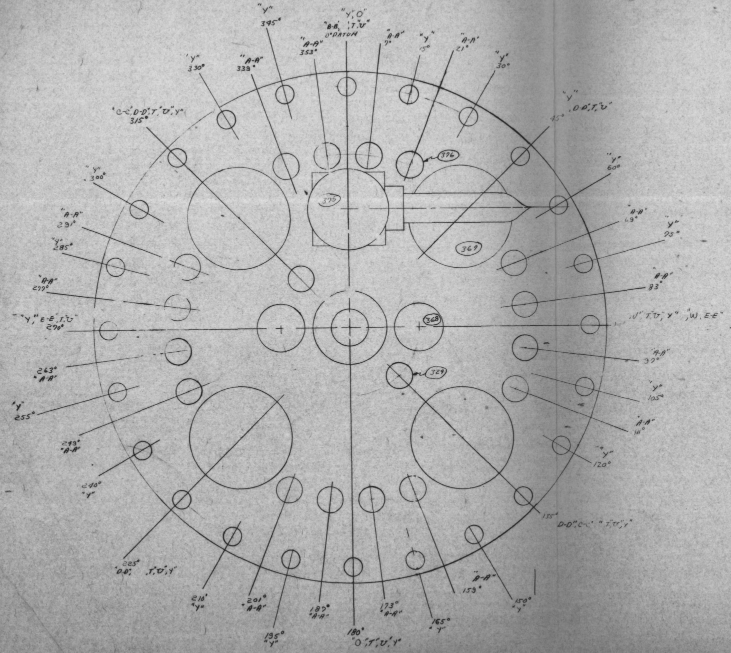
"Y"
345°
"Y", O
"B-B", "T" "U"
0° DATUM
"A-A"
353°
"A-A"
7°
"Y"
15°
"A-A"
21°
"Y"
30°
"Y"
330°
"A-A"
339°
"Y"
45° "D-D", "T", "U"
"C-C", "D-D", "T", "U", "Y"
315°
376
375
"Y"
60°
"Y"
300°
"A-A"
69°
"Y"
75°
"A-A"
291°
"Y"
285°
369
"A-A"
83°
"A-A"
277°
"Y", "E-E", "T", "U"
270°
368
"U", "T", "U", "Y", "W", E-E"
"A-A"
97°
263°
"A-A"
329
"Y"
105°
"Y"
255°
"A-A"
111°
249°
"A-A"
"Y"
120°
240°
"Y"
135°
D-D", C-C" "T", "U", "Y"
225°
"D-D", "T", "U", "Y"
"A-A"
159°
150°
"Y"
210°
"Y"
201°
"A-A"
187°
"A-A"
173°
"A-A"
165°
"Y"
195°
"Y"
180°
"O", "T", "U", "Y"

"E-E"

UNCLASSIFIED

UNCLASSIFIED

UNCLASSIFIED

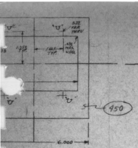
"U"
"U"
8-32 TAP THRU
1.250 TYP.
1.025 TYP.
.032 MAX. RAD.
"U"
"U"
450
6.000

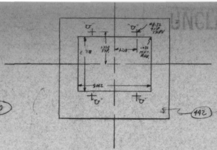
"U"
"U"
#8-32 TAP THRU
2.38
1.250 TYP.
1.210
.032 MAX. RAD.
3.062
"U"
"U"
442

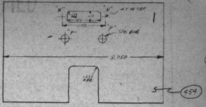
"N"
"N"
#3-48 TAP.
"P"
"P"
.516 DIA.
8.050
.250 RAD.
454

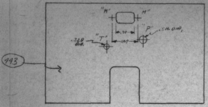
"M"
"M"
.39
"T"
.328 DIA.
"P"
.516 DIA.
443

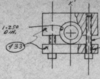
"R"
"K"
"R"
1.250 DIA.
433

SECTION "E-E"

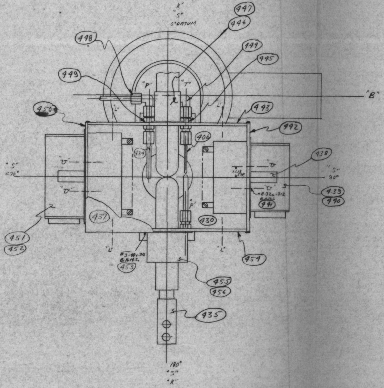
"K"
"S"
0° DATUM
447
446
448
449
449
445
"P"
"T"
"B"
"L"
"L"
450
443
442
406
434
438
"S" 270°
"U"
"U"
"U"
"U"
"S" 90°
439
440
#8-32 x .312
441
437
"P"
430
451
452
"L"
"L"
#3-48 x .312
453
454
455
456
435
180°
"S"
"K"

UNCLASSIFIED

UNCLASSIFIED

UNCLASSIFIED

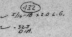
432
5/16-18 x 2.0 L.G.
.323 DIA.

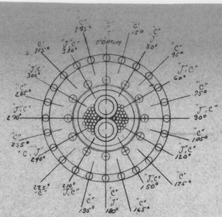
0° DATUM
"C" "J"
"C" 15°
"C" J 30°
"C" 45°
"J" "C" 60°
"C" 75°
"J", "C" 90°
"C" 105°
"J" "C" 120°
"C" 135°
"J" "C" 150°
"C" 165°
"C" "J" 180°
"C" 195°
210° "J" "C"
225° "C"
"C, J" 240°
"C" 255°
"J" "C" 270°
"C" 285°
"J" "C" 300°
"C" 315°
"J" "C" 330°
"C" 345°

SECTION "C-C"

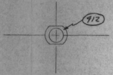

SECTION "D-D"

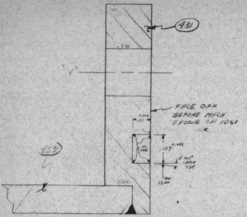
431
.241
"V"
FACE OFF BEFORE MACH GROOVE ON 1061
+.006 .101
.157 +.006
0° TO 5° TAPER TYP.
13.000
454
SEL.

VIEW "H-H" (5×1)

12.0

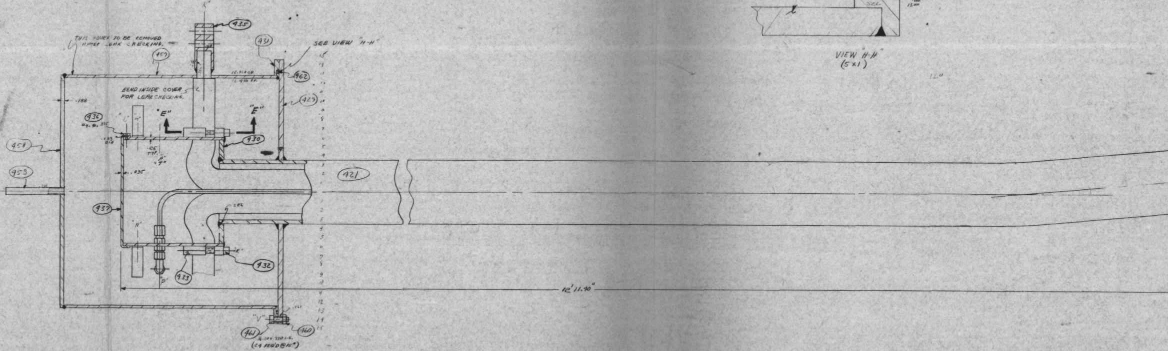
"K"
435
THIS COVER TO BE REMOVED AFTER LEAK CHECKING.
457
431
SEE VIEW "H-H"
462
12.750 O.D.
12.438 I.D.
BEND INSIDE COVER FOR LEAK CHECKING.
429
.188
436
#4-40 x .375
"L" "M"
"E"
"E"
430
.129 DIA
.125 TYP.
"P" "T"
458
.035
459
421
437
SEL
"N"
"R"
432
433
"P"
12' 11.40"
"V"
461
1/4-20 x .750 L.G. (24 REQ'D @ 15°)
460
15 14 13 12 11 10 9 8 7 6 5 4 3 2 1
1 2 3 4 5 6 7 8 9 10 11 12 13 14 15

UNCLASSIFIED

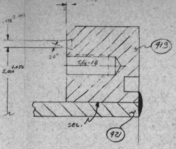
.088 ±.003
20°
5/16-18
5.000 +.050
419
SEL.
421

VIEW "GG"
(SCALE = 2x1)

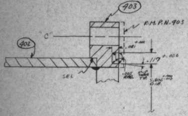
403
R.M.P.N. 403
"C"
402
.081 +.002
.117 +.006
SEL
.005 RAD.
0°-5° TAPER TYP.
5.800 +.000 -.010 DIA.

VIEW "F-F"
(SCALE = 2x1)

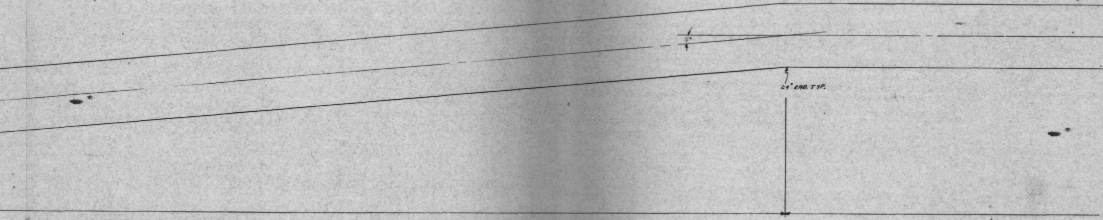

UNCLASSIFIED

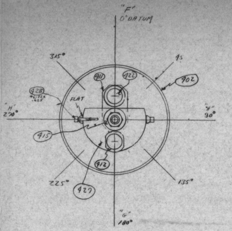
"F"
0° DATUM
315°
45
911
922
902
928
#6-32×.625
FLAT
"H"
270°
"H"
90°
915
912
225°
135°
927
"G"
180°

SECTION "B-B"

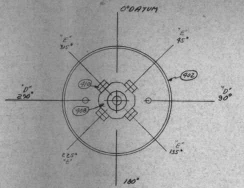
0° DATUM
"E"
315°
"E"
45°
916
902
"D"
270°
"D"
90°
908
225°
"E"
"E"
135°
180°

SECTION "A-A"

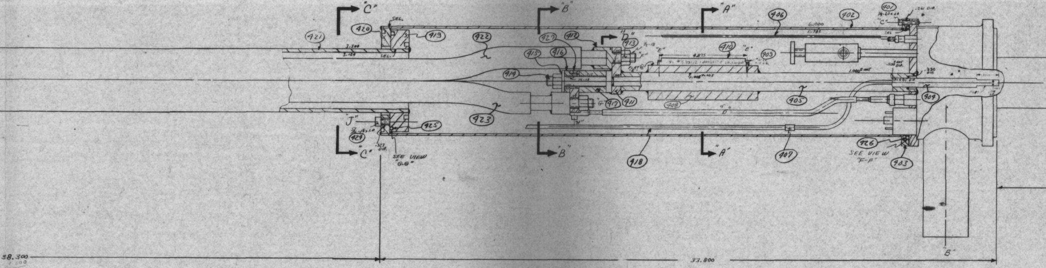
"C"
SEL.
920
919
921
3.500
3.124
SEL.
922
"B"
927
912
"D"
913
1/2-13
"F"
"E"
4.875
915
916
914
1/2-13
FLAT @ "E"
1.006 ±.005
917
911
"G"
908
923
"H"
"J"
5/16-18×1.0
924
.323 DIA.
925
"C"
SEE VIEW "G-G"
"B"
918
"A"
906
6.000
5.782
902
901
1/4-20×1.0
.261 DIA.
"C"
SEL
910
909
.500 ±.005 DIA.
1.000 ±.005
.390 DIA.
905
904
"D"
907
926
SEE VIEW "F-F"
903
"A"
"B"
38.300
33.800

UNCLASSIFIED

UNCLASSIFIED

REV	DESCRIPTION	DATE	BY	APPR
A	SEE OBS L.O. (9-3-65)	9-3-65	VP	

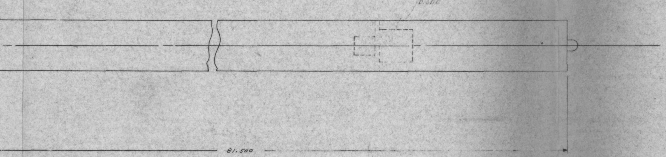
1.0 O.D.E
81.500

UNCLASSIFIED

PART	SIZE	REV	REQ	MAT'L	NOTES
					LAYOUT & SUB-ASSEM
1060			1		P.N. 903, 902, 920 WELD F.M.
1061			1		P.N. 931, 957, 9-8, 959 WELD F.M.
962	ND		1	—	"O" RING #2-[illegible] (PARKER)
961	ND		24	SS	#1/4-20 x 1/4 [illegible]
960	ND		24	SS	#1/4-20 NUT
959			1	SS	
958			1	SS	
957			1	SS	
956	ND		1	—	#57-40360 RECP. (AMPHENOL)
955	ND		1	—	#57-30360 PLUG (AMPHENOL)
954			1	Al	
953	ND		4	SS	#3-48 x .312 B.H.M.S.
952	ND		1	—	#S-510-DB CON (JONES)
951	ND		1	—	#P-510-CE CON (JONES)
950			1	Al	
949	ND		2	SS	#500-A1-5-316 BULKHEAD ADAPTOR (SWAGELOK)
948	ND		2	SS	#500-3-316 ELBOW (SWAGELOK)
947	ND		1	—	#57-40140 RECP. (AMPHENOL)
946	ND		1	—	#57-30140 CON (AMPHENOL)
945	ND		1	SS	#200-A1-2-316 BULKHEAD ADAPTOR (SWAGELOK)
944	ND		1	SS	#200-3-316 ELBOW (SWAGELOK)
943			1	Al	
942			1	Al	
941	ND		8	SS	#8-32 x .312 B.H.M.S.
940	ND		1	—	#S-508-DB CON (JONES)
939	ND		1	—	#P-508-CE CON. (JONES)
938	ND		2	—	#500-L LOCK (H.B. JONES)
937			1	Al	
936	ND		4	SS	#4-40 x .375 B.H.M.S.
935			2	CU	
934	ND		2	CU	5/16 O.D. TUBE
933			2	Al	
932	ND		4	SS	#5/16-18 x 2.0 LG. HSHS
931			1	SS	
930			1	Al	
929			1	AL	
928	ND		4	SS	#6-32 x .625 LG. HSHS.
927			1	Ni	
926	ND		1	"O" RING	#2-162 (PARKER)
925	ND		1	"O" RING	#2-153 (PARKER)
924	ND		12	SS	#5/16-18 x 1.0. LG. HSHS
923	ND		1	—	#500 CABEL (WESCO)
922	ND		1	—	#300 CABEL (WESCO)
921			1	Al	
920			1	SS	
919			1	Al	
918	ND		2	CU	5/16 O.D. CU TUBE
917			1	NYLON	
916			1	NYLON	
915	ND		1	SS	#1/2 WASHER
914			1	SS	
913	ND		3	SS	#1/2-13 NUT
912			2	Ni	
911			1	Ni	
910	ND		9	BAKELITE	#599-12 (H. SMITH) STRIP
909	ND		8	SS	#6-32 x .5 LG. B.H.M.S.
908			1	SS	
907	ND		2	CU	.312 O.D. TUBE SLEVE
906	ND		1	CU	.125 OD TUBE
905			1	SS	
904			1	CU	
903			1	SS	
902			1	SS	
901	ND		24	SS	1/4-20 x 1.0 LG. B.H.M.S.

UNCLASSIFIED

7 SEE FIXTURE LAYOUTS (3090, 3190 ETC.) FOR FIXTURE INFORMATION.
6 UNK = UNKNOWN N.D. = NO DRAWING, PROCURE FROM THIS L.O.
5 DOTTED LINES INDICATE ROUGH OR PRELIMINARY MACHINING.
4 ALL MATING CORNERS & FILLETS ARE .015 X 45° CHFR. AND .010 R. RES.
3 MAX. PERMISSABLE TAP DRILL DEPTH AND MIN. PERMISSABLE FULL THREAD DEPTHS ARE SHOWN.
2 SECTION LOCATIONS DEFINED BY LETTER LOCATION AT END VIEW.
1 NOTES 2 THRU 7 APPLY UNLESS OTHERWISE SPECIFIED.

NOTES

	A	B	C	D	E	F	G	H	J	K	L	M	N	P	R	S	T	U	V	W	Y	Z
1	✓	✓	✓	✓	✓	✓	✓	✓			✓	✓	✓	✓	✓	✓	✓					
2																						
V	✓	✓	✓	✓	✓	✓	✓															
∥																						
⊥																						
⊙																						

UNLESS OTHERWISE SPECIFIED

DECIMAL: .X ±.03, .XX ±.01, .XXX ±.005
FILLET RADIUS: .010 MAX
THREADS: CLASS 2
*DIA. CONC. WITHIN ___ T.I.R.
ALL OTHER DIA. CONC. WITHIN .005 ___ T.I.R.
SURFACES TO BE PERP. WITHIN .005 ___ T.I.R.
SURFACES TO BE PAR. WITHIN .005 ___ T.I.R.
HOLE ANGULAR TOL. 0-2.0 RAD. ±0° 9'
2.0-4.0 RAD. ±0° 5'
ALL OTHER ANGULAR TOL. TO BE ±0° 30'
REMOVE ALL BURRS AND EDGES

SCALE: 1/2-1
FINISH: —
NEXT ASSY.
SIMILAR TO

THERMO ELECTRON
ENGINEERING CORPORATION
85 FIRST AVENUE · WALTHAM, MASS 02154

DRAWN	CHECKED	ENGINEER
P-18		

TITLE: Figure 3.2

SIZE	DRAWING NUMBER	SHEET	REV
H	509-1010	4	A

OSTI #04601361 NYO-3434-7

and the bottom of the getter about 100°C. The variation in temperature along the entire getter insured that portions of the getter operated at the correct temperature for selective gettering of different gases. Two getter temperatures are particularly important. Gettering of O_2, N_2, CO and CO_2 occurred primarily in a temperature range from 600 to 800°C. Hydrogen was gettered most copiously at about 300°C.

Above the housing tube was the offset connection chamber which was joined to the capsule lead tube. The capsule lead tube contained all the leads leaving the housing tube and extended approximately twenty-five feet up to the top of the reactor pool. The inside of the lead tube was dry, and was filled with helium gas during in-pile operation. The offset connection chamber prevented streaming of neutrons from the core to the top of the pool and provided a convenient arrangement for connecting the leads from the housing tube to the capsule lead tube. At the top of the lead tube provision was made for connecting all the in-pile leads to the instrumentation and test setup located on the reactor working floor.

B. ASSEMBLY

The assembly of SD-4 into the in-pile capsule was accomplished without encountering any significant problems. Figure 3.3 shows a side view of the lower section of the capsule, the section which is partially within the reactor core. This section, approximately 7 feet long, was evacuated after its outer stainless steel tube was placed over it and welded. The long sheathed heater, thermocouple, and voltage leads are visible in the picture. At the bottom end, the terminal disk which connects the sheathed leads to the converter leads is visible. Figures 3.4 and 3.5 show the connection region between

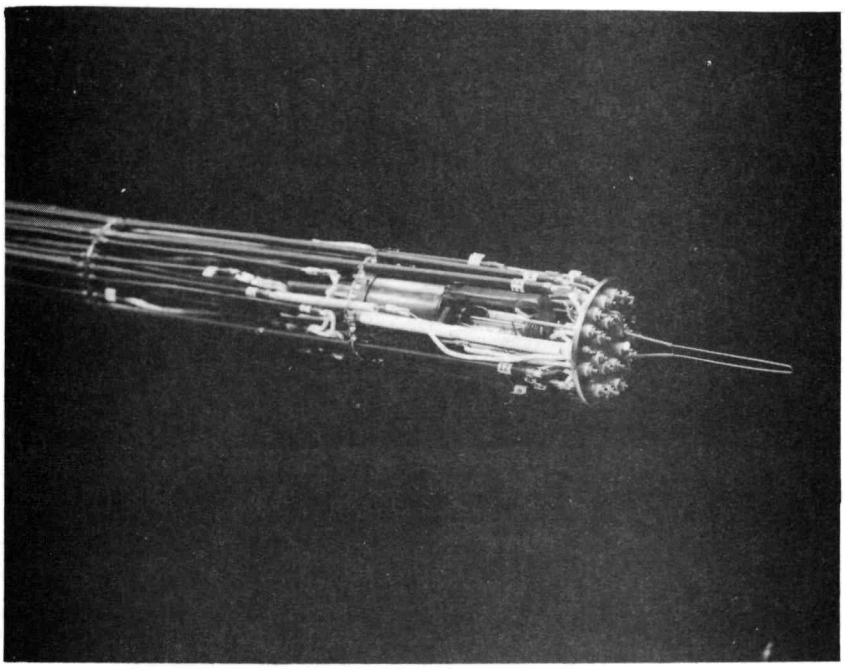

Figure 3.3. In-Pile End of Lower Section of In-Pile Capsule

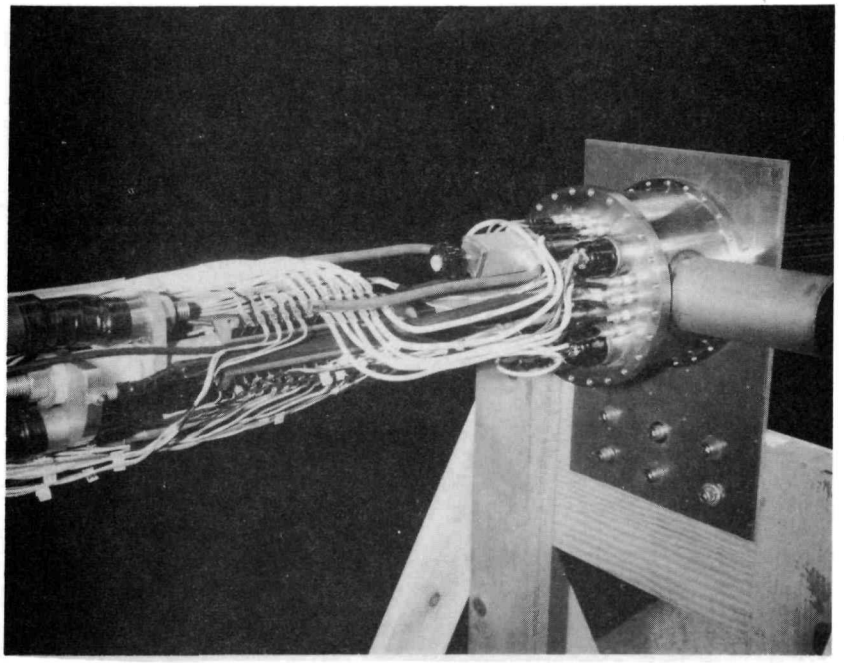

Figure 3.4. Connection between Upper and Lower Sections of the In-Pile Capsule

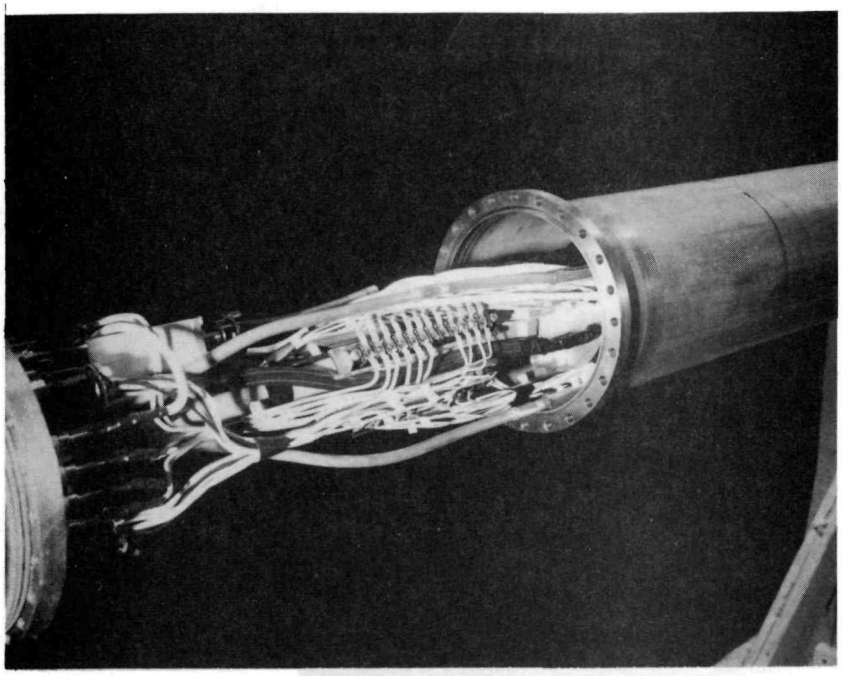

Figure 3.5. Connection between Upper and Lower Sections of the In-Pile Capsule

the lower section and the upper lead tube. All joints made in this region were designed for easy disconnection to facilitate post-irradiation handling. The penetrations made through the seal plate of the lower section included two water lines, six heater leads, twenty thermocouple leads, six voltage leads, the emitter and collector bus bars, and an evacuation line. All connections were successfully made and maintained during shipping and in-pile operation. Figures 3.6 and 3.7 show the in-pile end of the lower section. The exterior of the water-cooling jacket, the cesium reservoir, and the diode lead-through are visible inside the sheathed heater leads. The filament extending from the bottom of the terminal disk is the heater intended to control the temperature of the getter. This heater was the only part of the capsule assembly which was not functioning after shipment to the BMI reactor. Apparently, an open circuit developed at one of the connecting terminals leading to the heater supports.

The outgassing of the lower section was carried out over a ten-day period. The long lengths of sheathed leads evolved large volumes of gas which necessitated long outgassing times. The exterior of the 2.75-inch pipe, housing the lower section, was wrapped with heaters. For one week these heaters maintained the temperature of the pipe above 700°C. The internal temperatures ranged from 600°C to 20°C, the temperature of the cooling water tubes. The adequacy of this outgassing procedure can be evaluated only by post-irradiation inspection of the niobium components of the converter and by the performance of the converter during in-pile operation.

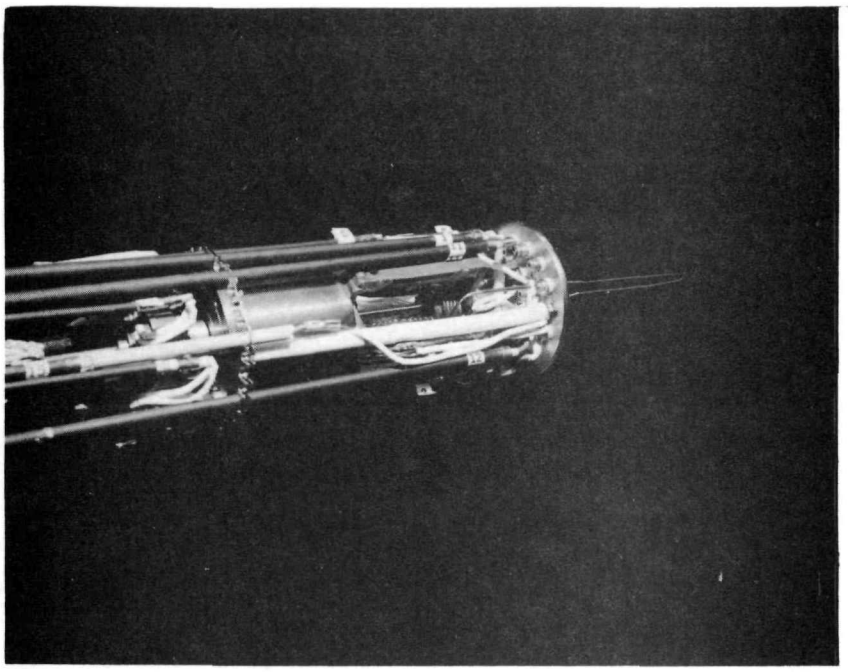

Figure 3.6. In-Pile End of Lower Section of In-Pile Capsule

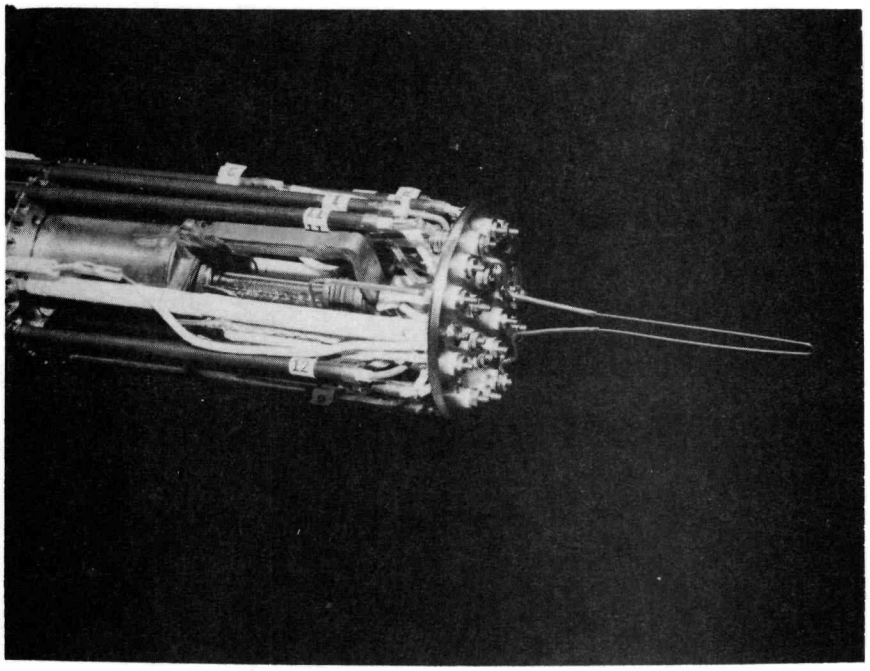

Figure 3.7. In-Pile End of Lower Section of In-Pile Capsule

C. HAZARDS ANALYSIS

The detailed hazards analysis of the in-pile test assembly was completed and reviewed by the Reactor Subcommittee of the Battelle Radiological Safety Committee. Recommendations of the Subcommittee were to delete the emitter thermocouples to provide more adequate fission product primary containment and to substitute helium for argon as the lead-out tube cover gas. These recommendations were followed and the changes incorporated into the test unit.

Reactor safety interlocks reflecting the operation of the diode in-pile are as follows:

1. Coolant flow rate - Reactor scram at coolant flow rates of less than 1/8 gpm;

2. Diode output current - An audible and visible alarm if output current drops 25 amps below the normal operating level and a reactor scram if the output current drops 50 amps below the normal operating level;

3. Temperature - Reactor scram when heat exchanger temperatures rise to 175°C. Out-of-pile loss of coolant information indicates that this temperature would indicate a coolant loss and not cause damage to the diode. This interlock serves primarily as a loss-of-coolant back-up safety feature.

D. COOLANT SYSTEM

The coolant system design has been completed and is shown schematically in Figure 3.8. The system is closed and the surge tank is purged with air to minimize possible gas buildup due to radiolytic decomposition of the demineralized water. The anticipated coolant flow rate is 0.3 gpm. Approximately 7 gallons of water are contained in the system.

The pump is interlocked with the flow sensing switch to shut down 2 seconds after a loss of low reactor scram. This is to prevent filling the diode test section with water should a coolant leak develop within the test section.

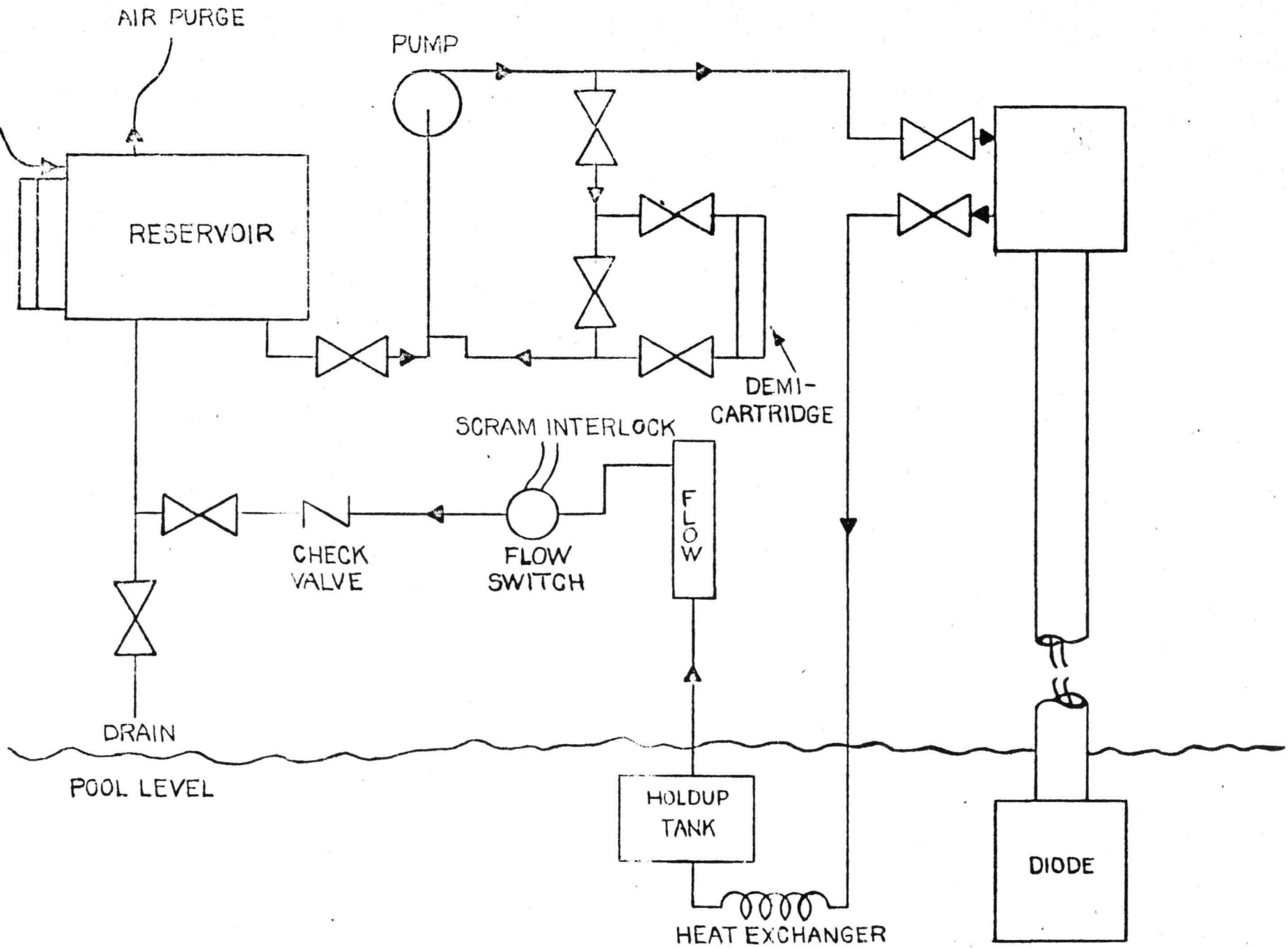

Figure 3.8 Schematic of In-Pile Coolant System

CHAPTER 4

DIODE TESTING

A. SUMMARY

Converter SD-4 has been operated for 100 hours out-of-pile and about 8125 hours in-pile. The results obtained during most of the test period are summarized in Figure 4.1, which displays power input, power output, efficiency, cesium reservoir temperature, and collector temperature. The points shown represent the data recorded at periodic intervals by the reactor operating technicians. In general, the cesium reservoir and collector temperatures were maintained near optimum levels. However, day-to-day drifts in cesium reservoir temperature and in collector temperature occurred throughout the test duration.

The total testing time can be divided into eight periods. The first period was the 100-hour out-of-pile test, shown in Figure 4.1 to the left of zero hours of in-pile operation. The second period was the initial 25 hours of in-pile testing. The third period consisted of a transient in emitter temperature caused by a reduction in power input to the emitter. This transient lasted until the 600-hour point, although it was virtually over by the 300-hour point. The fourth period was a steady run of about 300 hours at a slightly reduced reactor power level necessitated by another experiment on the reactor. The fifth period was a steady run from about the 1400-hour point to about the 2600-hour point at full reactor power levels. The reactor was shut down for modifications at about the 2600-hour point. The sixth period was a fairly steady run after the reactor was restarted until the 6100-hour point, when a malfunction in the cesium reservoir heater occurred. The seventh period consisted of operation without the cesium reservoir

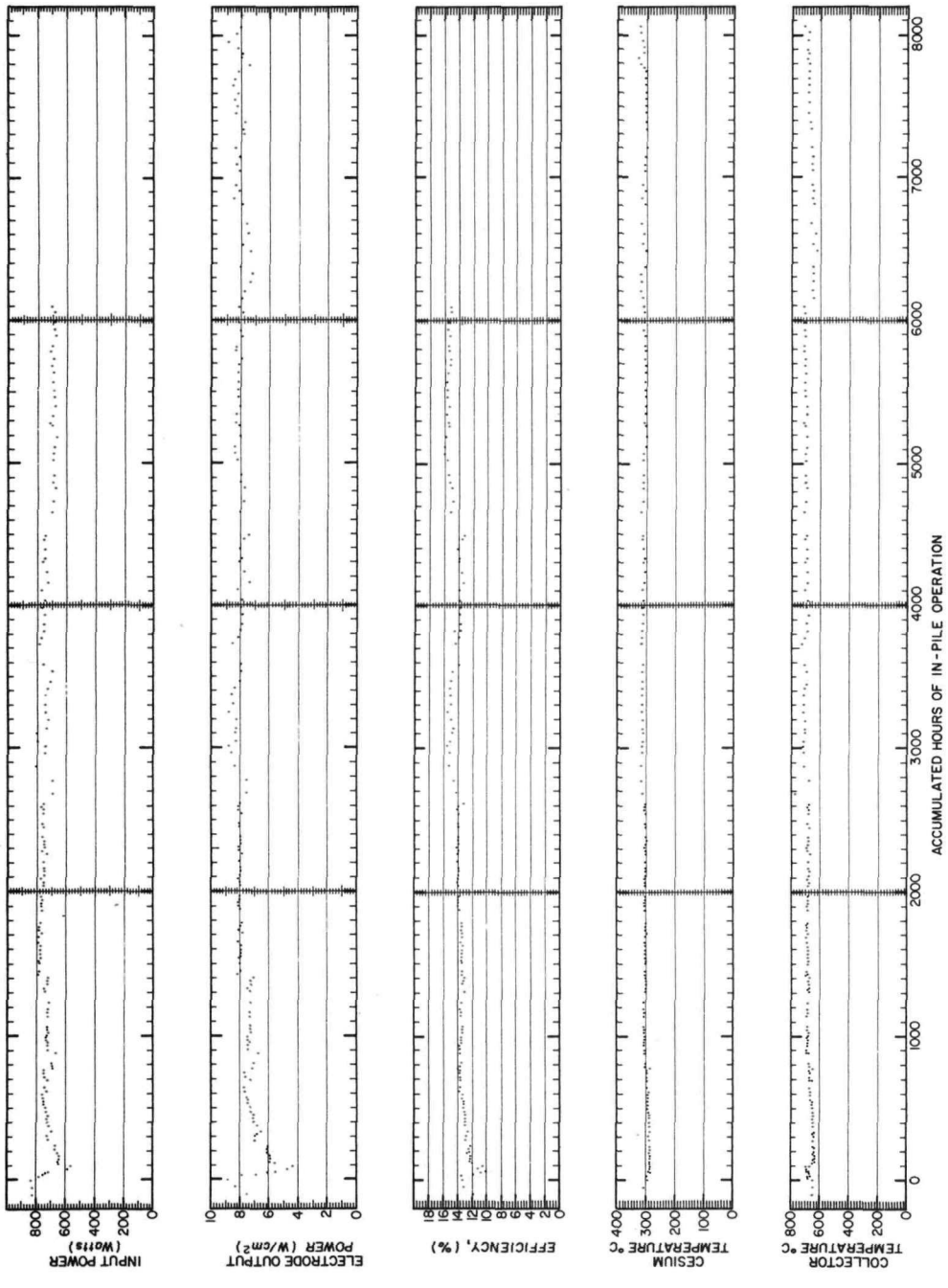

Figure 4.1 Performance Summary

heater and extended from the 6100-hour point to the 7327-hour point. During the initial part of this period, Dowtherm was used instead of water as a coolant to achieve the desired cesium reservoir temperature. This period ended when the cooling lines became clogged with a carbon-type substance caused by dissociation of the Dowtherm. The eighth test period was started after the carbon scale was flushed out of the coolant lines. However, the scale built up again during this period and finally led to termination of the test after 8125 hours. In the following paragraphs, each of these test periods is summarized.

Throughout all eight test periods, no performance degradation of the converter was observed. At periodic intervals the cesium temperature, collector temperature, and power input were reset at reference levels corresponding to a data point taken during the first 25 hours. These points are shown in Figure 4.2 at the 25-hour, 1711-hour, 2615-hour, 3110-hour, 4300-hour, 7000-hour, and 7890-hour points. These points are shown in relation to a sweep curve taken during the initial out-of-pile tests. During the first 2615 hours, the reference points were taken at very closely set cesium reservoir and collector temperatures. As mentioned in the following discussion, a shift in the cesium reservoir thermocouples occurred during the shutdown after the 2615-hour point. Therefore, the indicated cesium reservoir temperatures shown for subsequent points are somewhat higher. However, no significant difference is believed to exist in the actual cesium reservoir temperature for any of the points shown in Figure 4.1 at less than 5000 hours. At about the 6150-hour point, one of the cesium reservoir thermocouples failed completely. For the last two points (7000 and 7890) it was impossible to get the cesium reservoir temperature lower than those values

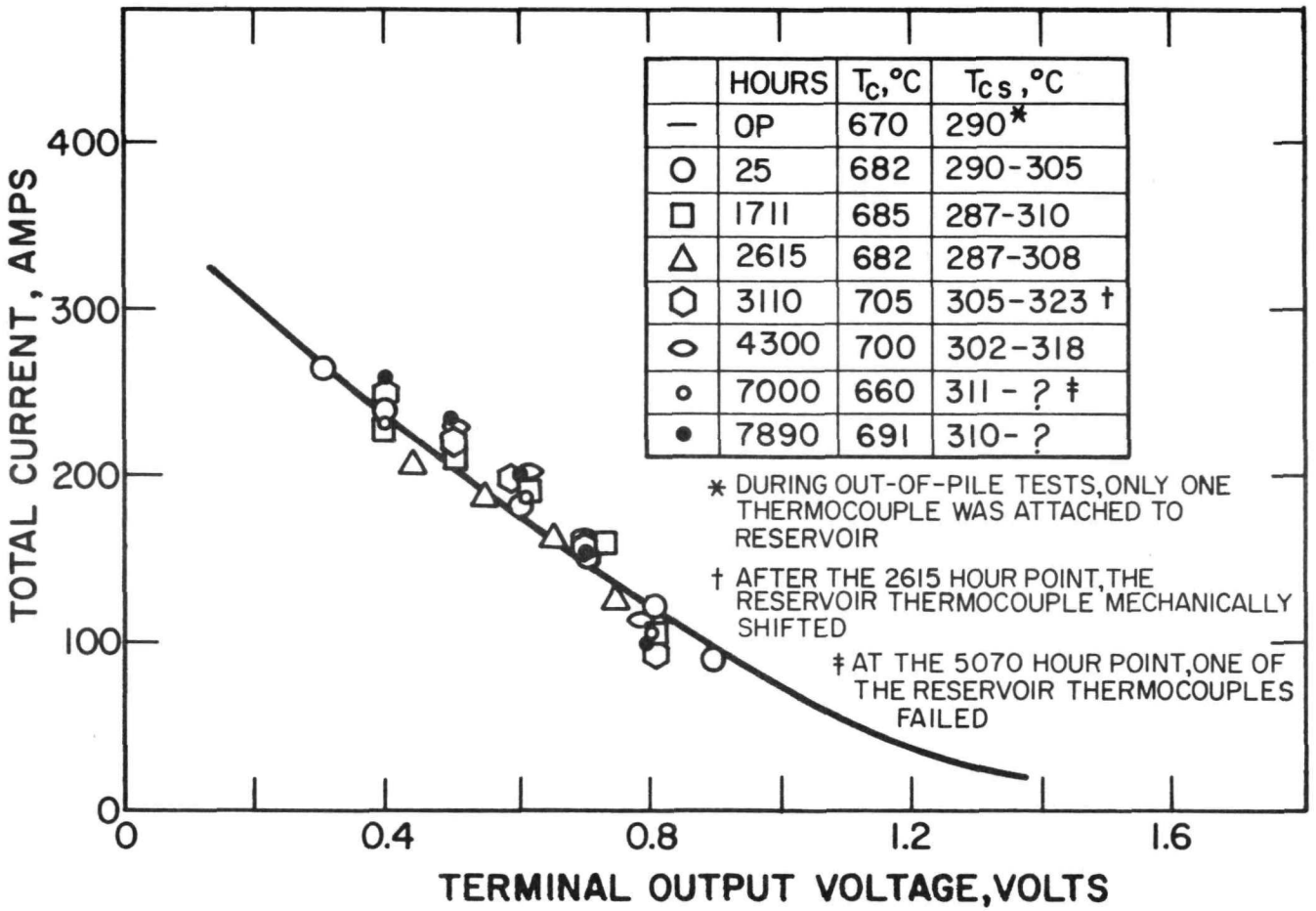

Figure 4.2 Comparison of I-V Sweep Data at Controlled Reference Points During Out-of-Pile and In-Pile Operation.

shown in Figure 4.1. Despite these difficulties, remarkably close agreement was observed over a wide range of the I-V curve throughout the 8125 hours of testing. A summary of the operating characteristics of the converter over its test history is shown in Table 4.1.

B. DETAILED DESCRIPTION OF TEST PERIODS

1. Out-of-Pile Test Period

The converter was operating out-of-pile for approximately 100 hours at a variety of test conditions. Over 90 percent of the operating time was at output power levels about 8 w/cm^2 (electrode power density). In Table 4.2, a typical operating point during these tests is described. No evidence of performance degradation was observed between the beginning and end of the test period. In addition to steady-state operating data, parametric sweep data were obtained as shown in Figure 4.2.

Heat transfer measurements were made on the cesium reservoir straps and the heat choke fins. The thermal resistance of the straps was determined by measuring the cesium reservoir temperature as a function of power input to the cesium reservoir heater. Since gamma heating of the reservoir and the straps occurs during in-pile operation, this resistance was critical to the achievement of reservoir temperature control in-pile. Since the heat choke fins represent a fixed thermal resistance through which the heat rejected from the collector must flow, the temperature drop across the fins can be used as a thermal power indicator. Therefore, the relationship between power input and this temperature difference was determined for SD-4 during the out-of-pile tests. These data provided input and efficiency measurements during in-pile operation.

TABLE 4.1

SUMMARY OF SD-4 OPERATING CHARACTERISTICS

Out-of-Pile:	
Test Time, hours	100
Average Electrode Power Density W/cm^2	8.0
Average Overall Efficiency, * %	13.1
Average Estimated Emitter Temperature, °C	1600
Diode Characteristics	Stable
In-Pile:	
Test Time, hours	8125
Average Electrode Power Density, W/cm^2	7.8
Average Overall Efficiency, † %	13.7
Average Estimated Emitter Temperature, °C	1575
Diode Characteristics	Stable
Fuel Characteristics	
Power Density, W/cm^3	324
Equivalent Lifetime of Solid 0.9" Fuel Rod, hours	26,700
Average Burnup, $fiss/cm^3$	3.1×10^{20}
Maximum Burnup, $fiss/cm^3$	7.3×10^{20}
Average Burnup, U^{235} atom %	1.7
Maximum Burnup, U^{235} atom %	4.0
Total Number of Cycles	~80

* Power output at the terminals divided by total electrical power input (bombardment plus filament power).

† Power output at the electrodes divided by the total nuclear power input to the emitter as estimated by calorimetry.

TABLE 4.2

TYPICAL OPERATING CONDITIONS FOR SD-4
DURING OUT-OF-PILE TESTS

Typical Operating Time (hours)	100
Filament Power, watts	141
Bombardment Power, watts	705
Total Power Input, watts	846
Estimated Average Emitter Temperature, °C	1600
Average Collector Temperature, °C	650
Cesium Reservoir Temperature, °C	298
Output Current, amps	168
Voltage Drop in Emitter Lead, volts	0.101
Output Voltage (At Diode Output Terminals), volts	0.680
Output Power (At Diode Output Terminals), watts	114
Output Power Density (At Diode Output Terminals), watts/cm^2	7.60
Output Power Density (At Diode Electrodes), watts/cm^2	8.75
Overall Efficiency (Electrical Power at Terminals with no Heater Cavity Correction), %	13.5
Net Efficiency (Electrical Power at Terminals with a 60-watt Heater Cavity Correction), %	14.5
Net Design Efficiency (Electrical Power at Electrodes with a 70-watt Heater Cavity Correction), %	16.7

UNCLASSIFIED

UNCLASSIFIED

2. Initial In-Pile Test Period

During the first 25 hours of operation, the performance of the diode was steady and closely duplicated the performance observed in the 100-hour out-of-pile test. At periodic intervals during the in-pile test, diode current-voltage characteristics were determined by sweeping around the static operating point. In Figure 4.2, an in-pile I-V characteristic taken during this period is compared to one of the out-of-pile characteristics. The out-of-pile I-V curve corresponds to a measured cesium reservoir temperature of 290°C, a measured collector temperature of 670°C, and an estimated emitter temperature of 1575°C. The in-pile points (circles) correspond to a measured cesium reservoir temperature of 290°C - 305°C, a measured collector temperature of 682°C, and an estimated emitter temperature of 1575°C. The two measured cesium reservoir temperatures correspond to two different thermocouples attached to the cesium reservoir. The difference between the readings is attributed to the method of thermocouple attachment. In Table 4.3, the performance is described in more detail and compared to two subsequent operating periods. The excellent agreement between the in-pile and out-of-pile I-V characteristics strongly re-enforces the validity of the emitter temperature estimates. The agreement also indicates that the in-pile performance of diode SD-4 was virtually identical to its out-of-pile performance.

3. Third Period

After the first 25 hours of steady operation, a drop-off in power output was observed at a fixed reactor power level. The reduction in power output was accompanied by a corresponding reduction in optimum

TABLE 4.3

SUMMARY OF SD-4 REPRODUCIBILITY TESTS

Accumulated In-Pile Test Time, hours	25	1711	2614
Reactor Power Level, megawatts	2.0	2.0	2.0
Estimated Average Emitter Temperature, °C	1575	1575	1575
Average Collector Temperature, °C	680	685	682
Average Cesium Reservoir Temperature, °C*	298	299	298
Output Current, amps	150	148	149
Voltage Drop in Emitter Lead, volts	0.09	0.09	0.09
Output Voltage (At Diode Output Terminals), volts	0.70	0.70	0.70
Output Power Density (At Diode Output Terminals), w/cm^2	7.00	6.92	6.96
Output Power Density (At Diode Electrodes), w/cm^2	7.90	7.80	7.85
Estimated Input Power, watts	780	770	760
Overall Efficiency,† %	13.4	13.4	13.7

* This temperature is the average of the two thermocouples on the cesium reservoir.

† Power output at the terminals divided by the total nuclear heat generated in the fuel.

UNCLASSIFIED

UNCLASSIFIED

cesium reservoir and collector temperatures and by a shift of the diode ignition voltage to lower levels. The emitter temperature was obviously going down. The reduction in emitter temperature continued for about 75 hours and then started to recover. After 300 hours of in-pile operation, the diode output had recovered to within about 85% of its initial level. After 600 hours, the recovery in emitter temperature and output was essentially complete.

It is apparent that some heat loss mechanism existed during this period which prevented the emitter from receiving its "normal" fraction of the heat generated in the fuel. The "normal" fraction is defined here as that fraction which it received prior to and after the reduced emitter temperature test period. This normal fraction is about 98%, the 2% loss being caused by thermal radiation out of the cavity. Of course, of the heat reaching the emitter, a significant fraction is conducted and radiated from the emitter support sleeve. One possible mechanism for the additional heat loss could have been conduction from the fueled-emitter and its support sleeve through gases present in the cavity. Although accurate analytical predictions of such heat losses in the cavity would be extremely complicated, approximate calculations indicate that heat losses of a few hundred watts might occur if air or nitrogen were present at tens of millimeters of pressure.

A likely source of gas could have been the outgassing of the nickel plug which was used to close the gun cavity after out-of-pile operation was completed. Since the nickel closure plug was not exposed to the diode interior, it was not thoroughly outgassed at a temperature above its expected operating level. When the diode began

operation in-pile, gamma heating plus conduction from the emitter sleeve raised the temperature of the nickel to an estimated 800°C. Extensive outgassing undoubtedly occurred, causing the pressure in the sealed cavity to rise substantially. This gas could have been removed eventually from the cavity by the "gettering" action of the emitter support ring, which is made of well-outgassed molybdenum. Removal of the gas could have corresponded to the recovery in emitter temperature.

The gas might have been due to another source, communication between the cavity and the environment surrounding the diode. If a leak developed in the closure plug weld or in one of its brazes, gas could have entered the cavity from the capsule tube region. This possibility is enhanced by the fact that the pressure in the tube increased rapidly at the beginning of the in-pile operation and recovered rapidly after about 300 hours of operation. The initial surge in pressure was due to outgassing of the sheathed heater leads and other components in the tube, and the recovery in pressure resulted from the pumping action of the zirconium getter located at the bottom of the tube. The pressure gauge in the tube had a full scale reading of 25 microns. Within 25 hours, the needle on the pressure gauge went off-scale and did not come back on-scale until the 300-hour point. The close correspondence of this pressure transient with the emitter temperature transient suggests that they may have been related.

Regardless of the cause, there is no doubt that the temporary reduction in output power was due to a reduction in emitter temperature. If the diode had undergone degradation of emitter surface properties, the optimum cesium temperature would have increased rather than decreased. Furthermore, the complete recovery of the output and

all other diode temperature parameters essentially eliminates any effect other than a transient emitter heat loss. As additional confirmation, a test was performed during this period to show that the full output could be recovered by increasing the emitter temperature. This was accomplished by operating at a static point corresponding to terminal output voltage of 0.8 volt instead of 0.7 volt. The I-V sweep curves obtained at each condition are shown in Figure 4.3. The difference in the average current between the sweep curves is 18 amps, which corresponds to a difference in electron cooling of about 50 watts. Based on out-of-pile parametric results, this 50-watt difference corresponds to a difference in emitter temperature of about 35°C. The electrode power density for curve "A" at a terminal output voltage of 0.7 is 7.9 w/cm^2, instead of 7.0 w/cm^2 for curve "B". The 7.9 w/cm^2 is equal to the power density obtained under static conditions prior to and after the emitter temperature transient. Thus, by increasing the emitter temperature by 35°C, full output power density was recovered.

4. Fourth Period

As mentioned previously, the diode output had completely recovered by about the 600-hour point. The power input and power output remained essentially constant for about the next 200 hours. At the 760-hour point, the reactor power level was reduced to accommodate another experiment in the reactor. This reduced reactor power level was maintained until the 1400-hour point, when the other experiment was withdrawn from the reactor. The reduced reactor power resulted in a reduction in diode input power of about 30 watts

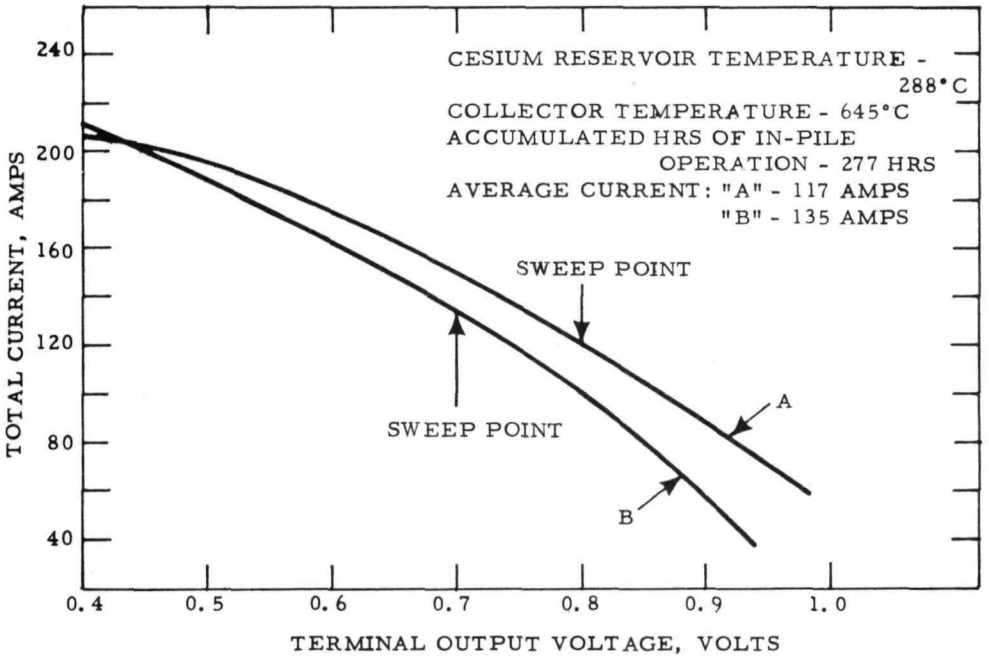

Figure 4.3 I-V Sweep Data During Emitter Temperature Transient.

and a corresponding reduction in diode output power of about 9 watts. The diode output power density at the electrodes averaged about 7.3 w/cm^2 during this period.

5. Fifth Period

After the reactor power was restored to its normal level, a constant power test period of over 1200 hours was accomplished. The average electrode power density during this time was about 8 w/cm^2, and the overall efficiency varied from about 13.5% to 14%. The diode characteristics remained very constant except for a slight improvement in overall efficiency with increasing time. At the 2615-hour test point, the diode was removed from the reactor to permit modifications to be made to the reactor.

At about the 1700- and 2600-hour points, experiments were performed to examine the diode characteristics very carefully for traces of degradation. At each point, the cesium reservoir temperature, the collector temperature, and the power input were set at the same levels as existed at the 25-hour point. Both static and sweep data were taken at each point. The results of the static experiments are summarized in Table 4.3. The reproducibility of the three points is quite remarkable, the only noticeable change being a slight improvement in overall efficiency. Since there is some uncertainty in the determination of input power, this improvement is probably not significant.

6. Sixth Period

When the reactor was restarted at the 2615-hour point after the three-month shutdown, the diode returned to its former performance

level. Since the reactor fuel elements had been reshuffled, some uncertainties existed in neutron and gamma flux levels and distributions. A period of several days was required to re-establish equilibrium. After stable operation was restored, at about the 2800-hour point, the diode output and input were slightly higher. The only significant change in conditions was a 12°C increase in the optimum indicated cesium reservoir temperature. Since the cesium reservoir thermocouples are only mechanically attached, their position could have been shifted by handling of the capsule during the reactor modifications. Consequently, it is not certain that a 12°C change in actual cesium reservoir temperature did occur. As is evident in Figure 4.1, the collector temperature also increased by about 20°C. In Figure 4.2, the data points taken from sweep measurements at 3110 hours and 4300 hours are shown with previous results. The striking reproducibility of all the data points strongly suggests that no significant changes in diode operating conditions or performance have occurred. This stable operation continued until the cesium reservoir heater failed at the 6100-hour point.

7. Seventh Period

After remote attempts to repair the cesium reservoir heater were unsuccessful, the water coolant surrounding the collector was replaced with Dowtherm "A", an organic liquid capable of higher operating temperatures. Since the cesium reservoir is connected to the cooling jacket through two copper straps, the increased temperature of the cooling jacket resulted in higher cesium reservoir temperatures. Control of the cesium reservoir temperature was achieved by varying the flow rate and inlet temperature of the Dowtherm.

Operation of the diode for the seventh test period was resumed using this control technique, which proved quite adequate. However, during startup and early operation of the seventh period, the collector thermocouples indicated absurdly low temperatures. After about twenty hours, the indicated temperatures increased but still were about 60°C lower than the previous data. Since the reactor power level and core position were unchanged, it is assumed that the difference was caused by movement of the thermocouples within the test capsule. This movement could have been caused by the higher pressures within the coolant tubes, resulting from the higher pressure drops necessary with Dowtherm as compared with water. Since the input power measurements are based upon the measured temperature differences between the collector and the coolant jacket, no input power or efficiency estimates were made beyond the 6103-hour point.

During the first few hundred hours of the seventh test period, an increase was noted in the thermal impedance between the coolant and the cesium reservoir. To offset this increase, the Dowtherm flow rate was increased, thus lowering the coolant jacket temperature, and thereby the cesium reservoir temperature. At about the 6360-hour point, the impedance had increased enough to permit water to be used instead of Dowtherm as the coolant. Accordingly, the Dowtherm was flushed out of the lines and replaced by water, and operation was continued until the 7327-hour point. During the last few hundred hours, the pressure drop in the water coolant system increased appreciably. Eventually, the pressure drop caused too great a reduction in flow rate to permit safe operation. Therefore, testing was stopped to examine the condition of the coolant lines and system. A carbon-type

scale was found in the water coolant, which was causing clogging of the flow passages. Apparently, this scale was created by radiation damage to the residual Dowtherm left in the system after it was flushed with water. Several attempts were made to remove this scale. Reverse flushing with water and soaking and flushing with acetone were performed alternately for several weeks. Finally enough scale was removed to allow the original flow rate to be restored, and operation of the converter was resumed. Except for the problems with the flow rate and the collector thermocouples, the performance of the diode was quite stable throughout the seventh test period. The electrode power density averaged about 8 watts/cm^2, with fluctuations of $\pm$ 1 watt/cm^2. These fluctuations were caused by day-to-day changes in reactor power level and in cesium reservoir temperature.

8. Eighth Test Period

The eighth and final test period ran from the 7327-hour point to the 8125-hour point. Dowtherm was used initially as the coolant, and control of cesium pressure was achieved by varying the Dowtherm flow rate. As before, fouling of the coolant jacket surface gradually occurred due to decomposition of the Dowtherm. Eventually this fouling caused a very high pressure drop and consequent reduction in flow rate. At about the 7890-hour point, the Dowtherm was replaced by water to reduce the coolant jacket temperature, and thereby the cesium reservoir temperature. This permitted an additional 235 hours of testing before the clogging became too great to keep the cesium reservoir temperature down to acceptable levels. After further

attempts to unclog the coolant passages were unsuccessful, the diode was removed from the reactor for hot cell examination. As can be seen in Figure 4. 1, the performance of the diode was normal throughout this test period. During the last 65 hours the clogging caused the cesium temperature to be well above its normal level, and therefore caused a slight reduction (~15%) in the converter output. However, the reduction was about that expected for such off-optimum cesium reservoir conditions.

CHAPTER 5
HOT CELL EXAMINATION SUMMARY

A. INTRODUCTION

This section summarizes briefly the results of the hot cell examination which was conducted by BMI following the 8125 hours of in-pile operation. The complete BMI report covering this portion of the work is included in Appendix B.

B. SUMMARY OF FINDINGS

The findings of the hot cell examination are summarized as follows.

1. Fission Gas Release

Gas sampling of the sealed vacuum capsule in which the diode had been irradiated showed the presence of fission gas in the capsule. The sampling was performed utilizing a Toepler pump to transfer the gas from the capsule to an evacuated collection system of known volume. Samples were then removed from the collection system and analyzed by mass spectroscopy for total krypton and xenon. The amount of krypton and xenon released (6.7 cm^3) was approximately 80% of the amount formed during irradiation, as calculated from burnup obtained by isotopic analysis.

2. Dimensional Stability

The diode was disassembled and the emitter neutron radiographed and dimensioned by micrometer. The fueled area of the emitter had experienced a slight amount (2.7 percent average on the

external diameter) of swelling. This is approximately 0.006 to .007 inch of radial expansion, or about one half the initial interelectrode spacing. The swelling was greatest, about 3%, at the bottom of the emitter and least, about 1.7%, at the top of the emitter adjacent to the sleeve or electrode lead.

3. Fueled Emitter Examination

Figures 5.1 and 5.2 show the condition of the irradiated fuel from SD-4 versus the unirradiated fuel from SD-2 which was operated 2500 hours with electrical heat. As can be seen, the irradiated fuel particles have more porosity and larger cracks than do the unirradiated particles. Figures 5.3 and 5.4 show composites of an axial section and a radial section of the fuel and emitter with higher magnifications of selected areas.

Figure 5.3 shows deposition of the UO_2 at the top of the inner tungsten fuel liner, which was severely cracked over its whole length. This deposition also occurred at the bottom of the liner. These cracks, plus a leak which developed in the gas sampling tube at the top of the emitter cavity, allowed the fission gas to escape from the fuel to the in-pile capsule. The liner did, however, effectively prevent excessive fuel loss by vaporization. Figure 5.4 shows an axial cross-section of the fueled emitter.

Figure 5.5 is a highly magnified view of the void area in Figure 5.4. It shows that the UO_2 in this area has taken on a columnar grain structure. It is thought that most of the redistributed UO_2 at the ends came from areas such as this. The reason for the nucleation

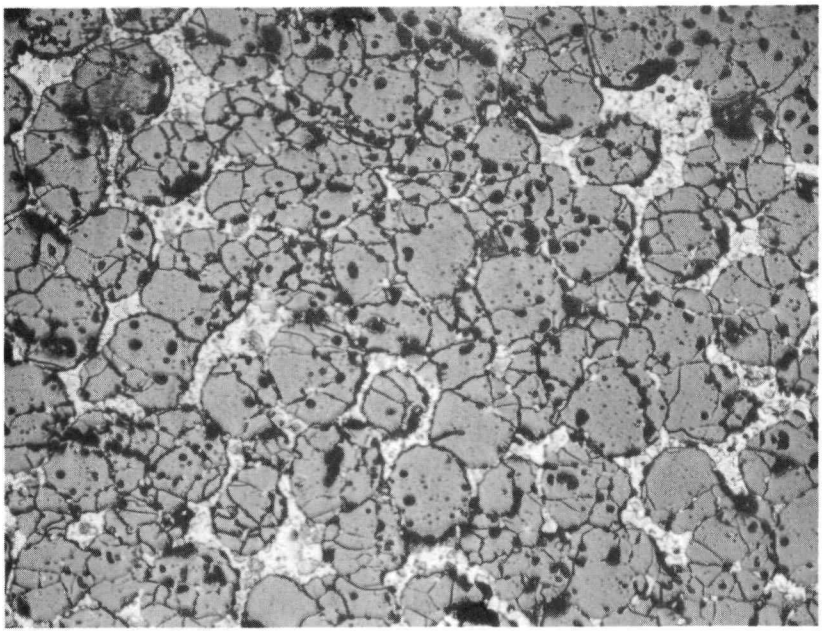

100X HC21572

SD-4: Irradiated

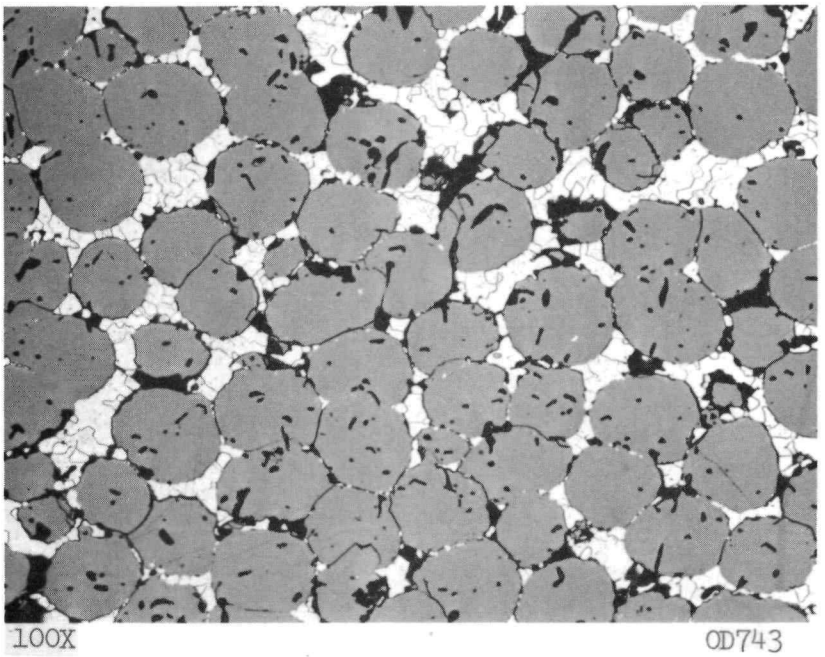

100X OD743

SD-2: Unirradiated

Figure 5.1 Microstructures of Fuel in Irradiated SD-4 and Unirradiated SD-2 Diodes.

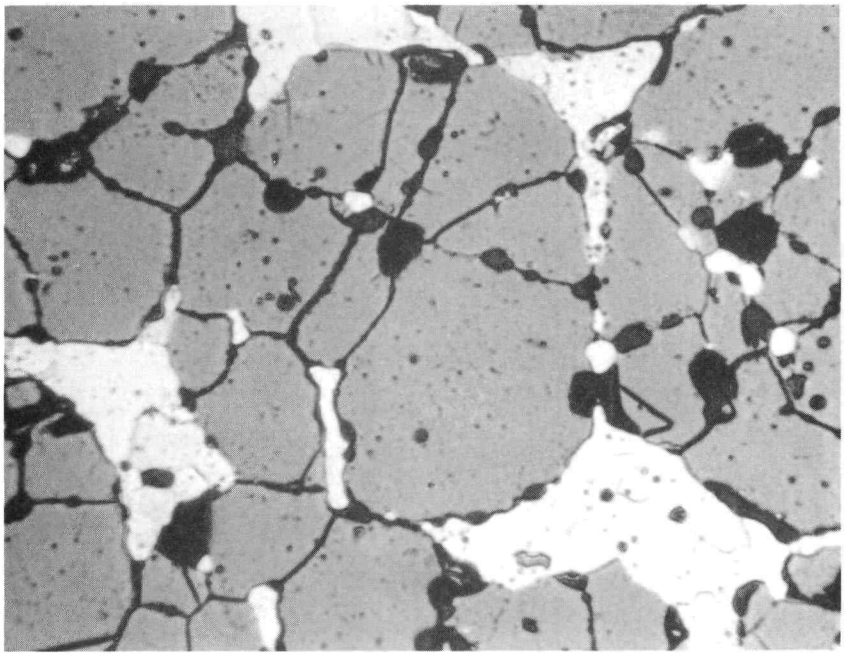

500X HC21581

SD-4: Irradiated

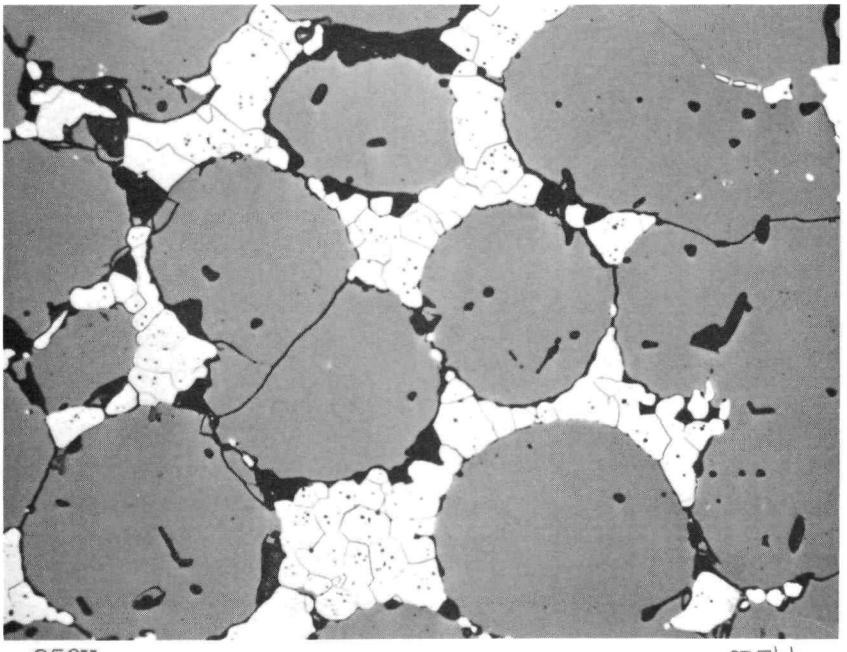

250X OD744

SD-2: Unirradiated

Figure 5.2 Microstructures of Fuel in Irradiated SD-4 and Unirradiated SD-2 Diodes.

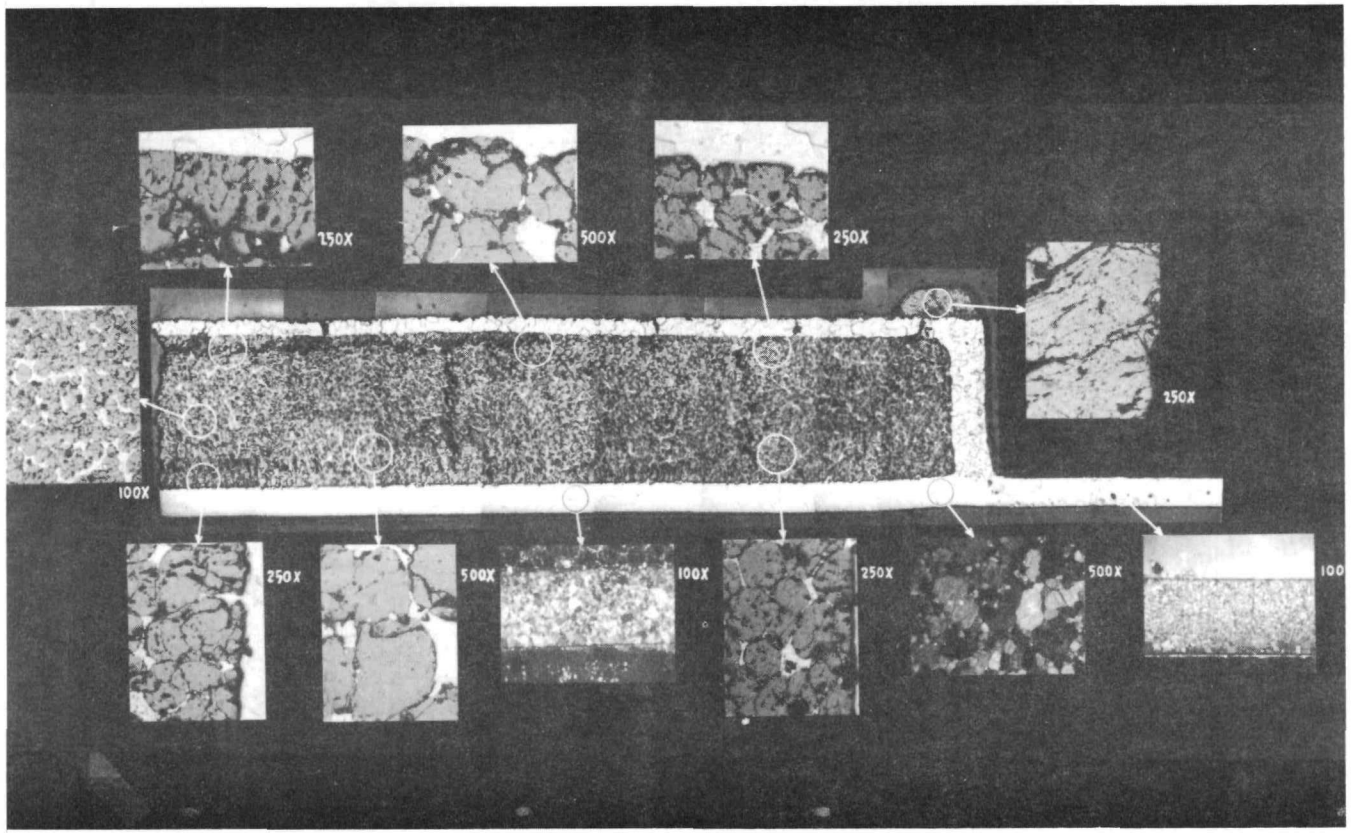

Figure 5.3 Composite Photographs of Longitudinal Section Through Top Half of Emitter.

CONFIDENTIAL

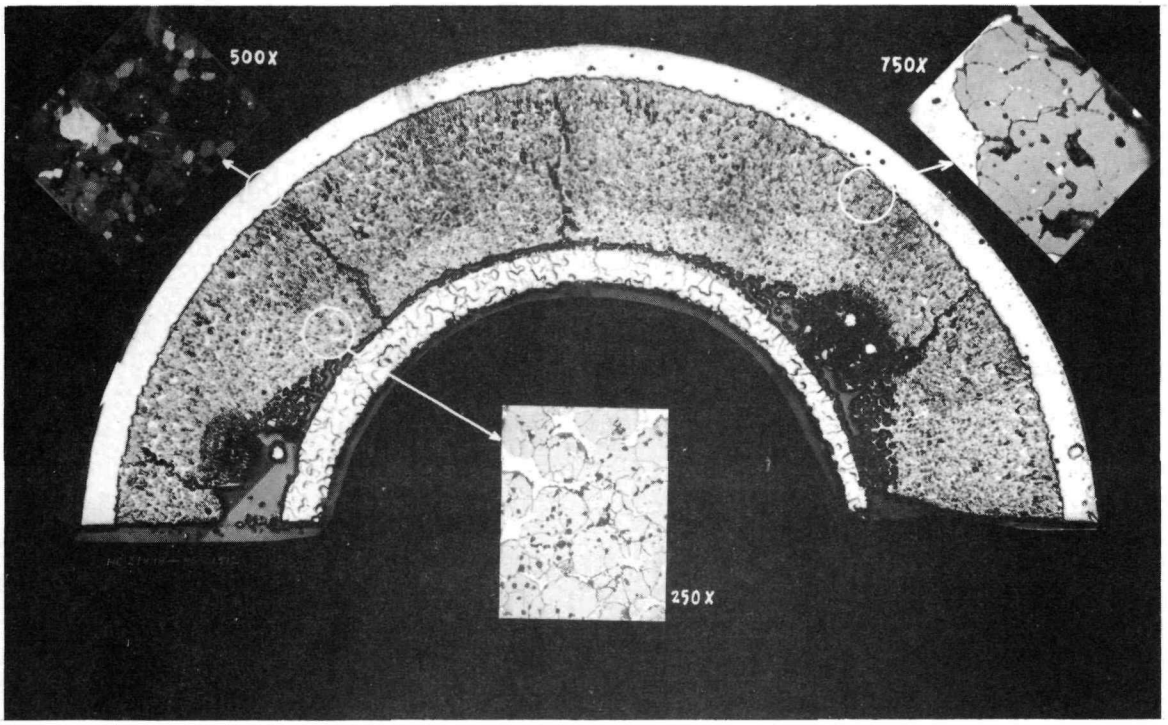

Figure 5.4 Composite Photographs of Transverse Section near Axial Center of Emitter.

CONFIDENTIAL

CONFIDENTIAL

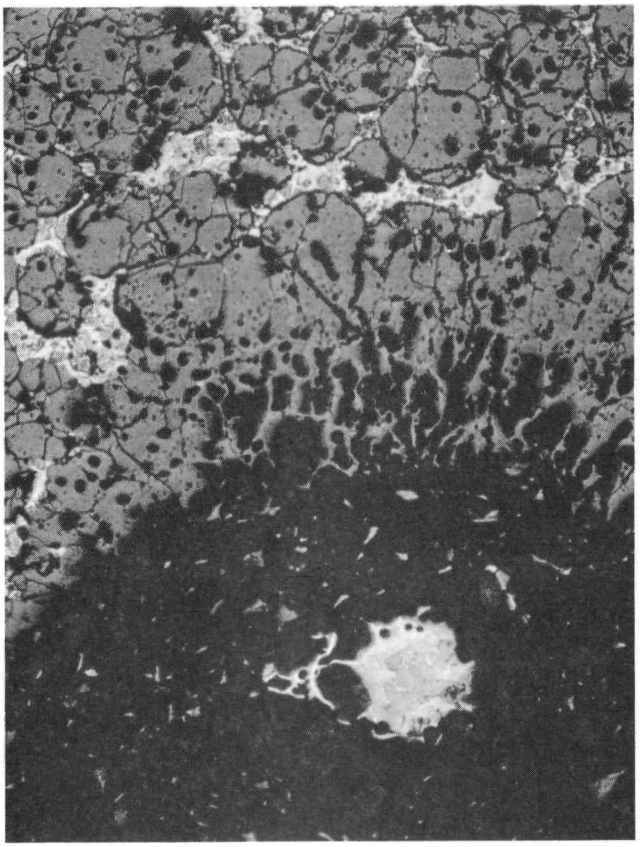

100X HC21569

Figure 5. 5 Apparent Hot Spot in Fuel Near Inner Clad-Core Interface.

CONFIDENTIAL

of these localized apparent high temperature areas has not been established. The white inclusions in this zone were found by autoradiography not to be a fission product alloy.

Figure 5.6 shows the microstructure of the rhenium emitter in several areas. In general, the grains at the emitting surface were much larger than the grains in the interior of the clad and at the clad-fuel interface. Also, the grain size in the interior of the clad and at the clad-fuel interface is much larger in the fueled area of the emitter than in the unfueled area. The grain size at the emitting surface, however, does not appear significantly different in the fueled area of the emitter than in the unfueled area. Machining of the rhenium resulted in cold-working the outer surface layer of metal, which provided a driving force for recrystallization and grain growth on the whole surface during a subsequent high temperature anneal to stabilize the surface treatment. Grain growth to a lesser extent occurred in the unworked interior rhenium opposite the fuel. Little or no grain growth occurred in the unworked interior rhenium in the unfueled area of the emitter.

4. Diode Structure Examination

The niobium collector of SD-4 had been coated with molybdenum by vacuum evaporation during construction of the diode. Figure 5.7 shows this molybdenum layer after irradiation. Although the thickness and uniformity of this layer before irradiation was not measured, it appears that after irradiation the molybdenum layer is very uniform and about 0.4 mils (10 microns) thick. There is no evidence of any

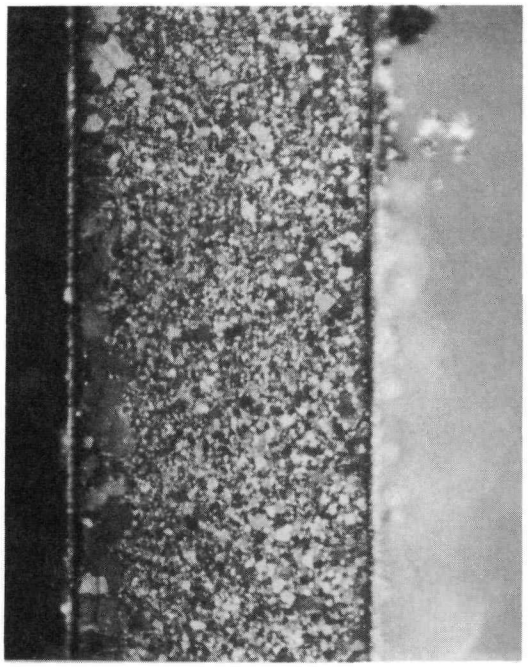

100X

(a) Above the fueled area

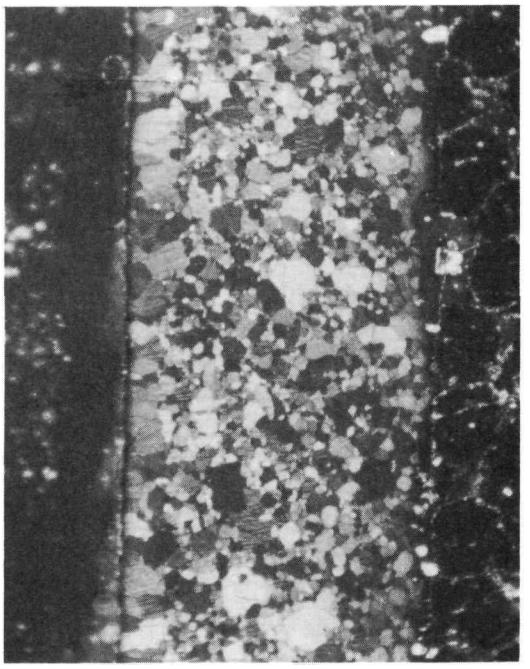

HC21592

(b) Near the top of the fueled area

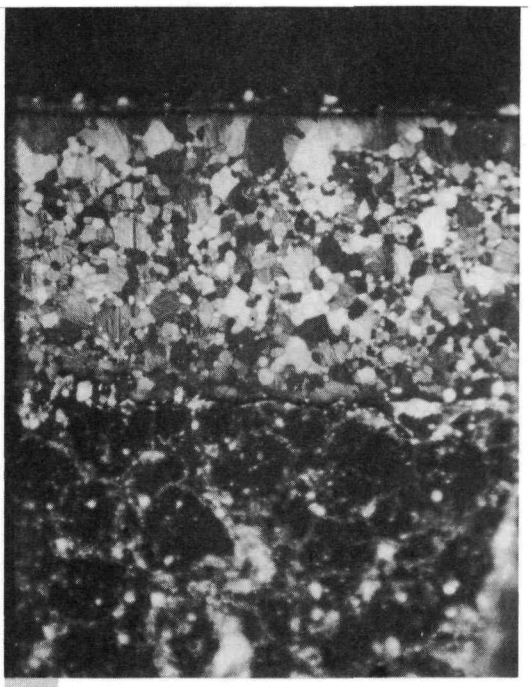

100X

(c) Near the center of the fueled area

HC21600

(d) Near the bottom of the fueled area

Figure 5.6 Representative Microstructures of the Rhenium Clad (Emitter) - Polarized Light.

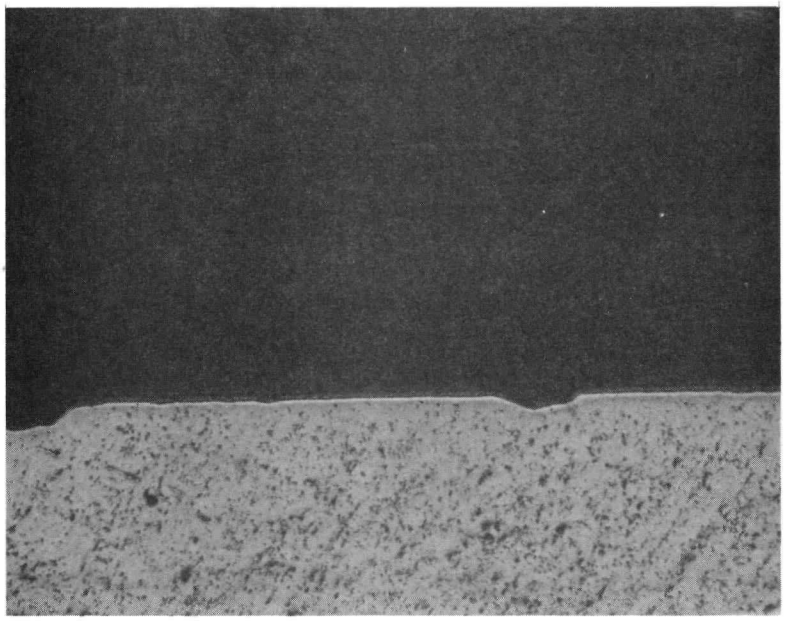

(a) As polished with oblique lighting

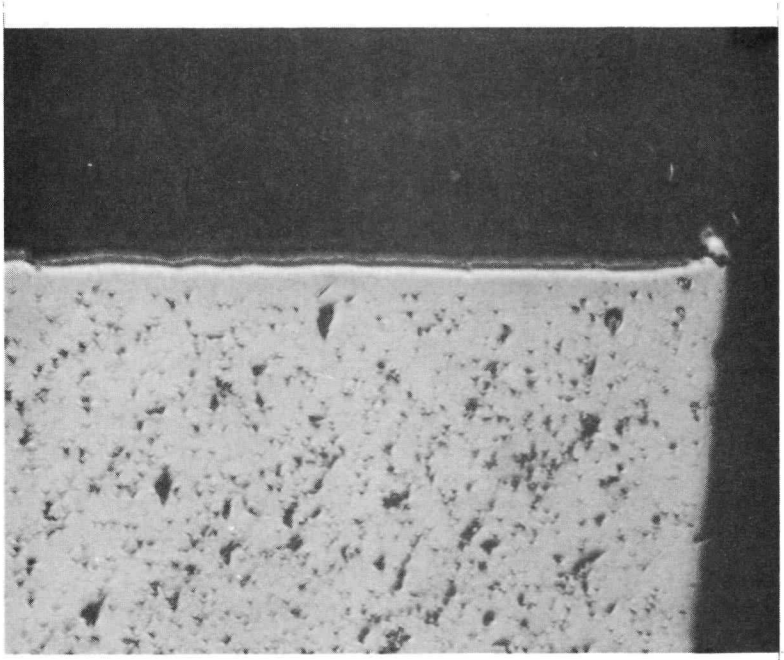

(b) As polished with oblique lighting, cut surface is at right.

Figure 5.7 Vapor-Deposited Layer of Molybdenum on the Niobium Collector Surface.

reaction or corrosive attack to this surface. Figure 5.8 shows several areas of the brazes in the collector, the collector heaters, and heat exchanger. These brazes appear unaffected by the irradiation.

The diode insulator was Al 300 alumina (97% Al_2O_3) metallized and copper-nickel brazed. After irradiation, the resistance of the insulator at ambient temperature was 510 ohms. After surface cleaning with a wire brush, the resistance increased to 3200 ohms.

Figure 5.9 shows the irradiated alumina insulator from SD-4 versus the unirradiated insulator from SD-2.

Table 5.1 shows microhardness data from the insulators from SD-2 and SD-4. The irradiated material shows a slightly higher hardness, but not significantly so.

5. Burn-up Analysis

The burn-up sample was a complete circular cross section of the fuel about 1/4 inch long, removed from the axial center of the emitter. The rest of the emitter was sectioned longitudinally and one-half of each of the upper and lower sections were used for longitudinal metallographic samples; the remaining two were used for transverse samples.

The SD-4 irradiated fuel sample for burn-up determination was sent to Idaho Nuclear Corporation along with an unirradiated specimen, SD-2, for uranium isotopic analysis. The results of this analysis are:

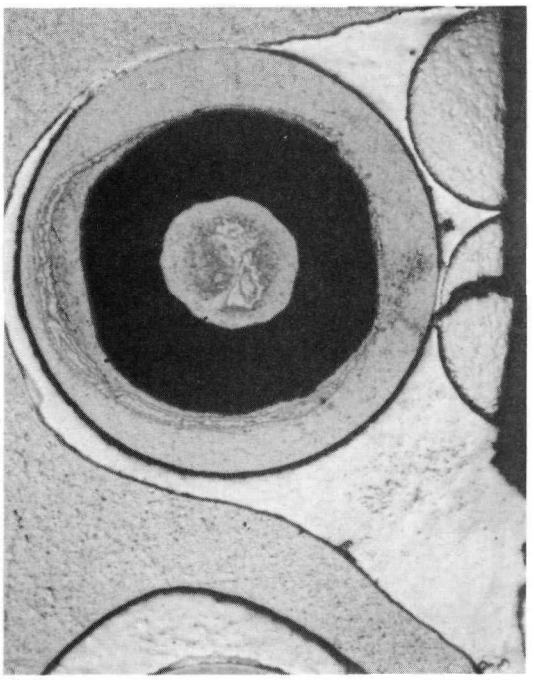

40X HC21624

(a) Heaters and braze area

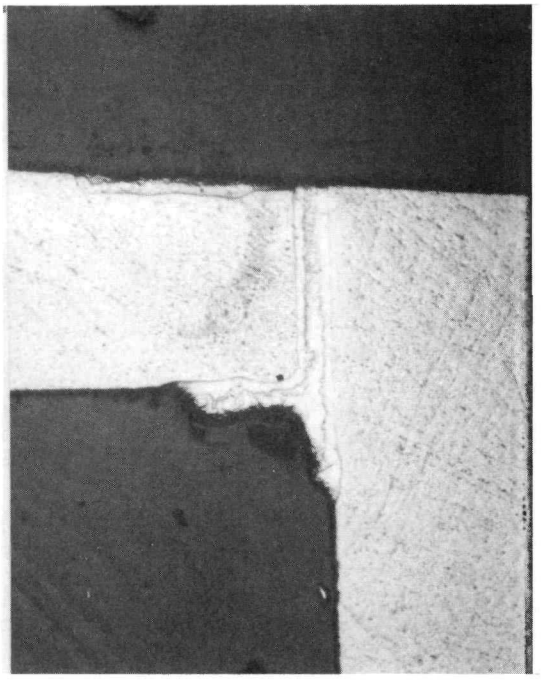

40X HC21622

(b) Heat choke fin braze to heat exchanger

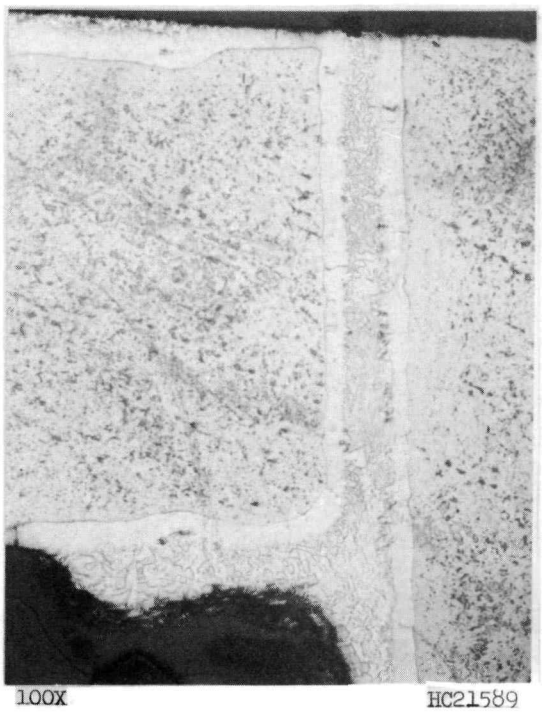

100X HC21589

(c) Heat choke fin braze to heat exchanger

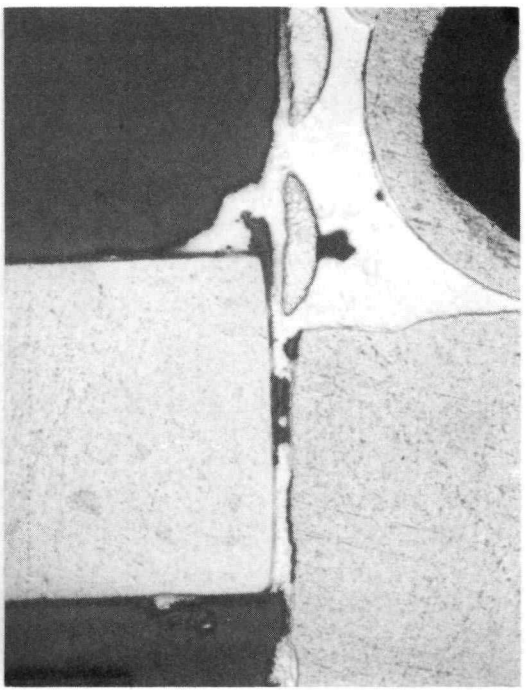

40X HC21623

(d) Heat choke fin braze to collector

Figure 5.8 Microstructures of Representative Areas of the Heat Exchanger.

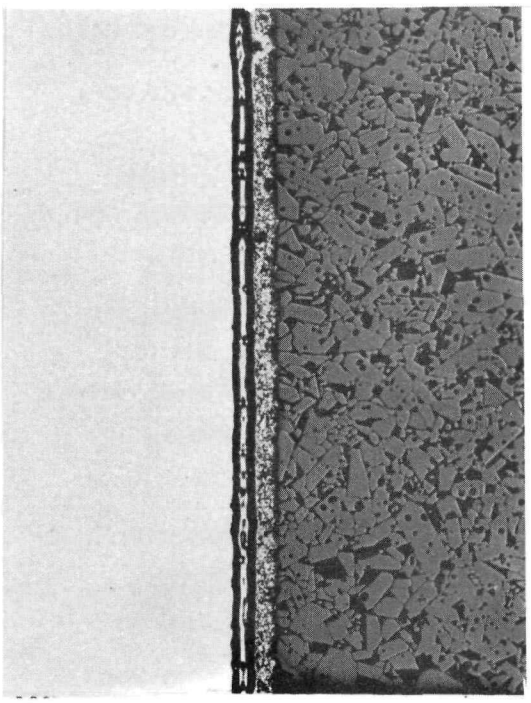

(a) Out-of-pile Diode, SD-2

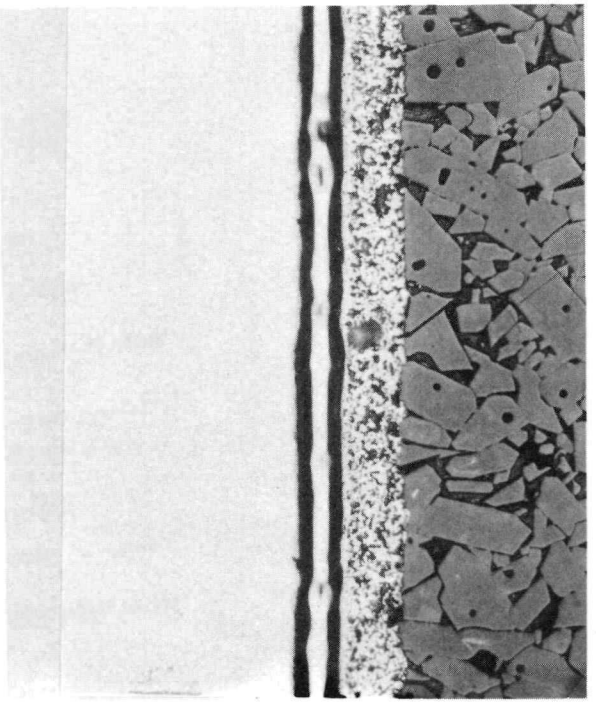

(b) Out-of-pile Diode, SD-2

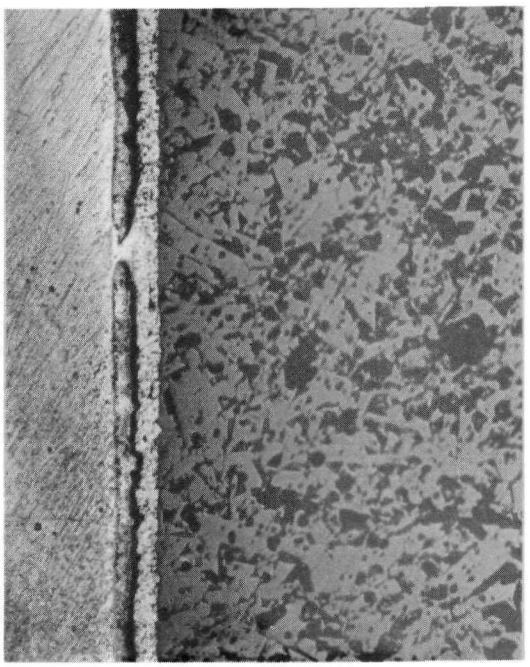

(c) In-pile Diode, SD-4

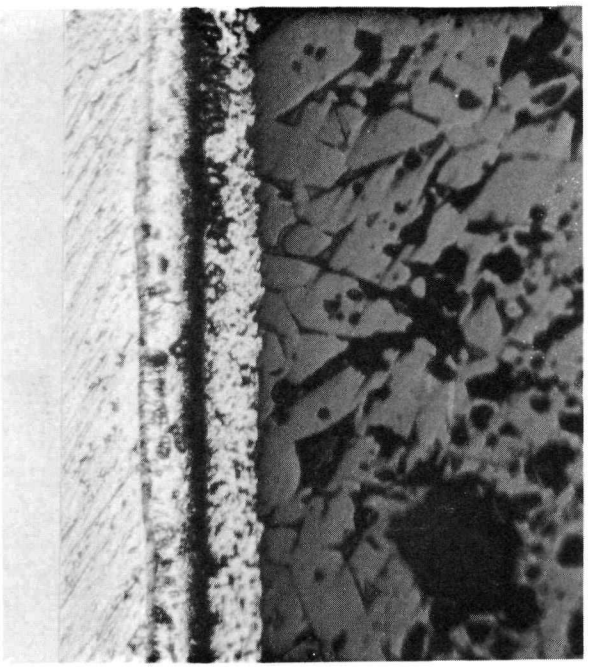

(d) In-pile Diode, SD-4

Figure 5.9 Comparison of Ceramic Insulators Used in Out-of-Pile and In-Pile Diodes.

TABLE 5.1

KNOOP MICROHARDNESS MEASUREMENTS ON THE CERAMIC INSULATORS FROM SD-2 AND SD-4

Sample Condition	Sample Number	Knoop Hardness Number	
		100 gm load	5 kg load
Unirradiated (SD-2)	1	1098	908
	2	1390	1176
	3	1162	870
	ave.	1217	985
Irradiated (SD-4)	1	1186	931
	2	1266	898
	3	1288	1217
	ave.	1247	1015

	Fraction of Isotope Present, W/O			
	U^{234}	U^{235}	U^{236}	U^{238}
SD-2 unirradiated	1.01	93.02	0.21	5.76
SD-4 irradiated	1.02	92.46	0.64	5.88

The burn-up was calculated from the relationship:

$$\text{Burnup} = 100\left(\frac{R_{6/5} - R^{\circ}_{6/5}}{\frac{\alpha}{1+\alpha} + R_{6/5}}\right)$$

where:

$R_{6/5}$ = ratio of post irradiation fractions of U^{236} to U^{235}

$R^{\circ}_{6/5}$ = ratio of preirradiation fractions of U^{236} to U^{235}

α = ratio of the cross sections for fission and capture of $U^{235} = 0.185 \pm 0.004$

The burn-up values calculated using the above methods along with estimated burn-ups determined by calorimetry measurements during irradiation are given in Table 5.2. The burn-up calculated from isotopic analysis is based on one segment of the fuel, while the calorimetry measurements give an average for the whole fuel emitter assembly.

C. CONCLUSIONS

1. The UO_2-fungsten cermet fuel released 80% of its fission gas.
2. The fission gas escaped from the diode through the cracked gas sampling tube.
3. There was some loss of UO_2 through the cracked tungsten inner liner.

TABLE 5.2

BURN-UPS OBTAINED FROM ISOTOPE ANALYSIS

	Burn-up a/o U-235 Fissioned	Burn-up 10^{20} Fissions/cm^3
Isotopic Analysis	2.74	3.85
Calorimetry	1.70	3.09

4. There was a 2 to 3% increase in outside diameter of the fueled emitter, which was not enough to affect significantly the rhenium emitter performance at the operating temperature of about 1600° C.

5. There was only slight grain growth in the interior of the rhenium emitter along the fueled zone, and no significant difference in grain growth at the surface of the rhenium emitter between the fueled zone and the unfueled zone. This indicates that the rhenium surface was stabilized by the preirradiation treatments.

6. The vacuum-deposited molybdenum surface layer on the niobium collector was apparently unaffected by the irradiation.

7. The diode structural welds and brazes were apparently unaffected by the irradiation.

8. The alumina insulator was not significantly affected by the irradiation.

CHAPTER 6

ELECTRICAL TESTING OF SD-2 PROTOTYPE DIODE

A. INTRODUCTION

The SD-2 diode was the first converter built under this program. Its purpose was to demonstrate that the basic converter structure and the fueled emitter to be used on SD-4 would be capable of stable and sustained operation. In addition, it provided both prototype testing for the SD-4 diode structure and thermal and electrical performance data required to confirm the design characteristics of the in-pile diode, SD-4.

B. ASSEMBLY AND PROCESSING

The SD-2 was assembled according to the design shown in Figure 6.1. The diode used an emitter identical to that used in SD-4. The diode design was also the same, except for minor changes in the cesium reservoir, in the coolant inlet tubes, and in the location of the thermocouple.

The diode was outgassed for 30 hours at temperatures well above expected operating levels. During the outgassing of the emitter, a temperature gradient of nearly 200°C was indicated by the emitter thermocouples. Since the internal pressure of the diode chamber was quite insensitive to changes in emitter temperature, no attempt was made to raise all areas of the emitter to the peak temperature of 1900°C. Thus the indicated emitter outgassing temperature ranged from 1700°C to 1900°C. As will be mentioned in the next section, the accuracy of these temperature measurements is in doubt. After outgassing, the diode was installed into the test stand, as shown in Figures 6.2a and 6.2b.

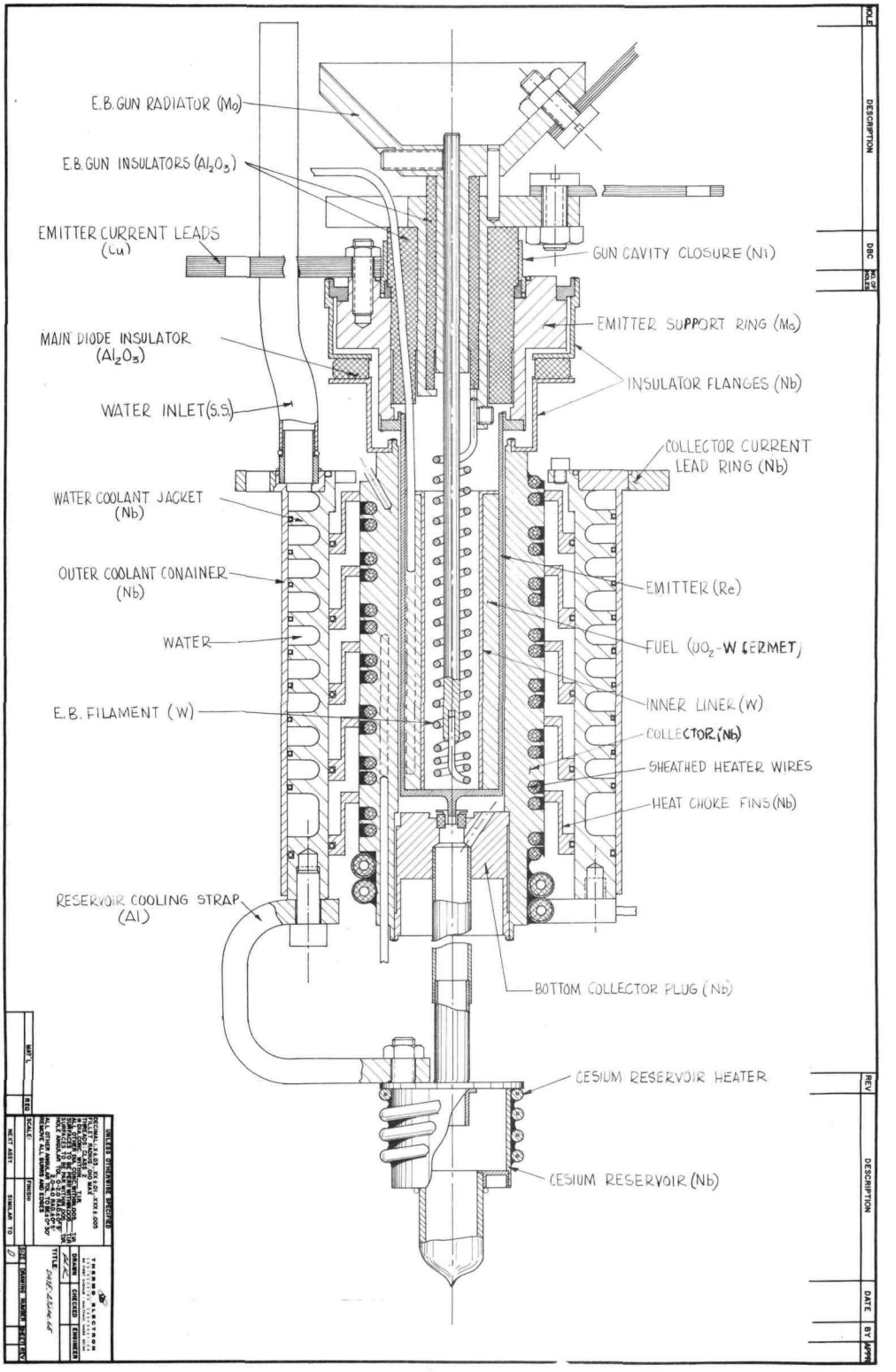

UNCLASSIFIED

Figure 6.1 SD-2 Electrically Heated Diode

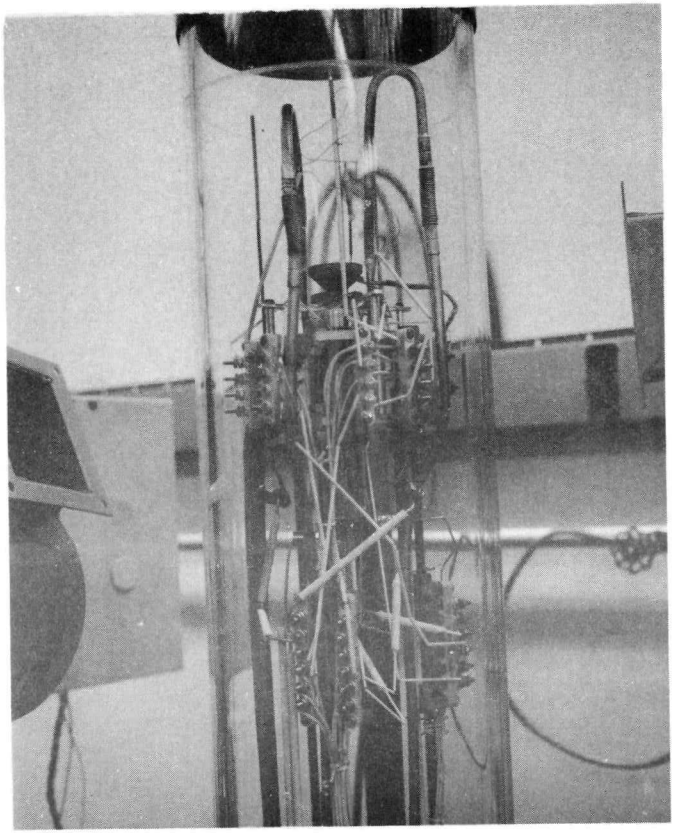

Figure 6.2.a. Diode SD-2 in Test Stand

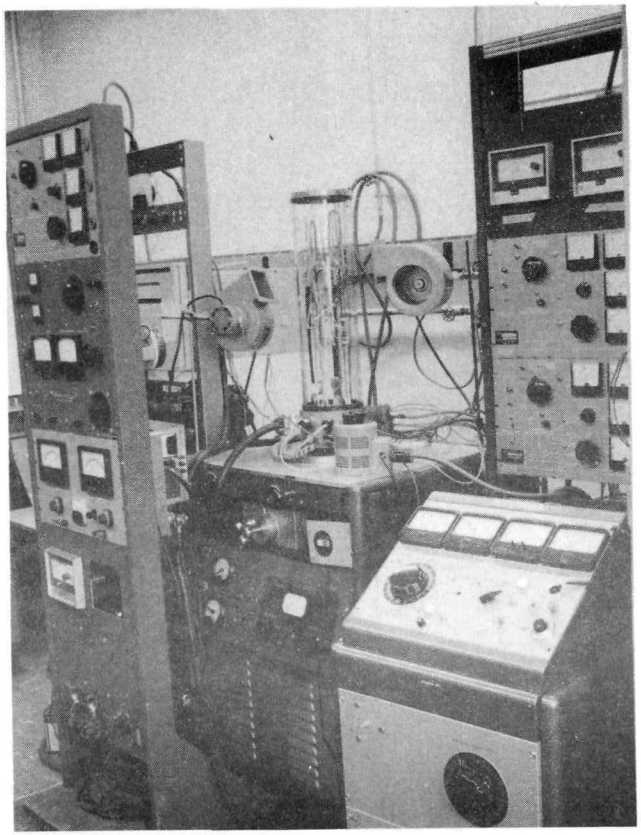

Figure 6.2.b. Diode SD-2 in Test Stand

UNCLASSIFIED
77
UNCLASSIFIED
8851

C. TESTING

The initial testing period covered 96 hours and consisted of parametric performance measurements at emitter temperatures in the range of 1300°C to 1500°C. When unattended (such as overnight), the diode was run at a fixed power input at output power levels between 4 and 5 watts/cm^2 and at an efficiency of about 10%. Figure 6.3 shows typical performance data obtained during this period. The emitter thermocouples indicated that the shallow end of the emitter was operating about 150°C above the rest of the emitter. Since this gradient precluded the possibility of obtaining complete and meaningful performance maps, the diode was shut down to replace the filament and examine the emitter thermocouples.

In attempting to remove the deep thermocouple, the thermocouple broke off at the edge of the fuel cylinder. The center thermocouple was also stuck in the fuel and could not be removed, but was not damaged. The shallow thermocouple was removed and replaced with a newly-calibrated thermocouple consisting of a two-holed Al_2O_3 tube enclosed in 0.001" molybdenum foil to prevent possible interaction between the Al_2O_3 and the cermet fuel. A new filament was wound with fewer turns at the shallow end. The original filament is shown in Figure 6.4.

Using the new filament and the shallow and middle emitter thermocouples, operation of the diode was resumed. No appreciable change in emitter temperature distribution was observed after operating temperatures were reached. It was noticed, however, that some change in temperature distribution could be achieved by variations in filament current. Higher filament currents tended to make the

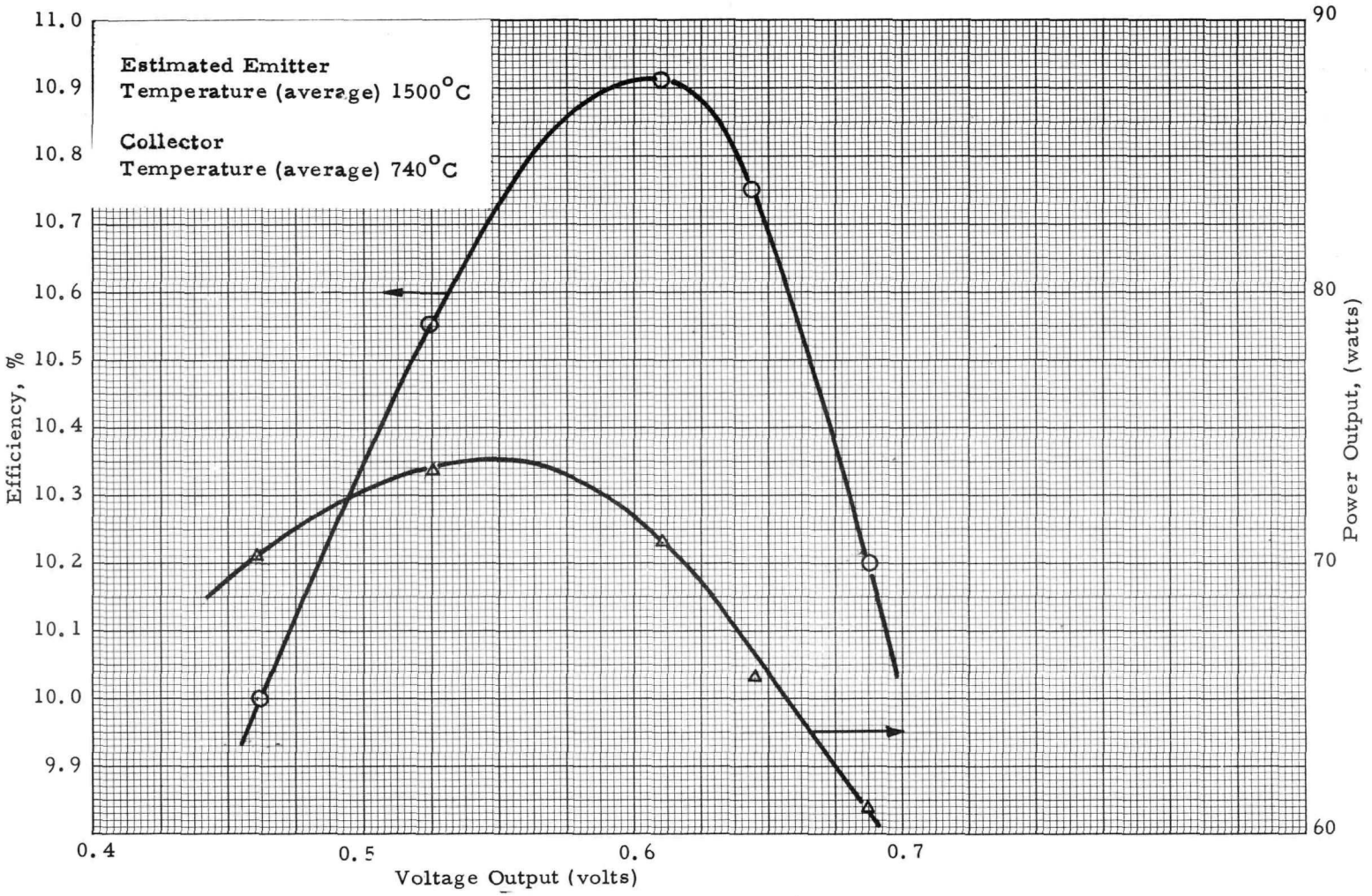

Figure 6.3. Typical Performance Data for Diode SD-2.

shallow end of the emitter relatively higher in temperature. While the diode was operated at an unattended fixed power level of about 4.5 watts/cm^2 for 160 hours, a further investigation of emitter temperature distributions was carried out on a dummy emitter test setup.

In the test setup shown in Figure 6.5, a number of filaments were used to heat a dummy tantalum emitter which was an exact dimensional mockup of the fueled emitter in the diode. A filament consisting of one full turn at the deep end and several compact turns at the shallow end produced an emitter temperature difference of less than 20°C at 1650°C. The diode was then shut down and this filament was installed. When the diode was restarted, the indicated temperature difference over the emitter was worse than before. The shallow and middle thermocouples indicated a temperature difference of about 200°C at an average temperature of 1550°C. After operating at a power output of about 4 watts/cm^2 for 16 hours, a high voltage arc caused an abrupt loss of input power.

While the diode was shut down, the top emitter thermocouple was replaced by a newly-calibrated thermocouple consisting of a two-holed BeO ceramic tube containing W-Re wires and enclosed in 0.001" molybdenum foil. The filament which replaced the original filament was re-installed. When operation was resumed, an emitter temperature variation of 140°C was measured by the middle and shallow thermocouples. Because of program schedule requirements, further temperature profile investigations were not carried out.

3

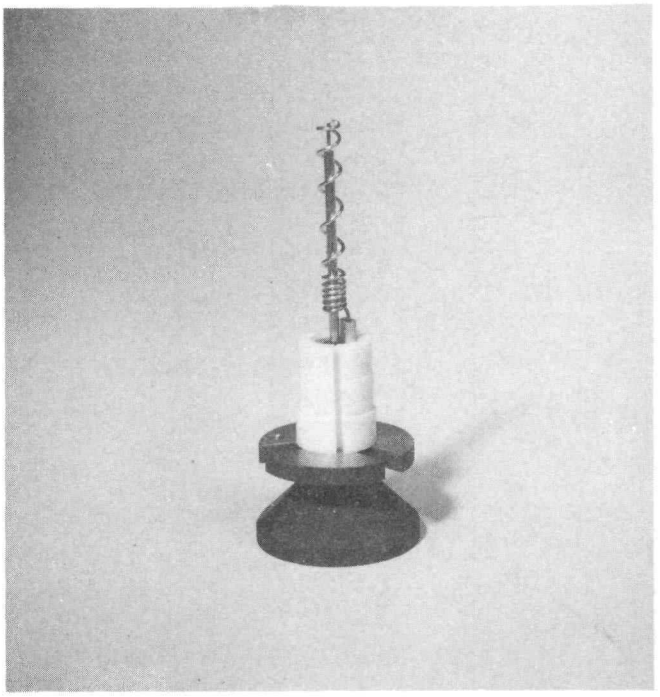

Figure 6.4. Filament Used in Diode SD-2

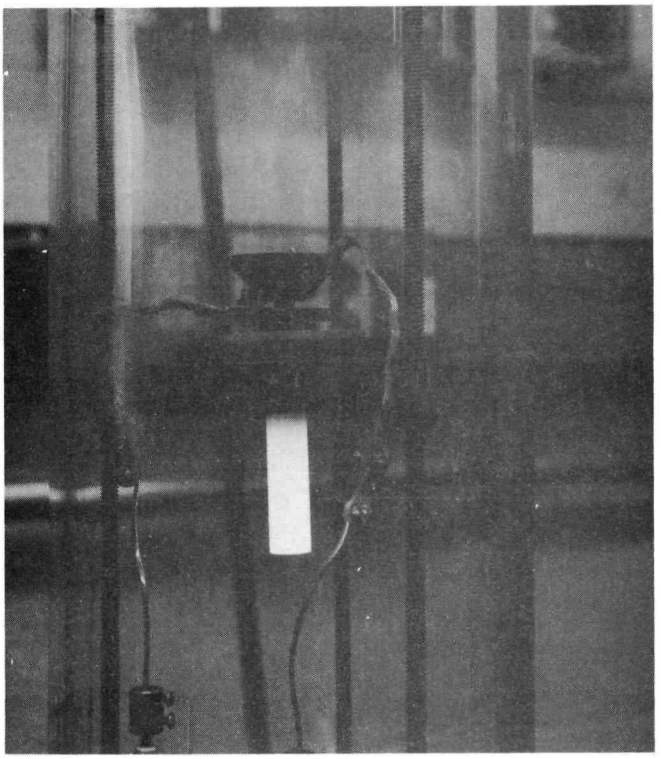

Figure 6.5. Dummy Emitter Test Set-Up.

Life testing at a fixed operating point was initiated. Two additional diode shutdowns were required during the next 20 hours to alter the test setup before sustained operation was achieved. Over the next 60 hours, at a fixed power input, the diode output increased from 7 watts/cm^2 and 11.4% efficiency to 8.3 watts/cm^2 and 13.2% efficiency. The gradual increase in power output is believed to have resulted from improved diffusion bonds between the inner tungsten liner and the cermet fuel ring. A total testing time of 425 hours has been logged without evidence of degradation. For the next 70 hours, the power level was maintained between 7.8 and 8.8 watts/cm^2 at efficiencies between 12.2 and 14.3%. The fluctuations are caused by changes in power input resulting from the input power control system. In Table 6.1, typical operating conditions are described at various times during the life test.

From approximately 275 hours to 605 hours, the diode ran without interruption. During most of this run the power output was about 8.25 w/cm^2 and the overall uncorrected efficiency was above 13.5%. At the 612 hour point, the filament burned out, causing a very rapid shutdown transient. A few hours after this transient, cesium was visible within the bell jar. Inspection of the diode showed that a leak had occurred in the Mo-Mo braze joint at the base of the emitter support tube. (See Figure 6.1) The leak was caused by evaporation of the braze material due to the excessive operating temperature of the joint. The overheating resulted from a shift made in the position of the filament which caused more heat to be transferred down the emitter support tube. This shift had been made during the experiments with the filaments to achieve better uniformity in emitter temperature.

TABLE 6.1

COMPARISON OF OPERATING CONDITIONS DURING LIFE TEST OF #SD-2

Total Operating Time, hours	425	710	1250
Filament Power, watts	154	136	114
Bombardment Power, watts	768	810	678
Total Power Input, watts	922	946	792
Estimated Average Emitter Temperature, °C	1625	1635	1575
Average Collector Temperature, °C	780	740	688
Cesium Reservoir Temperature, °C	302	304	310*
Output Current, amps	182	188	162
Voltage Drop in Emitter Lead, volts	0.087	0.090	.078
Output Voltage (at Diode Output Terminals), volts	0.72	0.72	.70
Output Power (at Diode Output Terminals), watts	131	135	113.2
Output Power Density (at Diode Output Terminals), watts/cm^2	8.7	9.0	7.56
Output Power Density (at Diode Electrodes)	9.8	10.1	8.43
Over-all Efficiency (Electrical Power at Terminals with No Heater Cavity Correction), %	14.2	14.3	14.30
Net Efficiency (Electrical Power at Terminals with a 70 watt Heater Cavity Correction), %	15.3	15.4	15.71
Net Design Efficiency (Electrical Power at Electrodes with a 70 watt Heater Cavity Correction)	17.3	17.4	17.53

*New thermocouple installed in reservoir after inner sleeve replaced

When the emitter was removed from the diode to re-braze the joint, the surfaces of both the emitter and collector were inspected. Both were very clean, and no evidence of contamination was visible on any other internal diode surface. The Mo-Mo joint was rebrazed with a lower-vapor-pressure braze material and the diode was re-assembled. After out-gassing and one inadequate cesium loading, a full charge of cesium was distilled into the diode. Operation was resumed with a new filament (#209A) at about the same conditions as before the interruption. In columns one and two of Table 6.1, a comparison of two data points, before and after the test interruption at 425 hours and 710 hours, is shown. Within the limits of the measuring accuracies, this comparison shows that the performance characteristics were unchanged.

Over the next 400 hours, several filament burn-outs were encountered which caused severe thermal cycling of the fueled-emitter structure. As can be observed in Figure 6.6, these cycles had no noticeable effect on the rhenium emitter. For a given power input, the power output remained quite constant. The slight variations observable in Figure 6.6 are due to differences in other diode parameters, such as collector and cesium reservoir temperatures. Inspection of the electron bombardment gun insulators after each filament burnout showed an increasing amount of UO_2 condensation. At about the 800 hour point, the UO_2 evaporation in the gun cavity started to cause instabilities in the filament emission. At the 815 hour point the instabilities were too severe for sustained operation. Inspection of the gun cavity showed that UO_2 had penetrated through the tungsten inner-liner of the fueled emitter. The penetration coincided with one of the fueled-emitter thermocouple holes which had wandered partially through the inner-liner during machining. Apparently, only a very thin layer of

tungsten remained after machining, and this layer eventually parted after sustained electron bombardment and thermal cycling.

To prevent further evaporation of UO_2 through the tungsten, a rhenium tube was inserted inside the tungsten tube. Rhenium was selected instead of tungsten because of its higher thermal expansion coefficient. It was hoped that thermal expansion at operating temperature would offset the room temperature clearance between the insert and the inner-liner. This clearance was unavoidable because of non-uniformities in the inside diameter of the tungsten liner.

A rhenium inner sleeve was installed in the emitter of SD-2, re-cesiating was accomplished, and laboratory testing was resumed. The use of rhenium instead of tungsten as the inner sleeve material greatly improved the stability of the electron bombardment heating. Unlike the tungsten sleeve, the rhenium did not form cracks and, therefore, uranium did not reach the electron bombardment filament. Either the superior ductility of rhenium or its better thermal expansion match to the cermet prevented the cracking problem.

Within twenty hours, the operation of the electron bombardment heater was back to normal and the output power of the diode for a given input power was within a few percent of its previous level. Some loss in overall efficiency was expected because of higher heater cavity losses caused by the temperature difference between the rhenium insert and the tungsten liner. To prevent excessive operating temperatures of the rhenium insert, the diode input power was limited to a level corresponding to an output power of about 7.4 w/cm^2 for the next 250 hours. At this point, the power output was raised to 8.25 w/cm^2 and held until a filament burnout occurred at 1240 hours. Apparently, the bond between

the rhenium and tungsten continued to improve during this period. As shown in Figure 6.6, the performance characteristics of the diode during the period were virtually identical to those observed prior to the insertion of the rhenium tube. The data shown in Table 6.2 also confirm this observation.

D. SIGNIFICANCE

Prior to the installation of the rhenium liner, high voltage kick-offs frequently occurred due to excessive bombardment currents which automatically tripped a high-voltage shutdown switch. Such currents would flow whenever the emitter temperature rose slightly, due to load changes or shifts in cesium reservoir temperature. Although these shutdowns caused thermal cycling of the fueled-emitter structure, they prevented excessive rises in emitter temperature. After the rhenium liner was installed, this emitter-temperature-limiting mechanism no longer existed because of the relative insensitivity of the bombardment current to emitter temperature. On two occasions, this led to large rises in emitter temperature when cesium reservoir heaters failed. These excursions in emitter temperature reached over 200°C and continued overnight for a total time of about 20 hours.

The emitter temperature surges coupled with some 90 severe thermal cycles finally caused distortion of the fueled emitter and a resultant emitter-to-collector short. Operation was terminated after 2460 hours and the diode was disassembled and is being inspected. Prior to the short, no significant change in performance was observed.

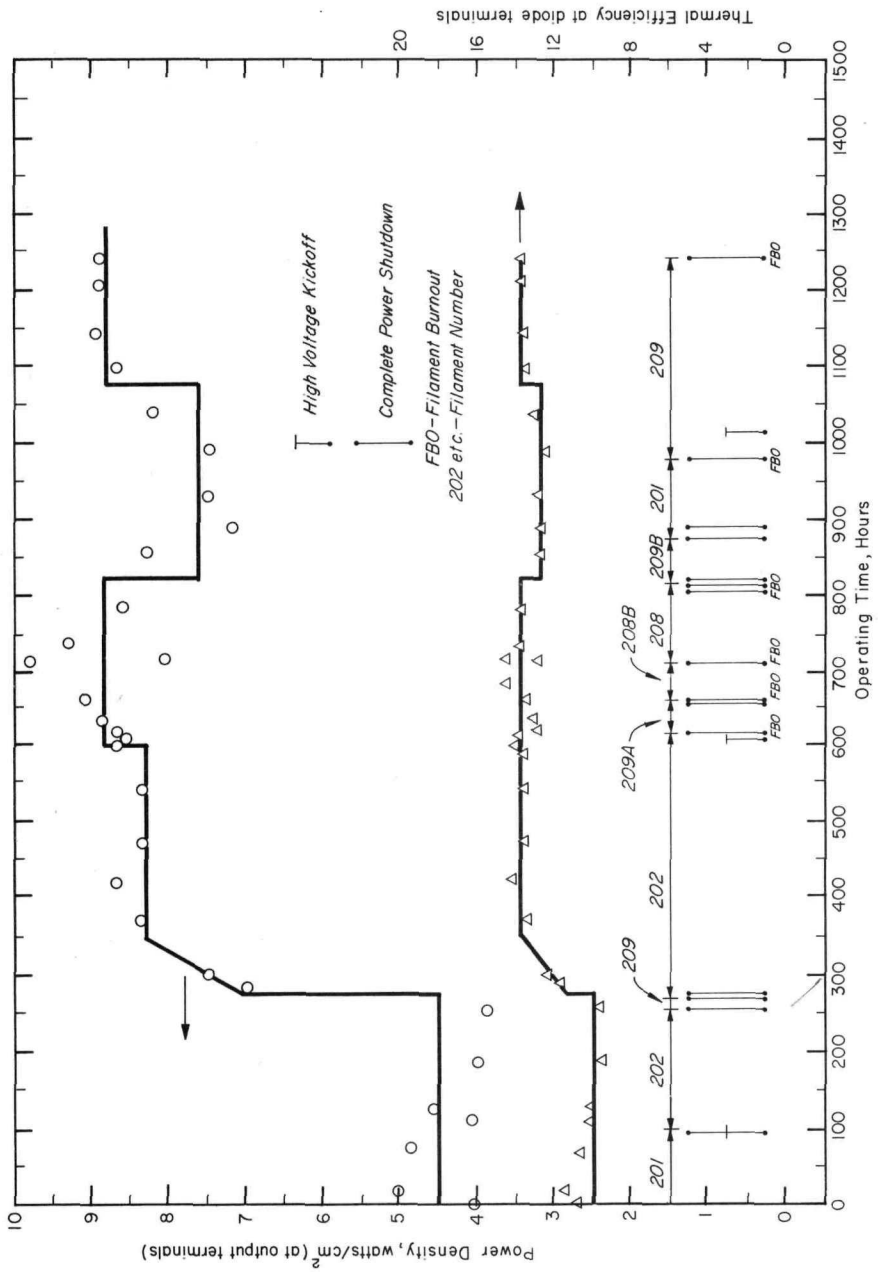

Figure 6.6 SD-2 Life Testing to 1250 Hours

In Table 6.1, a performance summary is presented for SD-2 at three different points during the life test. The first point was taken prior to the first test interruption, the second just after the first interruption and the third just after the rhenium inner sleeve was installed. In Figure 6.7, a performance versus time graph is shown with power inputs and cesium reservoir temperatures noted at some of the data points. The power input was not held constant throughout the operating life due to the electron bombardment heater problems previously discussed. Consequently, the scatter in data is much greater than it is for the in-pile testing of SD-4. However, inspection of Figure 6.7 indicates that no significant change in optimum cesium pressure occurred for a given power input (and emitter temperature). Therefore, it appears that no significant change in emitter work function occurred during the life test.

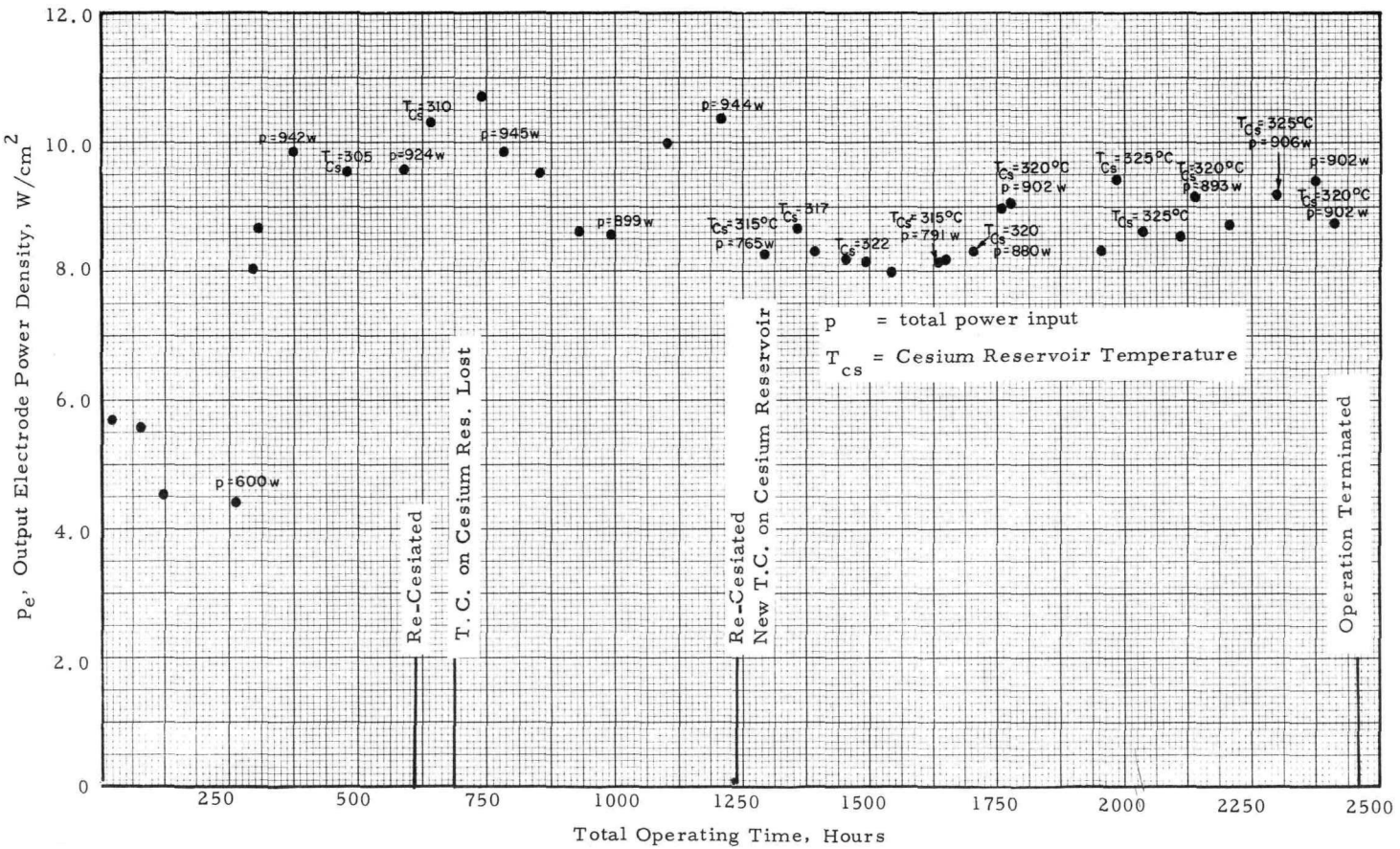

Figure 6.7. Out-of-Pile Life Test of SD-2

APPENDIX A
FUELED-EMITTER FABRICATION

A. SUMMARY

Two emitters were fabricated to the nominal dimensions shown in Figure A.1. Table A.1 lists the measured dimensions of each emitter. The emitters consisted of three major components: 1) a rhenium clad and emitting surface; 2) a UO_2-W cermet fuel cylinder; and 3) an interior tungsten clad. The rhenium and cermet components were fabricated by powder metallurgy techniques. The tungsten was machined from wrought rod. Densification of the cermet and bonding it to the tungsten were accomplished simultaneously by isostatic hot-pressing. The densified cermet was ground to size and the rhenium clad, consisting of a pre-sintered rhenium sleeve and a densified rhenium end plug, was isostatically hot-pressed onto the cermet, furthering densification of the rhenium sleeve and forming a metallurgical bond at the rhenium sleeve-rhenium end plug interface. The composite specimens were ground to the outside dimensions and the tungsten was drilled by electro-discharge machining, leaving the desired tungsten wall thickness for the inner cladding. Three thermocouple holes were drilled into the cermet of each emitter.

B. FORMING OF THE CERMET STRUCTURE

The two emitters were fueled with United Nuclear Corporation, fully enriched, -100 + 140 mesh, UO_2 shot. Table A.2 lists the vendor's characterization. The UO_2 powder was coated with 1 wt. per cent (of the fuel) of parawax by dissolving the parawax in enough carbon tetrachloride to completely cover the fuel in an evaporating dish, and then evaporating the carbon tetrachloride, leaving the parawax residue on the surfaces of the fuel particles. The coated powder was chilled to 6°C to harden the parawax coating and then forced

CONFIDENTIAL
UNCLASSIFIED

1 Rhenium Emitter

2 Cermet Fuel

3 Tungsten Clad

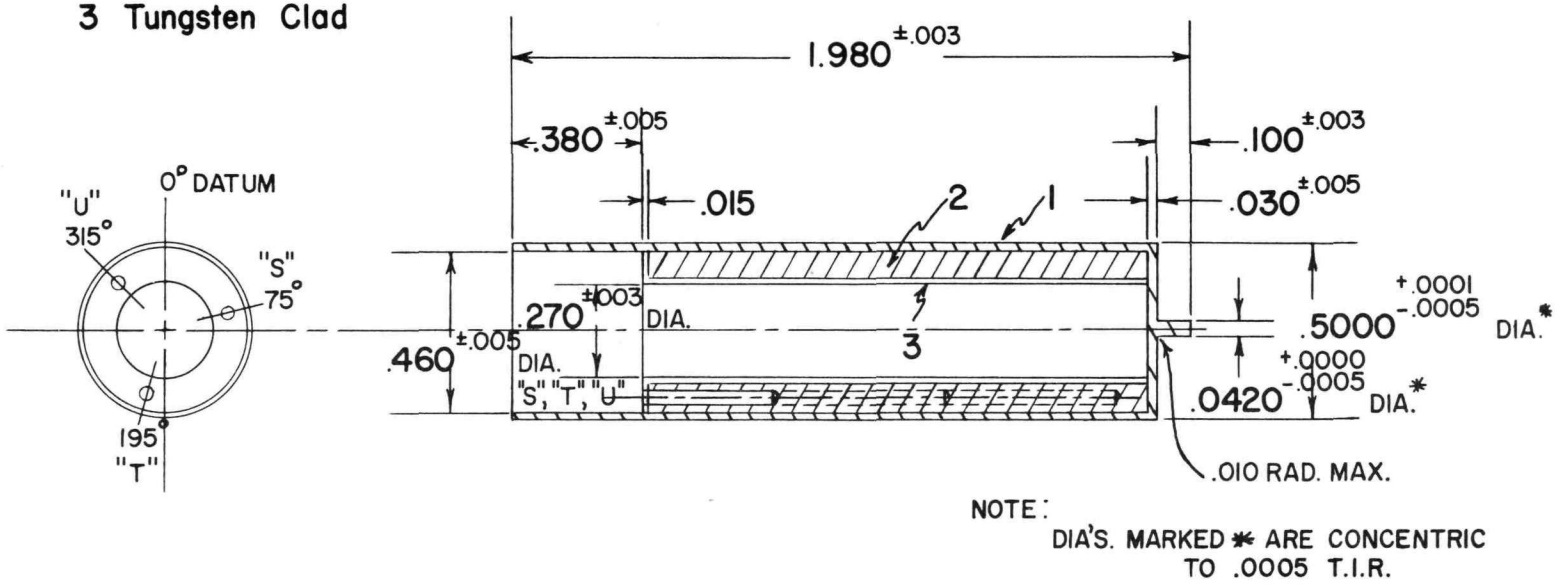

"S" $.043^{+.003}_{-.000}$ DIA. X $.400^{\pm.020}$ DP. TIP

"T" $.043^{+.003}_{-.000}$ DIA. X $.900^{\pm.020}$ DP. TIP

"U" $.043^{+.003}_{-.000}$ DIA. X $1.400^{\pm.020}$ DP. TIP

Figure A-1. Finished Emitter

CONFIDENTIAL
UNCLASSIFIED

TABLE A.1

SUMMARY OF FUELED EMITTER PROPERTIES

Emitter No.	Cermet	Per Cent Theoretical Density of Cermet	Total U, g[2]	U_{235} g	Cermet Length, inch	Cermet O.D., inch
0-1	80v/oUO_2-20v/o W	95.5	16.27	15.15	1.455	0.462
0-2	80v/oUO_2-20v/o W	95.2	16.22	15.11	1.454	0.462

Emitter No.	Tungsten Length, inch	Average Tungsten I.D., inch	Re Length, inch	Re I.D.,[1] inch	Re Plug Thickness, inch
0-1	1.470	0.270	2.000	0.462	0.149
0-2	1.469	0.270	1.999	0.462	0.150

(1) Inside diameter of open end.

(2) Calculated uranium contents.

TABLE A.2
VENDOR CHARACTERIZATION OF UO_2 SHOT

ISOTOPIC DATA: 93.14% U-235 (As reported by AEC)

CHEMISTRY DATA:

% Uranium 88.00

O: U 2.003 (Battelle Analysis: 2.006)

Impurities, PPM

Ag <.05	Bl <.5	Cu 1	Ni 30	Sn 1
Al 5	Cd <.2	Fe 10	P <20	Total
B .3	Co <1	Mg 5	Pb <1	Halides <10
Be <.1	Cr <5	Mn <2	Si 30	

Total Impurities 122 PPM

PHYSICAL DATA:

Density 10.265 G/CC 94.8% Theoretical (Determined by Mercury Pycnometer)

Particle Shape

D/D Ratio	Percent
1.1 to 2.1	100

Particle Size

Mesh Size	Weight Per Cent
-100	Trace
-100+140	95.7
-140	4.3

through a 100 mesh sieve to separate the particles. Tungsten powder (Fansteel Type 427) was then blended with the coated fuel in a six-ounce, wide-mouth glass jar canted 20° from horizontal and rotated at approximately 30 RPM at room temperature until the parawax became tacky.

Figure A.2 shows the mandrel apparatus used in compacting the blended cermet into sleeves. The mandrel with one plug removed was held vertically inside a 0.030-inch (0.076 cm) wall rubber tube. Blended powder was poured into the tube and the plug was placed onto the mandrel, pushing it down into contact with the powder. The rubber tube was pulled over the exposed ends of the plug and tied to seal out the pressing fluid. This assembly was submerged in a piston-type hydrostatic press and pressurized to 70,000 psi (4900 kg/cm^2). The cermet sleeves compacted to 72 per cent of theoretical density.

To obtain a uniform wall thickness, the green compacted cermet sleeves were held on a mandrel and the outside diameter turned on a lathe. To maintain sharp corners and squareness, and to remove the end effect produced in compaction, the sleeves were placed in a steel squaring block and approximately 0.2 inch (0.51 cm) was removed from each end with No. 240 grinding paper.

C. FORMING OF THE TUNGSTEN MANDRELS

Tungsten mandrels were machined from 1/2 inch (1.27 cm) diameter Fansteel tungsten rod stock as shown in Figure A.3. The mandrels were originally ground for a cermet inside diameter of 0.340 inch (0.864 cm). This diameter was reduced to 0.300 in. (0.762 cm) after nuclear mockup experiments showed a need for more fuel. As a result, the mandrels had to be reground to the smaller diameter without center holes. After the 0.340-inch (0.864 cm) diameter had been reground to 0.300 inch (0.762 cm), the concentricity was checked by chucking the 0.490-inch (1.245 cm) diameter end in a collet and turning the mandrel while a travel indicator rode the opposite end. The variation of the

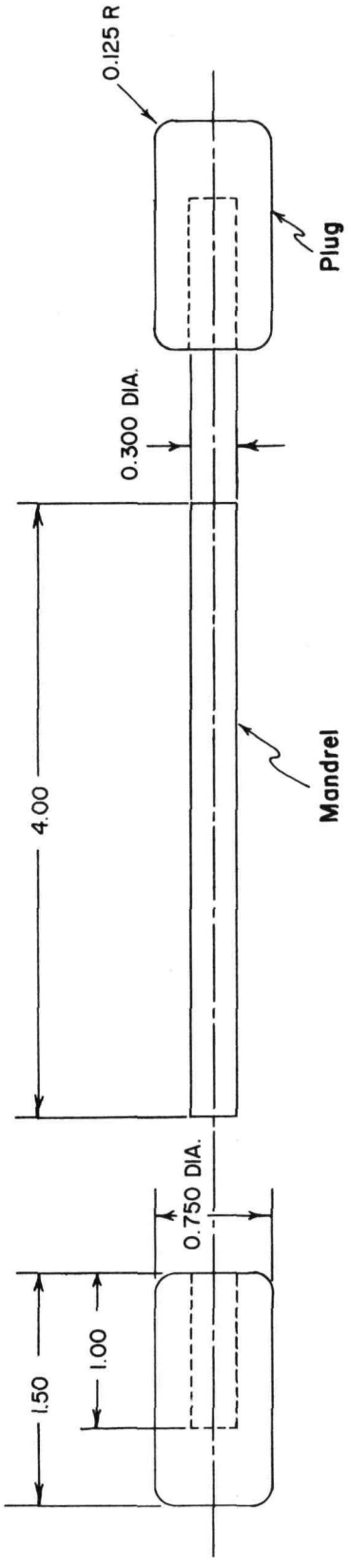

Figure A-2. Hydrostatic Pressing Assembly Components

CONFIDENTIAL
UNCLASSIFIED

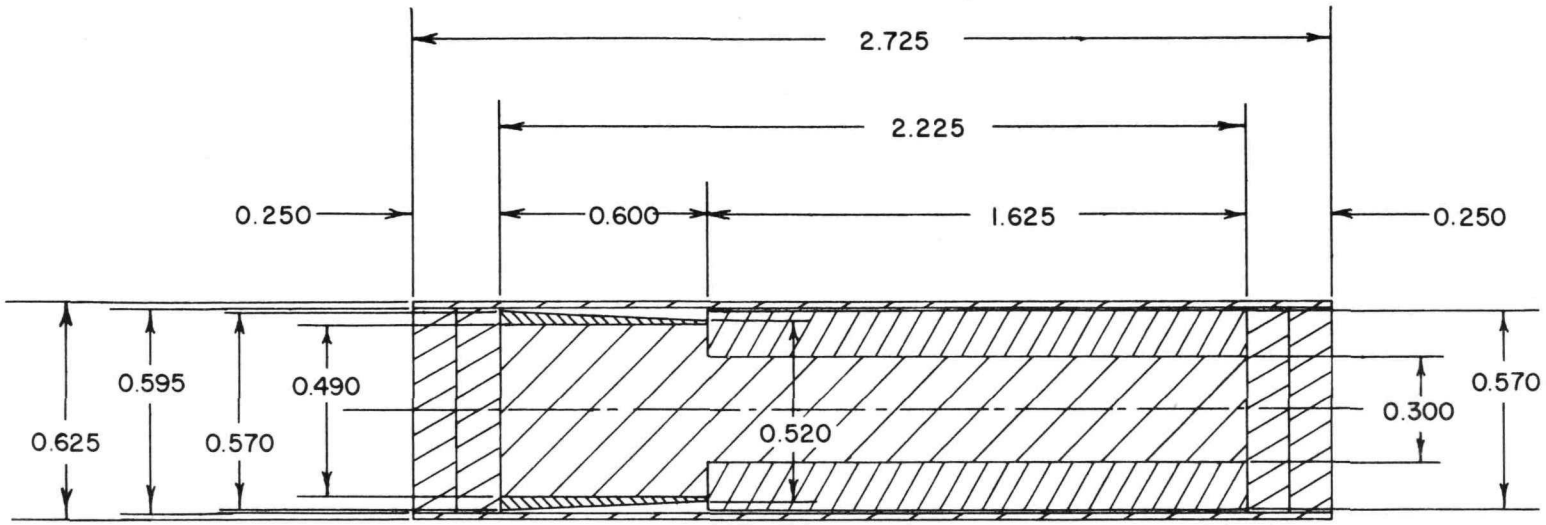

Figure A-3. Assembly for Cermet Densification

CONFIDENTIAL
UNCLASSIFIED

indicator was less than 0.0003 inch (0.00076 cm) for each mandrel, and this was considered to be satisfactory. A sharp corner was made at the step in the mandrel by finishing with a pointed tungsten carbide tool. The machined mandrels were degreased and vacuum-annealed at 1600°C for 1/2 hour.

D. ISOSTATIC HOT PRESSING OF THE CERMETS

Figure A.3 is a drawing of the assembly for densifying and bonding the cermet to the tungsten. The tapered graphite sleeve shown on the 0.490-inch (1.245 cm) diameter tungsten was designed to reduce the void space between the tantalum clad and the tungsten, and to help maintain a sharp transverse interface between the tungsten and the cermet. Not shown in the drawing was a layer of 0.006-inch (0.015 cm) thick graphite foil which completely lined the tantalum cladding to prevent its bonding to the internal components of the assembly. The assembly was heated at 1600°C in vacuum for a half hour to drive off the parawax in the cermet, and then vacuum-sealed by electron beam welding. These assemblies were then isostatically hot-pressed at 1600°C and 10,000 psi (701 kg/cm^2) for three hours.

The tantalum cladding was removed and center holes drilled in each end of the tungsten mandrels. The .300-inch (0.762 cm) diameter was centered by chucking the larger end of the tungsten mandrel in a collet and adjusting the piece until the .300-inch (0.762 cm) diameter ran true at the tungsten-cermet interface. The centered end was ground to a convenient collet size and the .490-inch (1.245 cm) diameter was centered. The pieces were then ground. The cermets at this stage are shown in Figure A.4. A 0.050-inch (0.127 cm) deep blind hole was machined in the 0.300-inch (0.762 cm) diameter end of the tungsten to press-fit onto a projection on the rhenium plugs as shown in Figure A.5. This was to prevent shifting of the plugs during subsequent hot-pressing. After machining, the specimens were ultrasonically degreased in ethyl alcohol

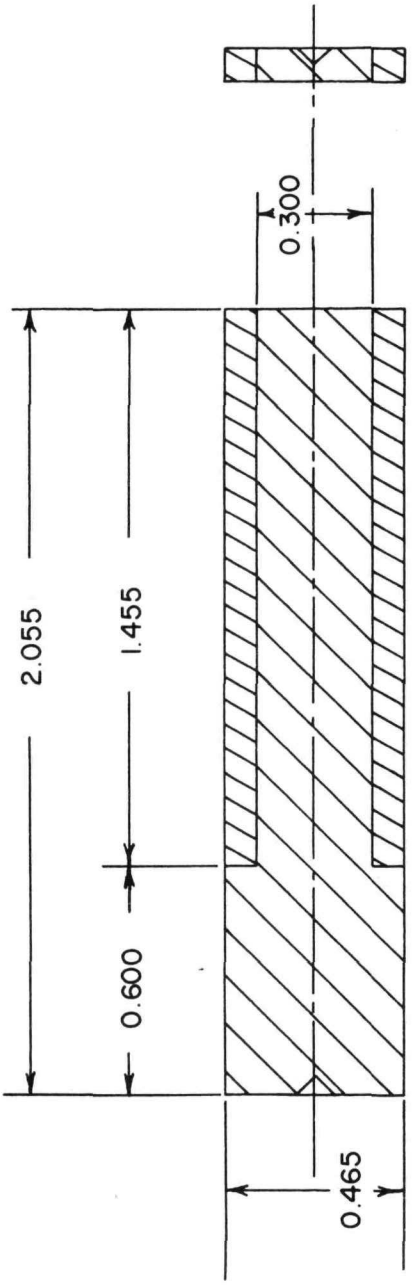

Figure A-4. Densified and Machined Cermet

CONFIDENTIAL

UNCLASSIFIED

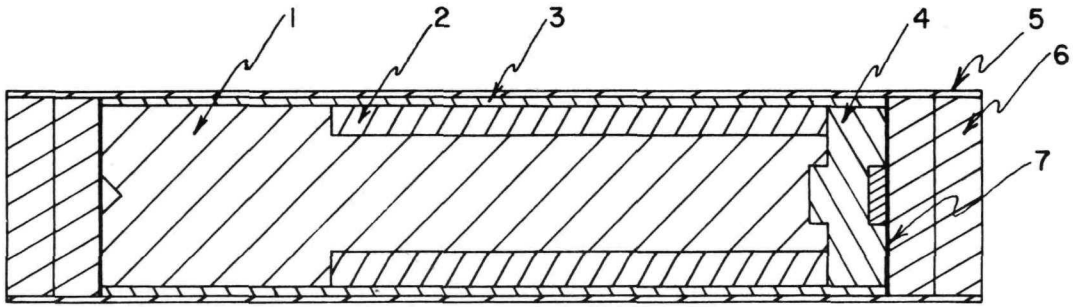

1. Tungsten Mandrel
2. Pressure Bonded Cermet – Bonded to W mandrel – Machined – Outgassed 30 min. at 1600° C.
3. Rhenium Sleeve – 80% of theoretical density – Machined 0.590" O.D. X 0.465" I.D. X 2.055" long – Outgassed 30 min. at 1600° C.
4. Rhenium Plug with Moly insert for centering
5. Tantalum Clad – 0.625" X 0.015" wall
6. Tantalum End Plugs – 0.125" thick – two in each end
7. Graphite Foil – 0.006" thick – separating the specimen from end plugs on each end

Figure A-5. Assembly for Simultaneous Densification and Pressure-Bonding Rhenium Clad

UNCLASSIFIED

CONFIDENTIAL

UNCLASSIFIED

CONFIDENTIAL

and vacuum heat treated at 1600° C for half an hour. The cermet sleeve lengths were determined by measuring the distance from the cermet-tungsten interface to the end of the cermet on an XLO shadow graph at 50X magnification. In calculating densities for each cermet, the weight of the cermet was obtained by subtracting the calculated weight of the tungsten mandrels from the total weights. The densities thus calculated showed the cermets to be approximately 95 per cent of theoretical density. Figure A. 7 is a photomicrograph of the densified cermet structure.

E. FORMING OF THE RHENIUM CLAD

The rhenium sleeve and the end plug for each emitter were fabricated from United Mineral and Chemical Corporation, 99. 9 per cent pure, -240 mesh, rhenium powder. This rhenium powder compacted to only 46 percent of theoretical density at 60,000 psi (4,210 kg/cm^2). To obtain a uniform wall thickness and to prevent sintering shrinkage during heat-up to the isostatic hot-pressing temperature, it was necessary to pre-sinter the rhenium sleeves. Previously, 46 percent dense rhenium sleeves which were sintered 2 hours at 1600° C were 76. 9 percent of theoretical density and the inside cross-sectional area reduced 35. 7 percent.

A pressing apparatus based on the above sintering data was prepared similar to that in Figure A. 2. Sleeves were pressed at 60,000 psi (4,210 kg/cm^2) to 45. 6 percent of theoretical density. These green-pressed sleeves were sintered 2 hours at 1600° C in vacuum. The average inside diameter of the sleeves was 0. 470 inch (1. 193 cm). To further reduce the inside diameter, the sleeves were sintered 2 more hours at 1600° C. After 4 hours of sintering, the average inside diameter was 0. 467 inch (1. 186 cm) and the average density was 84. 5 percent of theoretical density. The inside cross-sectional area reduced 32. 9%.

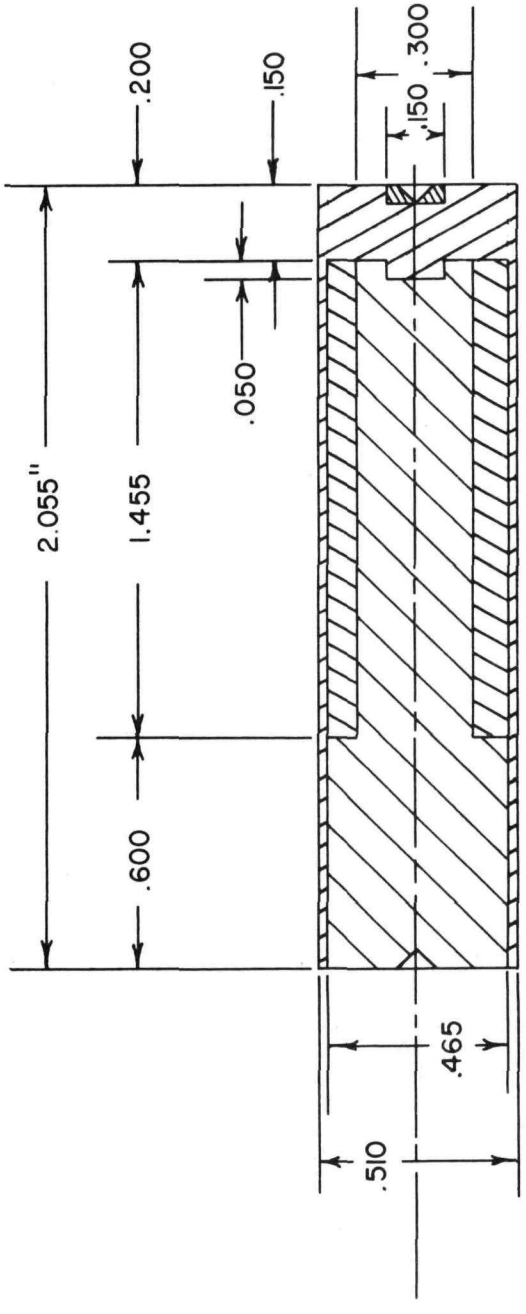

Figure A-6. Clad Emitter After Grinding

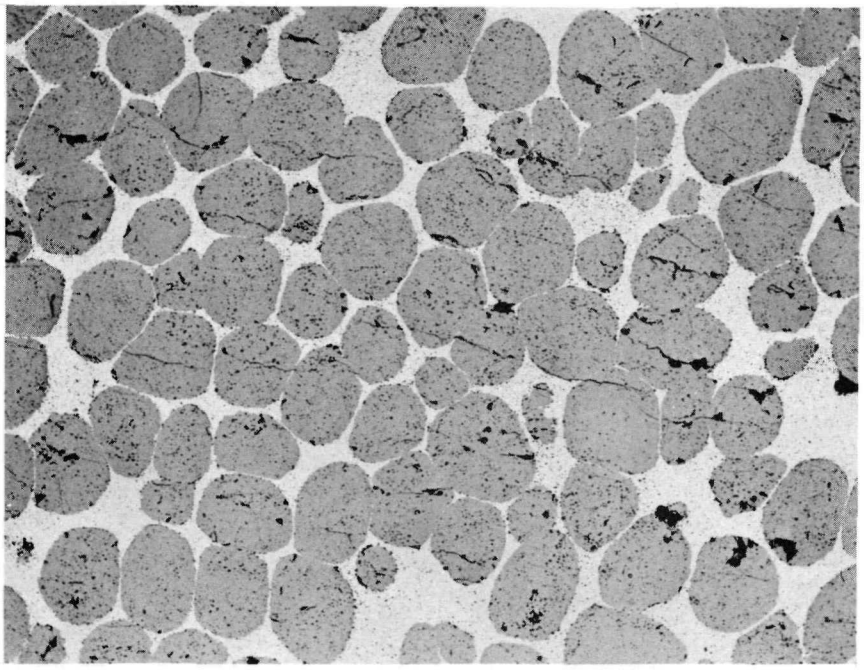

100X As Polished RM 41652

Figure A-7. Photomicrograph of Cermet Structure(Emitter No. 0-1)

The outside diameter of the rhenium sleeves was ground, the inside was honed smooth, and the sleeves were cut to remove non-uniformities at the ends. The sleeves were ultrasonically degreased in ethyl alcohol and outgassed at 1600°C for 1/2 hour.

Rhenium end plugs were fabricated to slip inside the rhenium sleeves. Powder compacts cold-pressed at 40,000 psi (2,800 kg/cm^2) were 0.595-inch (1.51 cm) diameter by 0.840-inch (2.13 cm) long and were 41.8 percent of theoretical density. These compacts were hot pressed in a 0.600-inch (1.523 cm) diameter graphite die at 1600°C and 8,000 psi (561 kg/cm^2) for a half hour in vacuum to greater than 99 percent of theoretical density. The densified plugs were ground to the configuration shown in Figure A.5. Because center-holes cannot be drilled in the rhenium clad end of the emitter after bonding, a blind hole was electrical discharge machined in the rhenium plug and a molybdenum insert fitted into the hole. The 0.150-inch (0.382 cm) diameter by 0.050-inch (0.127 cm) long centered extension opposite the blind hole was provided to maintain the central position of the plug with respect to the cermet by preventing shifting of the plug during isostatic hot pressing.

The cermet and rhenium components for each emitter were assembled and electron beam vacuum-sealed in tantalum cans, as shown in Figure A.5. The assemblies were isostatically hot-pressed at 1600°C and 10,000 psi (701 kg/cm^2) for three hours.

The tantalum end plugs were removed from each end of the assemblies, taking special care to leave the exposed face of the rhenium plug undisturbed, since this face had to be used as the reference for determining the cermet location and the final emitter and cermet lengths. Center holes were drilled in the molybdenum inserts. The centers in the tungsten were refinished. The rhenium clad emitters were ground to the outside dimensions.

F. FORMING OF THE INNER TUNGSTEN CLAD

The tungsten mandrel was removed by electrical discharge machining. A 0.015-inch (0.038 cm) thickness of tungsten cladding was left on the inside surfaces of the cermet. Figure A.6 shows the semi-finished emitter at this stage. Figure A.8 is a photomicrograph of a tungsten mandrel rhenium clad interface after hot pressing.

G. MACHINING OF THE THERMOCOUPLE HOLES

The three thermocouple holes shown in Figure A.1 were drilled through the tungsten clad and into the cermet by electrical discharge machining. The machined emitters were ultrasonically degreased in ethyl alcohol and shipped.

UNCLASSIFIED

E-67-38

100X As Polished RM 41485

Figure A-8. Photomicrograph of a Tungsten Mandrel-Rhenium Clad Interface

UNCLASSIFIED

APPENDIX B

POSTIRRADIATION EVALUATION OF THERMO ELECTRON CORPORATION'S SD-4 DIODE

The following section contains 58 pages.

Report No. BMI-X-538

Special Distribution

AEC Contract No. W-7405-eng-92

POSTIRRADIATION EVALUATION OF THERMO ELECTRON CORPORATION'S SD-4 DIODE (U)

by

James H. Saling, Edward O. Speidel, and Victor W. Storhok

July 22, 1968

GROUP I - Excluded from automatic downgrading and declassification

RESTRICTED DATA

This document contains restricted data as defined in the Atomic Energy Act of 1954. Its transmittal or the disclosure of its contents in any manner to an unauthorized person is prohibited.

BATTELLE MEMORIAL INSTITUTE
Columbus Laboratories
505 King Avenue
Columbus, Ohio 43201

TABLE OF CONTENTS

	Page
ABSTRACT	1
INTRODUCTION	1
RESULTS OF EXAMINATION	4
Visual Examination	4
Neutron Radiography	4
Gamma Scan and Burnup Analyses of the Diode	7
Fission-Gas Sampling	10
Disassembly of Diode and Dimensional Measurements	12
Emitter	12
Collector	12
Upper Ceramic Seal	15
Heat Shield	15
Copper Cooling Straps	15
Cesium Reservoir	20
Sectioning for Burnup and Metallography	20
Metallographic Examination	20
Determination of Fission-Product Distribution	39
Autoradiography	39
Gamma Scanning	39
Chemical and Vacuum-Fusion Analyses	55
CONCLUSIONS	56
ACKNOWLEDGMENTS	57
REFERENCES	57

POSTIRRADIATION EVALUATION OF THERMO ELECTRON CORPORATION'S SD-4 DIODE (U)

James H. Saling, Edward O. Speidel, and Victor W. Storhok

The SD-4 thermionic diode, which operated in the Battelle Research Reactor for about 8100 hr and acquired a burnup of 3.85 x 10^{20} fissions per cm^3, was subjected to a postirradiation examination which included visual inspection, fission-gas sampling, burnup analysis, dimensional measurements, metallography, fission-product distribution determinations, and chemical analyses. No gross swelling or warping of the emitter was observed. A 2.7 percent increase in emitter diameter was measured.

INTRODUCTION

In September of 1965, Thermo Electron Corporation started an in-pile test at the Battelle Research Reactor under USAEC sponsorship. The test assembly (Figure 1) consisted of a cylindrical thermionic converter with a rhenium emitter (Figure 2) fueled with a tungsten-80 v/o UO_2 cermet. The external environment of the converter was a static vacuum formed by an initial pump-out and seal-off of a stainless steel housing. The test assembly operated in-pile for 8125 hr over a period of about 2 years. More than 80 cycles between shutdown and full power occurred during this period. The average electrode power density throughout the test lifetime was 7.8 w per cm^2. For fixed reference levels of reactor power, cesium pressure, and collector temperature, the diode performance was stable throughout the test. The test was terminated when difficulties occurred in auxiliary heaters and coolant systems which caused a loss in control of the temperature of the cesium reservoir.

A postirradiation evaluation was conducted at the Battelle-Columbus Hot-Cell Facility and consisted of the following operations:

(1) Neutron radiography

(2) Visual examination

(3) Burnup analyses and gamma scanning of diode

(4) Fission-gas sampling

(5) Dissassembly of diode and dimensional measurements

(6) Metallographic examination

(7) Determination of fission-product distribution

(8) Chemical and vacuum-fusion analyses.

The following sections discuss each operation in detail.

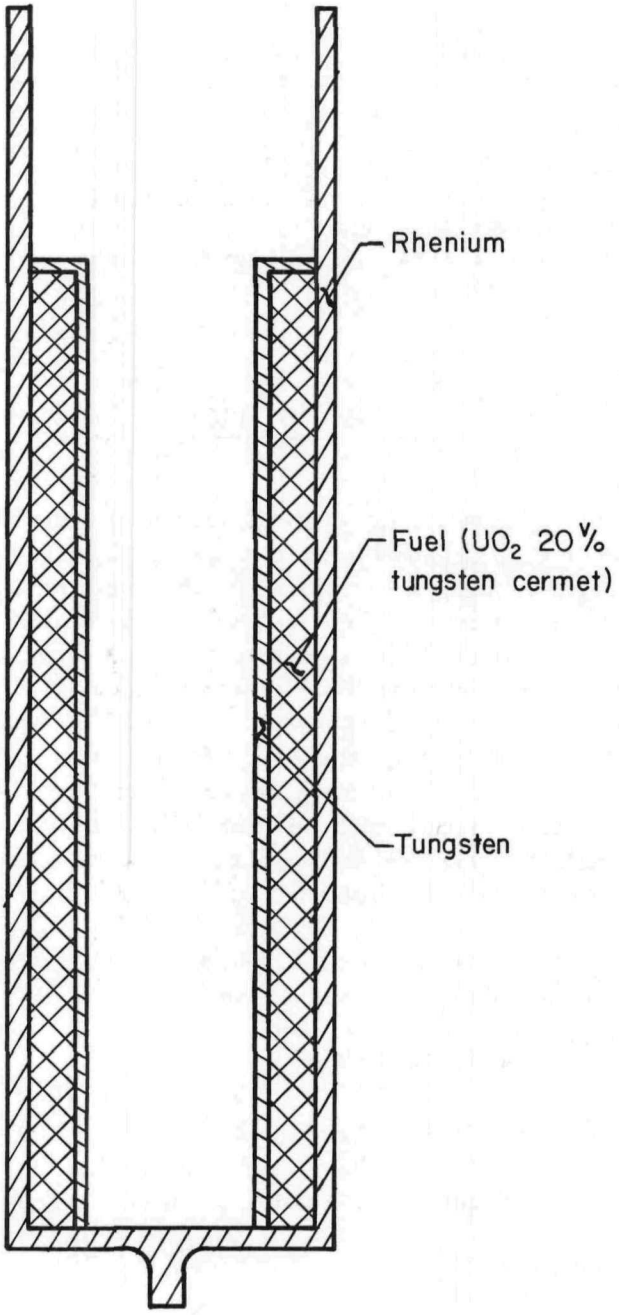

FIGURE 1. LONGITUDINAL CROSS SECTION OF EMITTER

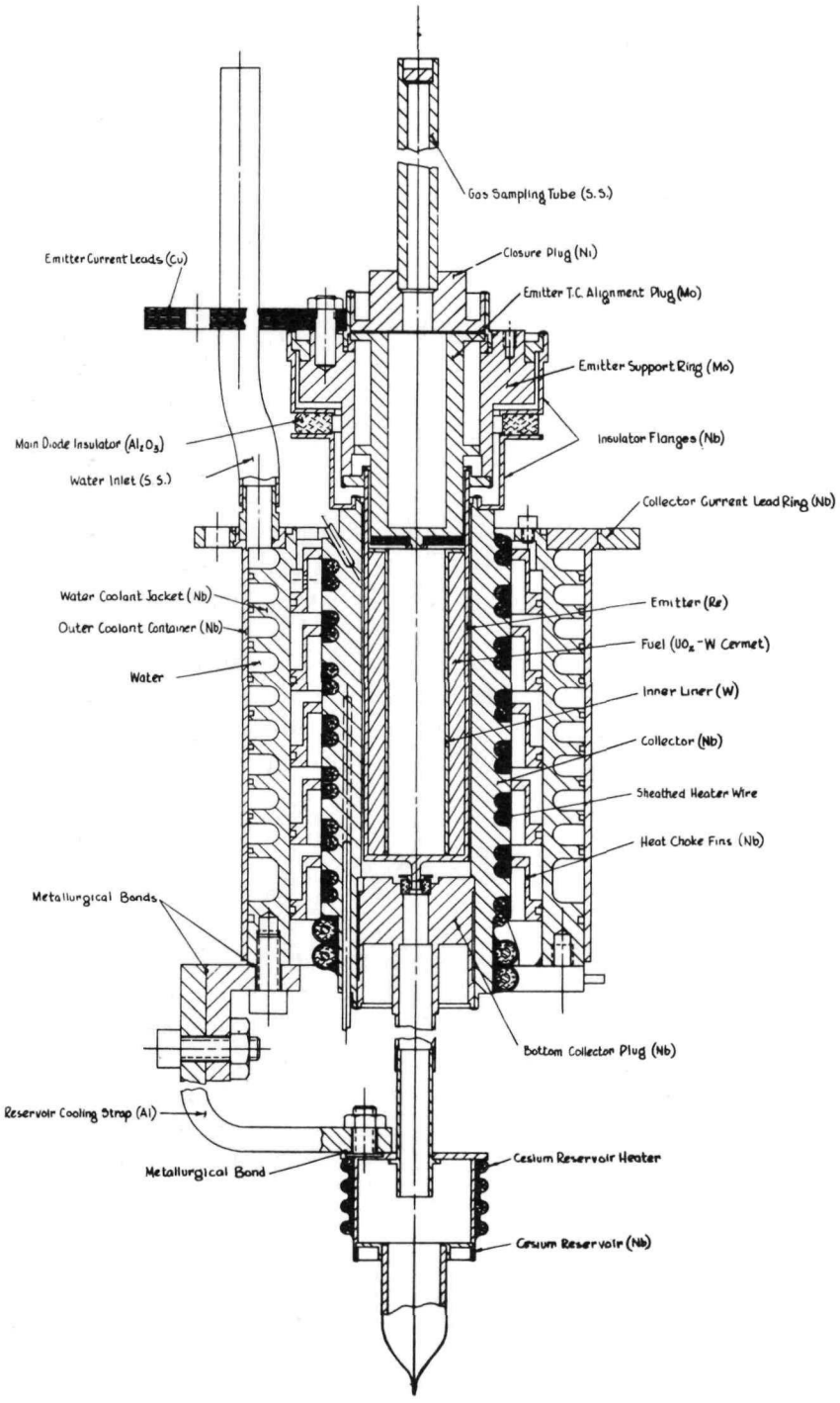

FIGURE 2. DESIGN OF DIODE SD-4

RESULTS OF EXAMINATION

Visual Examination

After sampling of the gases in the outer containment can, the diode was moved into the Remote Handling Facility and the outer containment can was removed. The thermocouple and heater leads were removed so that a visual examination of the diode could be made.

Visual examination of the diode assembly did not show any evidence of gross failure of any of the visible parts. Figure 3 is a photograph of the assembly after removal of the outer can. The color of the surface of the heat exchanger was probably darker than it was originally, but it still had a metallic luster. All exposed surfaces including the ceramic seal were examined at magnifications up to 12X. There was a faint line along the seam on the main diode insulator suggesting the possibility of a crack (Figure 4). Later investigations indicated that no crack existed and that the mark was probably a stain of the type frequently observed on similar insulators. The appearance of the rest of the ceramic seal was typical of similar as-constructed seals.

One of the emitter current leads and two of the cesium-reservoir heater leads appeared to be loose. These may have been pulled loose either during removal of the diode assembly from the containment can or during removal of the thermocouple and heater leads.

Neutron Radiography

Neutron radiographs of the diode were obtained before it was disassembled (Figure 5). The neutron radiographs were obtained by traversing the diode past a collimated beam of neutrons from the reactor. The emitter was then rotated 90 deg and the process repeated. Neutrons that passed through the diode activated an indium foil placed before each exposure on the opposite side of the diode from the neutron source. The indium foils were then used to expose photographic plates, producing images of the diode. Dark areas in the resultant pictures indicate where all or most of the neutrons were absorbed in passing through the diode.

These radiographs (Figure 5) indicated that no gross swelling or warping of the emitter had occurred. A dark, slightly conical area just above the top of the emitter fuel was seen in some radiographs and was thought to be the laminated heat shield. Later in the examination, it was found that this was UO_2 which had been vapor deposited onto the bottom of the heat shield during irradiation. The neutron radiographs did not show significant quantities of cesium in the cesium reservoir. However, the neutron radiographs would not detect cesium if it were distributed in thin films throughout the low-temperature portions of the diode structure. Since the diode had been handled prior to radiographing, it was concluded that the cesium could have been spread to other parts of the diode.

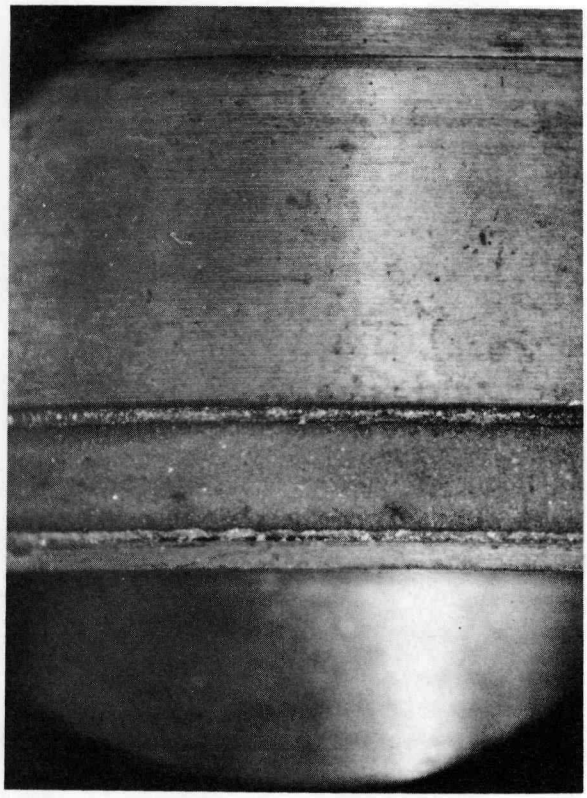

1/2X TEO1549A

FIGURE 3. SD-4 DIODE AFTER REMOVAL FROM OUTER CONTAINMENT CAN

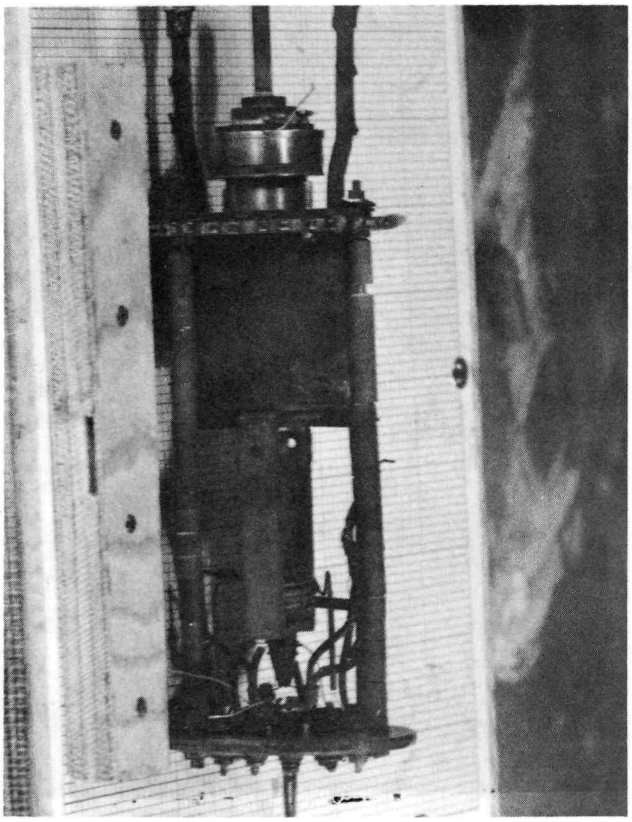

5X P1245

FIGURE 4. TOP CERAMIC INSULATOR ON SD-4

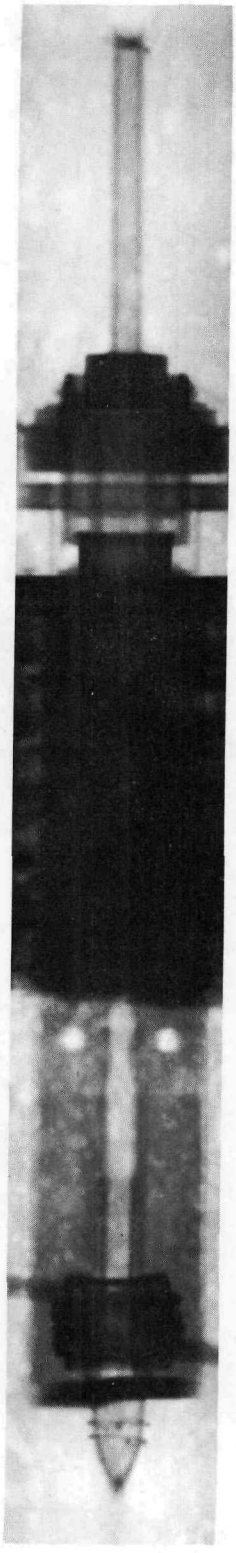

~1X TEO1582

a. Zero Rotation

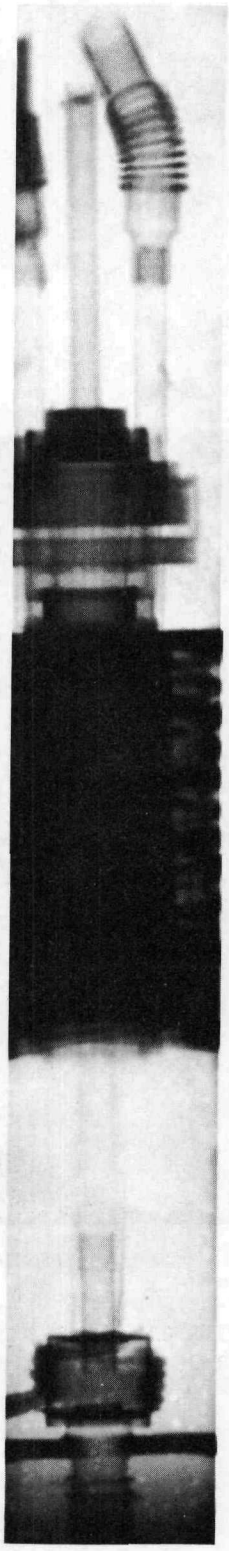

~1X TEO1582

b. 90-Deg Rotation

FIGURE 5. NEUTRON RADIOGRAPHS OF DIODE BEFORE DISASSEMBLY

After the emitter had been removed from the diode it was again neutron radiographed (Figure 6). Without the collector and heat exchanger a much clearer picture of the emitter itself could be obtained. It is obvious from these radiographs that the fuel in the emitter was cracked in several places. Later metallographic examination showed that relocation of UO_2 by vapor transport had occurred and that both the tungsten inner cladding and the fuel were extensively cracked. These neutron radiographs also indicated that the emitter had swelled in the fueled area. This observation was later confirmed by dimensional measurements.

Gamma Scan and Burnup Analyses of the Diode

As an initial step in determining specimen burnup, the relative intensity of gamma radiation emitted from the fuel was determined as a function of its length. Data from this operation were correlated with the analytically determined burnup to give the relative distribution of burnup over the length of the fuel. The 0.757-mev Zr^{95} photopeak was used to obtain the gamma intensity profile. Figure 7 shows a plot of the gamma activity of the fuel as a function of emitter length and indicates that there was some end effect, especially at the bottom of the fuel. Longitudinal sectioning of the sample later revealed that vapor transport of the UO_2 had occurred and appreciable amounts of UO_2 had been deposited at the top and the bottom of the emitter. It is probable that some of the increased gamma activity observed at the ends of the emitter was due to this increased amount of fuel at the ends. However, some might also have been due to flux peaking at the ends of the fuel.

A representative cross section of the fuel was removed from the axial center of the emitter for analytical burnup determination. This sample was sent to Idaho Nuclear Corporation for uranium isotopic analyses. The results of the isotopic analyses are given in Table 1. The burnup was calculated from the relationship:

$$\text{Burnup} = 100\,\frac{R_{6/5} - R^{\circ}_{6/5}}{\left(\frac{\alpha}{1+\alpha} + R_{6/5}\right)} \quad ,$$

where

$R_{6/5}$ = ratio of the postirradiation fractions of U^{236} to U^{235}

$R^{\circ}_{6/5}$ = ratio of the preirradiation fractions of U^{236} to U^{235}

α = ratio of the cross sections for fission and capture in $U^{235} = 0.185 \pm 0.004$.

The burnup values calculated using the above method along with estimated burnups determined by calorimetry measurements of the diode during irradiation are given in Table 2. The burnup calculated from isotopic analyses is believed to be the most accurate.

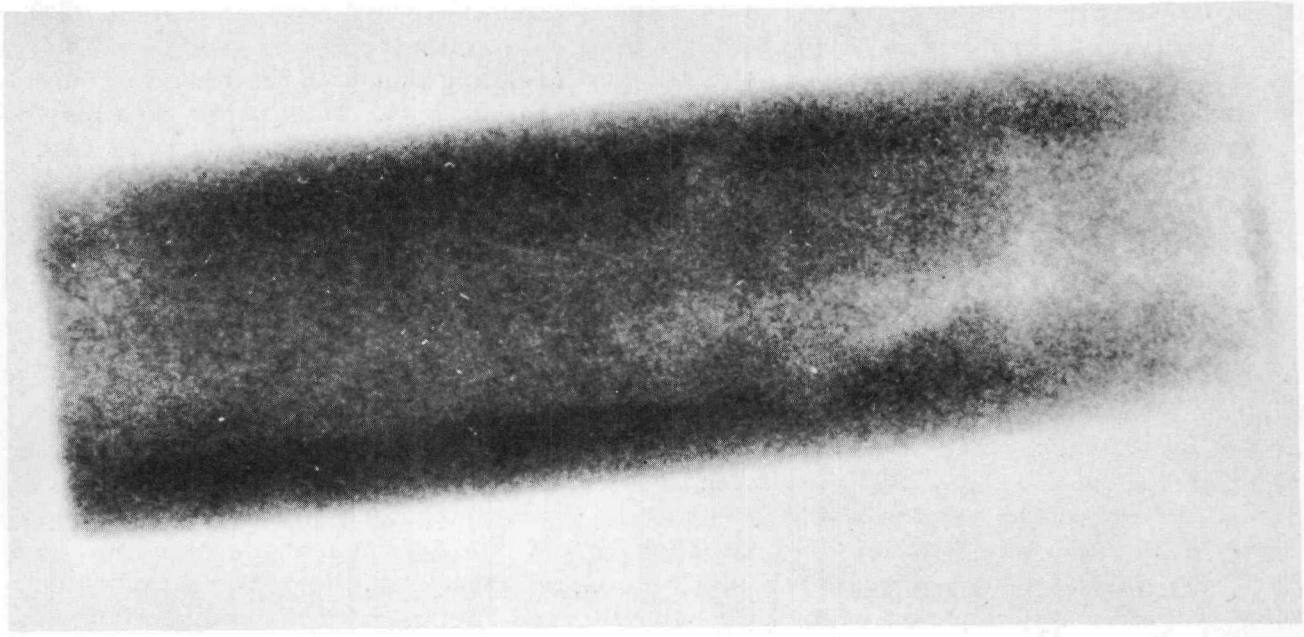

4X TEO1583

a. Zero Rotation

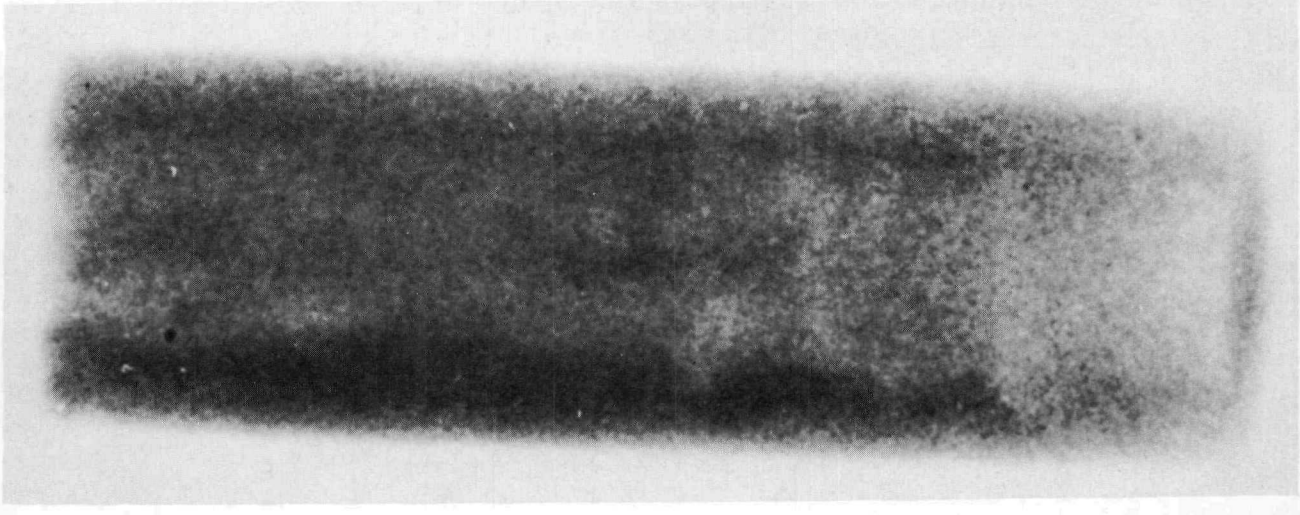

4X TEO1584

b. 90-Deg Rotation

FIGURE 6. NEUTRON RADIOGRAPH OF EMITTER

CONFIDENTIAL

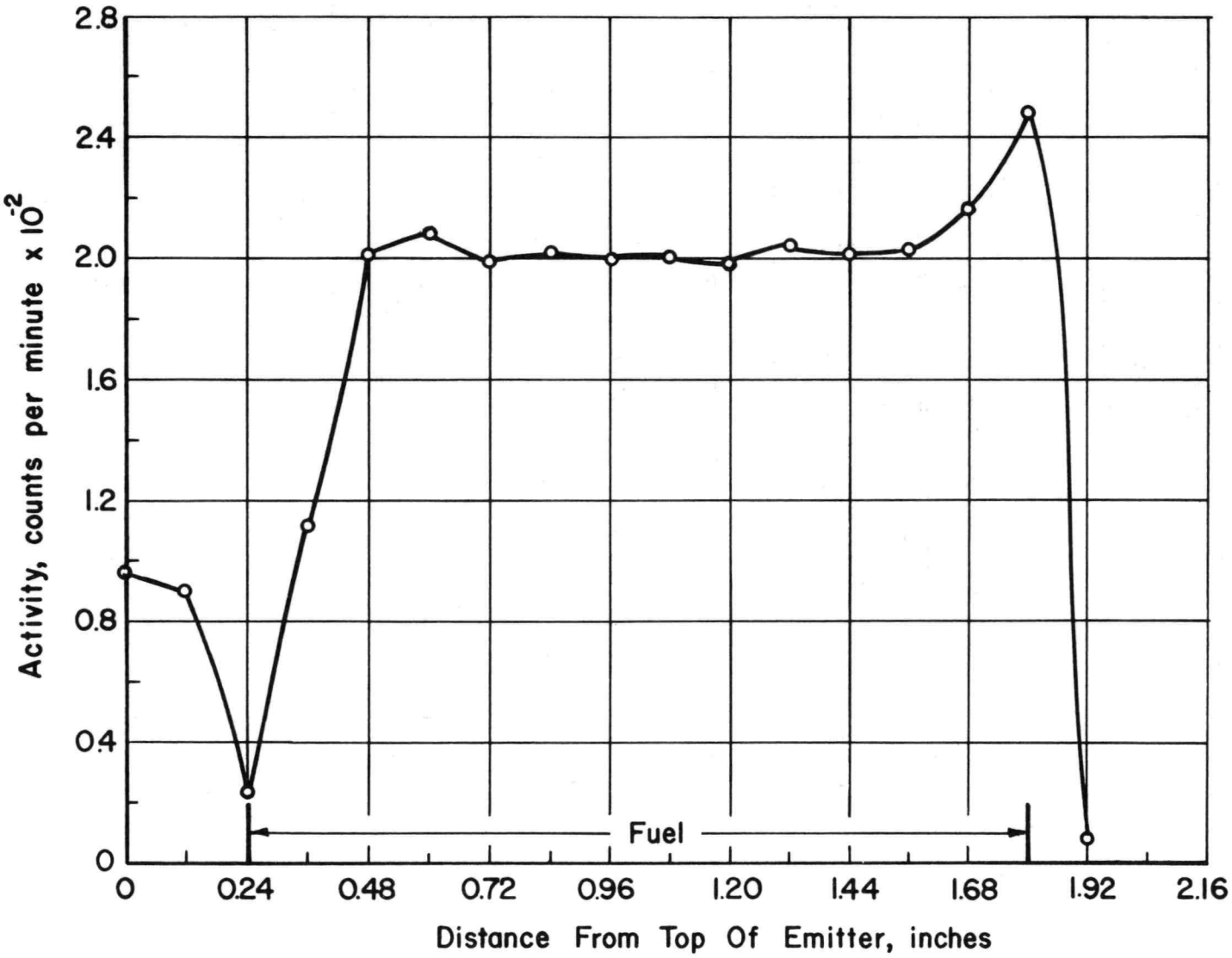

FIGURE 7. GAMMA SCAN OF SD-4 EMITTER

CONFIDENTIAL

TABLE 1. RESULTS OF ISOTOPIC ANALYSES OF FUEL FROM SD-4

Sample	Fraction of Uranium Isotope Present, w/o			
	U^{234}	U^{235}	U^{236}	U^{238}
SD-2 (control)	1.01	93.02	0.21	5.76
SD-4	1.02	92.46	0.64	5.88

TABLE 2. BURNUPS OBTAINED FROM ISOTOPIC ANALYSES AND POWER OUTPUT DURING OPERATION

Sample	Estimated Burnup Values			
	a/o U^{235} Fissioned		10^{20} Fissions per Cm^3 of Cermet	
	From In-Pile Calorimetry	From Isotopic Analyses	From In-Pile Calorimetry	From Isotopic Analyses
SD-4	1.7	2.3 ± 0.2	2.8	3.85

Fission-Gas Sampling

Fission-gas sampling of the outer can was accomplished through a special valve provided on the can.

The outer can containing the diode was initially evacuated through this valve which was then closed and its outlet sealed. Since this valve was above the vacuum-seal plate, the fission-gas sampling of the outer can was done before the diode was placed into the Remote Handling Facility. The gas-sampling procedure involved connecting an evacuated sampling system to the can through the valve provided. Then, using a Toepler pump, the gases contained in the can were transferred to a collection system of known volume. Samples were then removed from the collection system and analyzed by mass spectroscopy for total krypton and xenon. The amount of krypton and xenon released (6.7 cm^3) was 80 percent of the amount formed during irradiation, as calculated from the burnup measured analytically. Also, there was a large amount of helium (8.5 cm^3) in this volume which presumably leaked through the vacuum-seal plate. A low flow of helium was used continuously during the irradiation to purge the lead tube above the seal plate. Using a calculated volume of 6000 cm^3 for the void volume of the outer can, the total fission gases and helium would have resulted in a pressure of 1.93 mm of mercury in the outer containment can. In an effort to determine if the outer containment can leaked during irradiation, the can was evacuated through the special valve and a helium leak detector was connected into the system. Helium was then flowed around the outside of the can. The only detectable leak found was in one of the coolant lines. However, the size of this leak and the relatively short exposure to helium during a purge of the coolant lines would not seem to account for the amount of helium found in the can. It is possible

that the vacuum-seal plate, which was continually flooded with helium throughout the irradiation, could have had a very small leak that was not detectable by the measuring equipment available in the Hot Cell Facility.

The interelectrode space was sampled for fission gas by placing the entire diode into an evacuated chamber and drilling through the nickel tube connecting the cesium reservoir to the interelectrode spacing. The gases released from the interelectrode space were also pumped into an evacuated collection system of known volume by means of a Toepler pump. Samples of the gases were then removed from the collection system and analyzed by both gamma spectroscopy and mass spectroscopy. The emitter cavity of the diode was then sampled for fission gas in the same manner by drilling through the stainless steel gas-sampling tube at the top of the emitter. A very small amount, 8×10^{-4} cm^3 (0.01 percent of theoretical), of fission gas was found in the interelectrode space. A much larger amount (0.15 cm^3) of helium was found in this volume, however. The volume of the interelectrode spacing and the cesium reservoir was estimated to be about 7 cm^3. With a volume of 7 cm^3, the partial pressure of helium in the interelectrode space was calculated to be 16.7 mm of mercury. After termination of the irradiation, one of the water lines was evacuated in an effort to unplug them. Subsequent helium leak checks revealed a small leak in a water line at a point inside the outer containment can. It is, therefore, believed that some of the helium was removed from the outer can when the water line was evacuated. This accounts for the measured higher partial gas pressure (16.7 mm versus 1.93 mm of mercury) in the interelectrode space than in the outer can. This amount of helium could not have been present while the diode was operating as it would have cooled the emitter to the extent that no output would have been available. There is no readily apparent explanation of how the helium entered the interelectrode space.

Analyses of the gas collected from the emitter cavity indicated that no gases of any kind were present. The tube extending out the top of the emitter cavity broke off flush with the top of the diode during fission-gas sampling, but since the entire diode was within the sampling system, no loss of gas occurred. Since no gas was found in the emitter cavity, it was concluded that the emitter cavity leaked to the area outside the diode. Consequently, any gas contained in this volume was collected when the outer can was sampled, and any gas remaining in this volume was pumped out when the volume around the diode was evacuated prior to fission-gas sampling of the emitter cavity.

In order to determine the source of the fission gas in the outer can, the interelectrode space and the cesium reservoir were helium leaked checked prior to the attempt to sample for fission gas in the emitter cavity. This was accomplished by cutting the tube between the diode and the cesium reservoir, which had been drilled through for sampling of the fission gas, and then independently evacuating the interelectrode space and the cesium reservoir through the open ends of this tube. Helium was then flowed around the outside of the diode and the cesium reservoir. Any leak in the interelectrode spacing or the cesium reservoir would have been revealed by the helium leak detector connected into the evacuated system. No leak was found between the interelectrode space and the outside of the diode or in the cesium reservoir. After the emitter cavity had been sampled, which resulted in breaking off the tube at the top of the emitter cavity, the interelectrode space was again leak checked in the same manner as before. This was done to see if there was any leak between the emitter cavity and the interelectrode space. A leak was found, but additional tests indicated that it was in the weld between the stainless steel

tube provided for fission-gas sampling and the top of the emitter support ring. It is believed that this leak was introduced when the tube at the top of the emitter cavity broke off. The results of the fission-gas analyses support this theory. In an attempt to determine if volatile materials could have plugged any holes, the diode was heat treated in a vacuum furnace for 4 hr at 600 C and at 750 C. Helium leak checks after each anneal did not reveal any additional leaks in the diode. It therefore seems apparent that no leak developed in any part of the cesium envelope during the in-pile test.

Disassembly of Diode and Dimensional Measurements

In order to insure that adjacent surfaces of the diode components could be compared, all components which were to be separated were marked for orientation purposes. The diode was then dissassembled as follows. The emitter support ring and the emitter were removed from the diode by cutting the niobium insulator flange (refer to Figure 2) just below the ceramic seal. The ceramic seal was then removed by cutting the insulator flange just above it. Also, the bottom collector plug was removed by grinding away the weld at the bottom of the diode. Each of these parts, along with the cesium reservoir and the tube which had broken off of the top of the emitter, was examined in detail.

Emitter

A detailed visual examination of the emitter indicated that the fueled area had experienced a slight amount (2.7 percent on the diameter) of swelling but the surface appeared to be in excellent condition, as shown in Figure 8. Diameter measurements were obtained on the emitter using standard machinist micrometers at 0 deg and 90 deg of rotation at approximate 1/4-in. increments along the length. The results of these measurements are given in Table 3. The diameter of the short, nonfueled area at the top of the emitter was measured at several locations using a pair of ball-point micrometers. Both sets of measurements were estimated to be accurate to within 0.0005 in. It was assumed that the measurements at the top of the emitter had not altered during irradiation and were thus equivalent to the preirradiation data. On the basis of these data, the preirradiation diameter of the emitter was 0.4975 in. and the average swelling over the fueled area was 2.7 percent. There appeared to be some ovality of the emitter after irradiation with a diameter increase of 2.4 percent in one plane and 3.0 percent in the 90-deg plane. Measurement of the inside diameter of the emitter cavity indicated large variations. These data are also presented in Table 3. Later, visual and metallographic examinations revealed that the inner tungsten cladding had cracked and that fuel relocation had occurred both at the top and at the bottom of the emitter, causing the large variations of the inside diameter of the fuel that were observed.

Collector

Dimensional measurements were obtained on the inside diameter of the collector and the outside diameter of the heat exchanger in the same manner as that described for the emitter. The results of these measurements are presented in Table 4. The inside diameter was slightly larger at the bottom and uniformly became smaller toward the top. The uniformity of this taper suggested that it was present in the as-fabricated component and was not the result of irradiation.

CONFIDENTIAL/RD

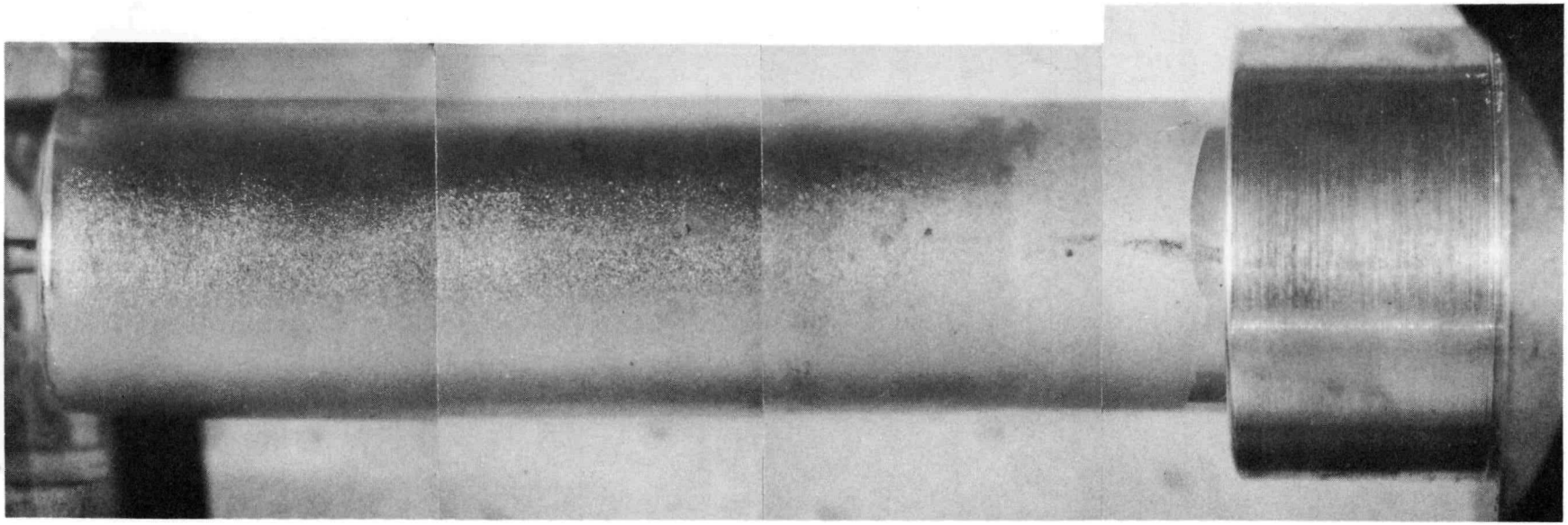

3.2X

P1282, P1285

FIGURE 8. CONDITION OF EMITTER SURFACE AFTER CLEANING

CONFIDENTIAL/RD

TABLE 3. DIMENSIONS OF EMITTER

Location of Measurement, in. from bottom of emitter	Outside Diameter of Emitter, in.			Increase in Outside Diameter of Emitter, percent		Inside Diameter of Emitter, in.			Change in Inside Diameter of Emitter, percent	
		Postirradiation					Postirradiation			
	Preirradiation	0 Deg	90 Deg	0 Deg	90 Deg	Preirradiation	0 Deg	90 Deg	0 Deg	90 Deg
0	0.4975	0.5120	0.5123	2.9	3.0	0.270	0.265	0.270	-1.9	0.0
0.25	0.4975	0.5114	0.5139	2.8	3.3	0.270	0.245	0.269	-9.3	-0.4
0.50	0.4975	0.5098	0.5140	2.5	3.3	0.270	0.274	0.270	+1.5	0.0
0.75	0.4975	0.5102	0.5131	2.5	3.1	0.270	0.274	0.266	+1.5	-1.5
1.00	0.4975	0.5101	0.5140	2.5	3.3	0.270	0.269	0.271	-0.4	+0.4
1.25	0.4975	0.5086	0.5122	2.2	3.0	0.270	0.270	0.272	0.0	+0.7
1.50	0.4975	0.5053	0.5063	1.6	1.8	0.270	0.237	0.235	-12.0	-13.0

TABLE 4. DIMENSIONS OF COLLECTOR

Location of Measurement, in. from bottom of collector	Outside Diameter of Heat Exchanger, in.		Inside Diameter of Collector, in.	
	0 Deg	90 Deg	0 Deg	90 Deg
0	1.6625	1.6647	0.5227	0.5231
0.25			0.5229	0.5230
0.50	1.6610	1.6603	0.5229	0.5229
0.75			0.5226	0.5226
1.00	1.6633	1.6630	0.5224	0.5224
1.25			0.5223	0.5222
1.50	1.6640	1.6592	0.5222	0.5223
1.75			0.5221	0.5223

After the dimensional measurements were obtained, the collector was sectioned longitudinally so that its surface could be examined in detail. Figure 9 shows photographs of the collector surface before and after cleaning. There was a fairly extensive discolored area (which shows lighter in the photographs) on the collector surface about one-third of the way down from the top and also a small area about two-thirds of the way down from the top. There was no evidence of similar markings on the mating emitter surface. Axial surface-profile measurements along the collector surface indicated that there was no detectable difference in surface roughness or surface level in the discolored areas as compared with nondiscolored areas.

Upper Ceramic Seal

Visual examination of the main diode insulator did not reveal anything unusual. The inside surface of the ceramic, as shown in Figure 10, appeared to be in excellent condition. Voltage-breakdown tests, however, indicated that arcing through the insulator occurred at voltage readings of 10 v or less, which was the minimum detectable reading on the measuring equipment used. Measurements indicated a resistance across the seal of 510 ohms, and attempts to clean up the surface of the ceramic with a wire brush to remove fused material and increase the voltage required for breakdown were unsuccessful. The resistance increased after each cleaning but after several cleanings, it was still only 3200 ohms, and no voltage reading could be obtained. Voltage-breakdown tests were also conducted on the top ceramic seal of a duplicate diode (SD-2) which was operated only out-of-pile. In this case the voltage required for breakdown was 500 v and, after the ceramic surface was cleaned with a wire brush after each test, this same value was measured several times. The bottom ceramic insulating bushing of SD-4 was examined and was found to have a coating of white material over a large portion of its top surface. There also appeared to be a small circumferential crack between the ceramic and the metal on one side as shown in Figure 11. The bottom ceramic insulating bushing otherwise appeared to be in good condition.

Heat Shield

The heat shield in the top of the emitter cavity was removed and examined. The bottom surface nearest the fuel was coated with a heavy deposit of a very coarse, friable material (Figure 12a) which looked very similar to vapor-deposited UO_2. Later chemical analyses revealed that it was indeed UO_2 which apparently had moved from the fuel by vapor transport. Figures 12b and 12c show that this coating was only on the bottom surface of the heat shield, i.e., the first tungsten-foil radiation shield. The top of the heat-shield plug appeared to be unchanged, with all machining marks still plainly visible.

Copper Cooling Straps

The copper cooling straps (Figures 13 and 14), connecting the heat exchanger to the cesium reservoir were removed and their dimensions were measured. The straps were 2.37 in. long by 0.42 in. wide by 0.23 in. thick. One of the straps had broken loose from the heat exchanger (Figure 14). It appeared that the failure occurred because of fracture of the bolt holding it to the heat exchanger. It is not known whether

CONFIDENTIAL

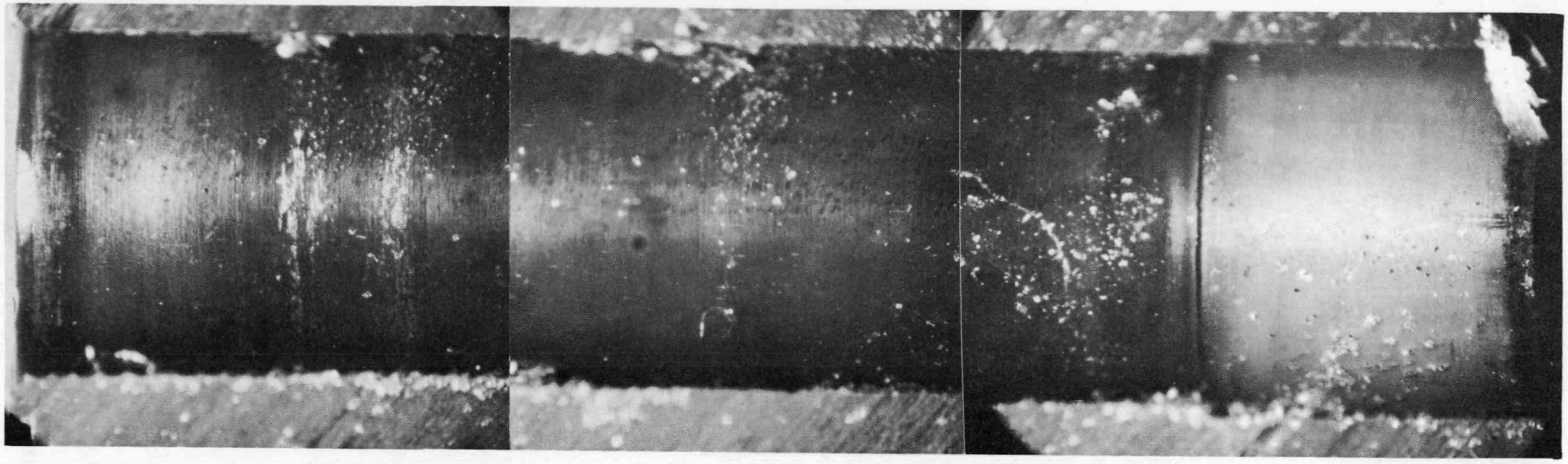

~ 3.4X

P1310, P1311, P1312

a. Before Cleaning

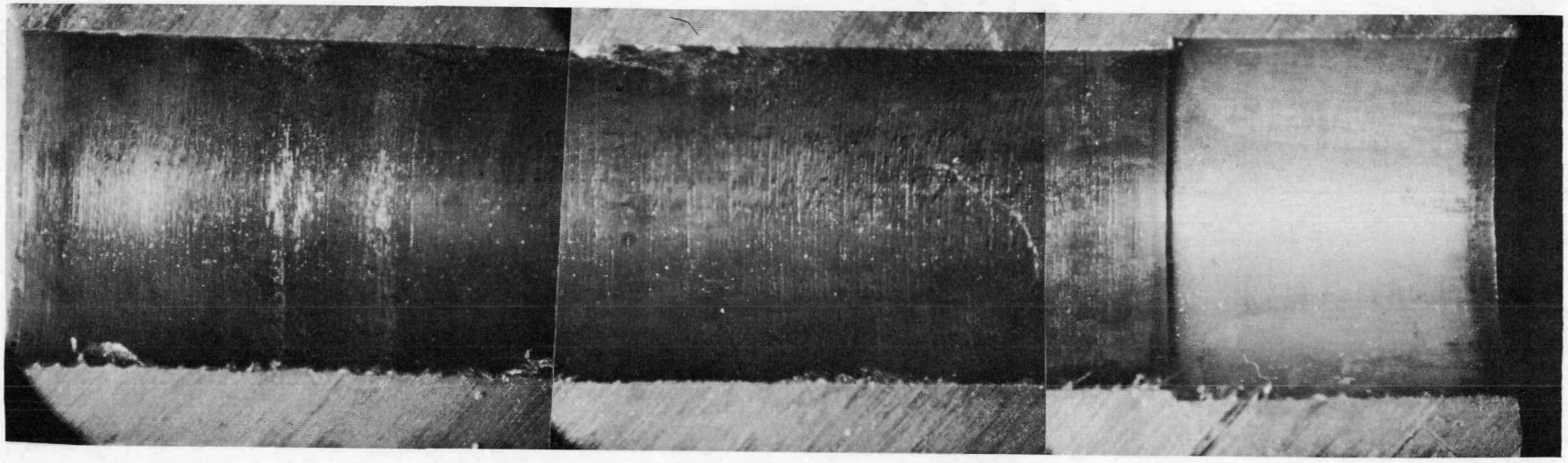

~3.4X

P1313, P1314, P1315

b. After Cleaning With Alcohol and Water

FIGURE 9. CONDITION OF COLLECTOR SURFACE

CONFIDENTIAL

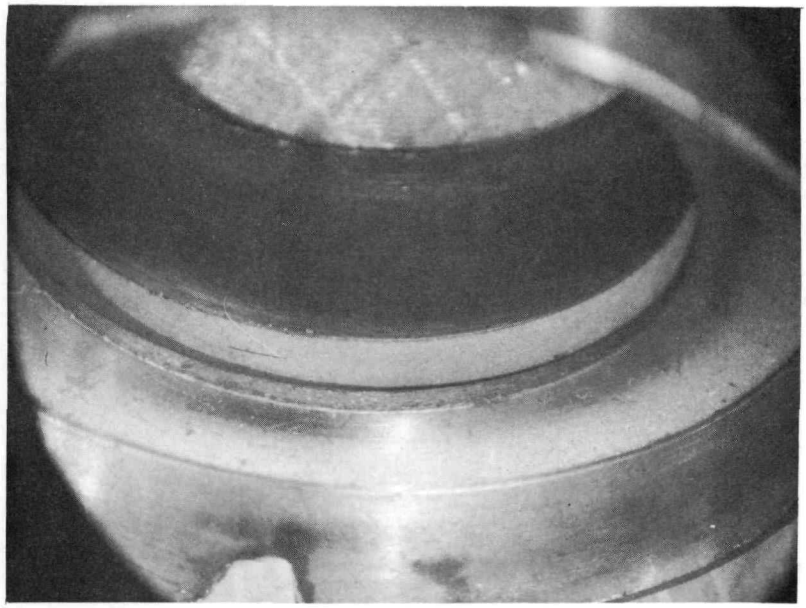

10X P1300

FIGURE 10. INSIDE SURFACE OF THE TOP CERAMIC INSULATOR

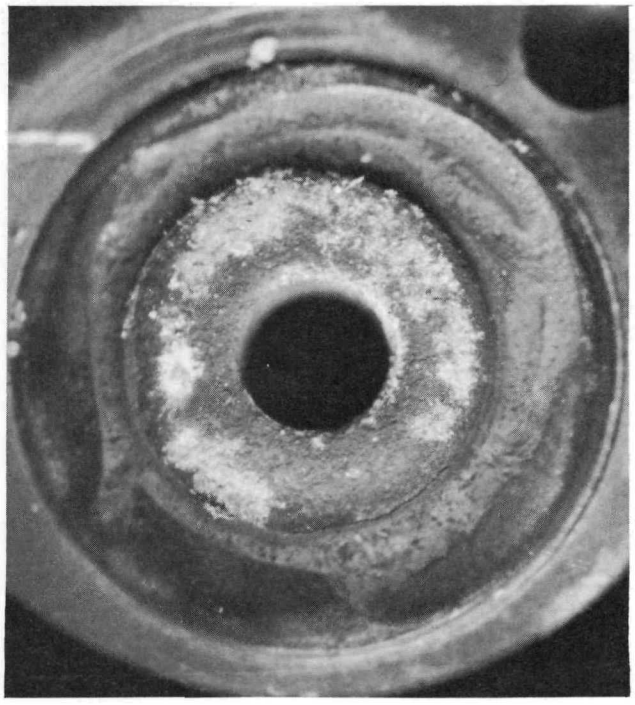

10X P1305

FIGURE 11. TOP SURFACE OF BOTTOM CERAMIC INSULATOR BUSHING

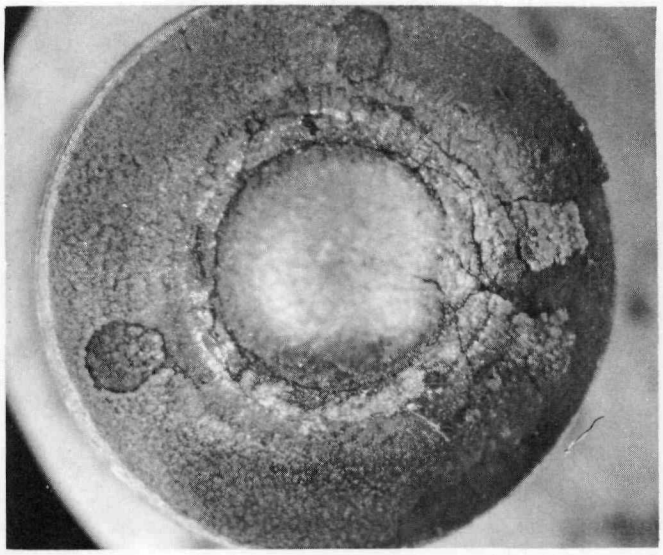

6X P1297

a. Bottom, or Surface Nearest Fuel

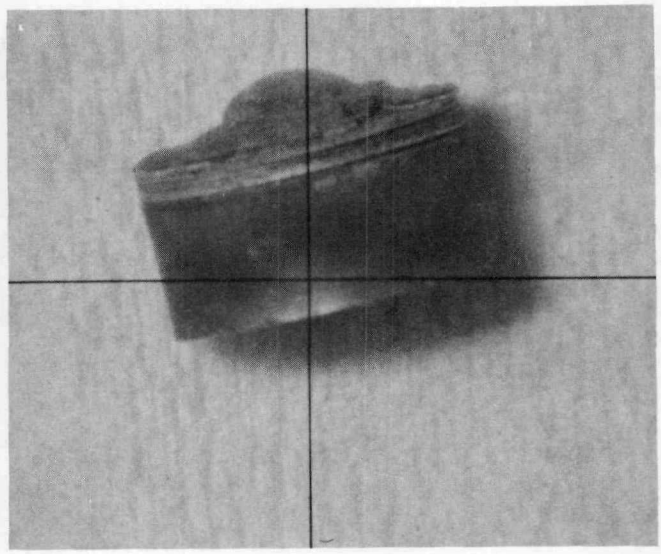

4X P1323

b. Side View of Heat Shield

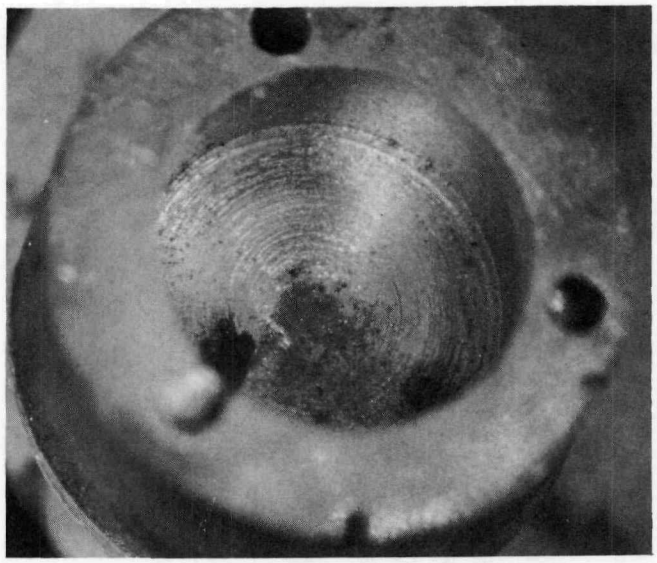

6X P1298

c. Top Surface of Heat Shield

FIGURE 12. SURFACE CONDITION OF THE HEAT SHIELD AT THE TOP OF THE EMITTER CAVITY

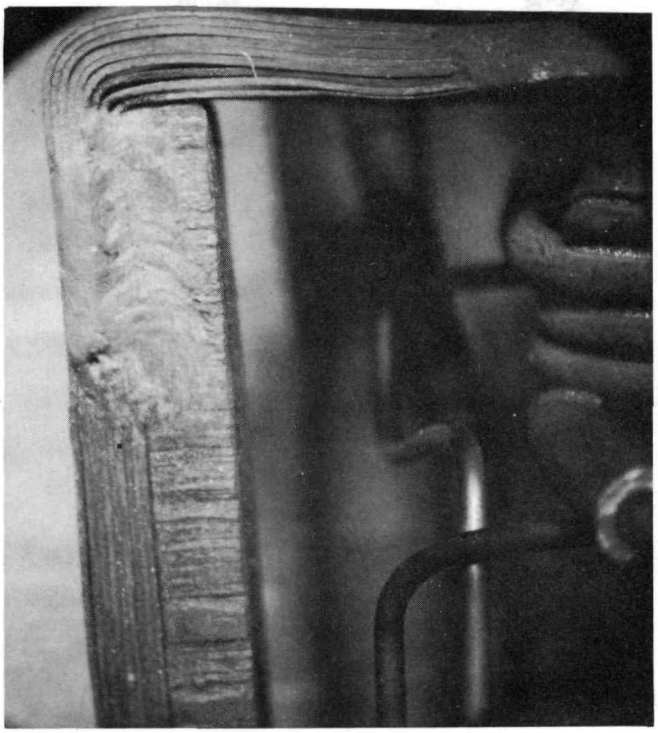

4X P1233

FIGURE 13. COPPER COOLING STRAP CONNECTING HEAT EXCHANGER TO CESIUM RESERVOIR

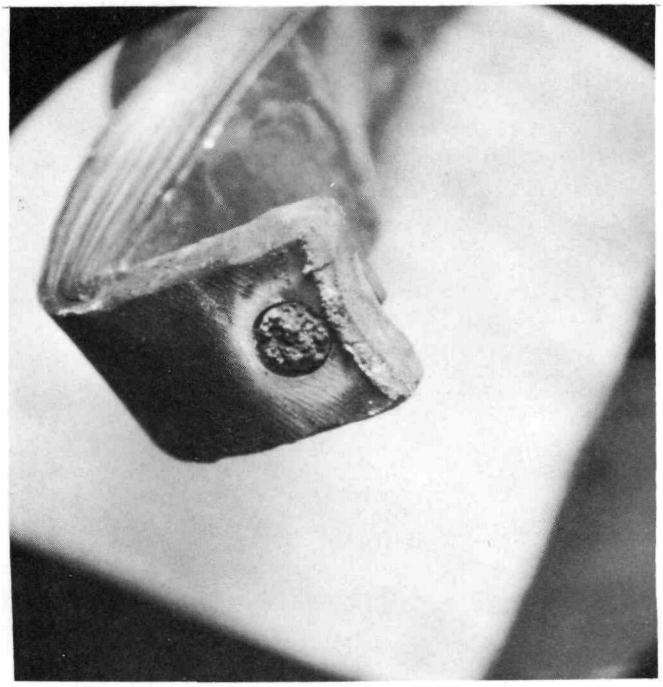

2X P1225

FIGURE 14. FRACTURED STUD THAT HELD COPPER COOLING STRAP TO HEAT EXCHANGER

this fracture occurred during irradiation or during subsequent handling of the diode. Other than this, the straps did not show any evidence of deterioration.

Cesium Reservoir

The cesium reservoir was examined for evidence of deterioration and none was found (Figure 15). An attempt was made to visually determine the amount of cesium remaining in the cesium reservoir but it was not possible to get sufficient light into the hole. The reservoir was weighed and then baked in a vacuum furnace at 650 C for 4 hr to vaporize and remove any cesium in the reservoir. The reservoir was again weighed. A weight loss of 0.0052 g, which was assumed to represent the weight of cesium in the reservoir prior to the heating, was measured. The cesium reservoir was then leak checked again with helium to see if the cesium removal had opened any leaks. The results of this leak test again indicated that there were no leaks in the cesium reservoir.

Sectioning for Burnup and Metallography

Further disassembly of the diode consisted of removal of small sections from component parts for metallographic examination and for burnup analysis of the fuel. A diamond cutting wheel was used to section the emitter and a coarse abrasive wheel was used for cutting all other components. The burnup sample was a complete cross section of the fuel about 1/4 in. long removed from the axial center of the emitter. The rest of the emitter was sectioned longitudinally and one half of each of the upper and lower sections were set aside for longitudinal metallographic samples. Also, the remaining half of the upper section of the emitter was set aside for a transverse metallography sample. Small longitudinal sections of the emitter support ring, the main diode insulator, the collector and heat exchanger, and the tube connecting the cesium reservoir to the diode were also removed for metallographic examination.

Examination of the surface of the inner tungsten cladding of the emitter revealed several cracks and a deposit of UO_2 at the top and bottom of the fueled section (Figure 16). No separation of the fuel from either of the claddings occurred during sectioning or subsequent handling.

Metallographic Examination

Sections of the irradiated SD-4 diode along with sections of the emitter and ceramic seal of the nonirradiated SD-2 diode heated electrically for 2500 hr were prepared for metallographic examination by mounting them in an epoxy resin. The samples were prepared by grinding through 240-, 400-, and 600-grit SiC paper and then rough polished with 1/2-μ-diameter diamond dust on a silk cloth with kerosene as a lubricant. The final polish was made with Linde A on a Microcloth with water as a lubricant. The fuel was etched with a solution of 10 cm^3 of H_2SO_4, 90 cm^3 of H_2O_2, and 1 cm^3 of HF. The rhenium cladding was examined under polarized light so that no etchant was required. Also, the Al_2O_3 in the ceramic seal was not etched. The etchant used for the collector, which was primarily niobium with a vapor-deposited layer of molybdenum on the collector surface, was a solution of 50 cm^3 of lactic acid, 30 cm^3 of HNO_3, and 2 cm^3 of HF.

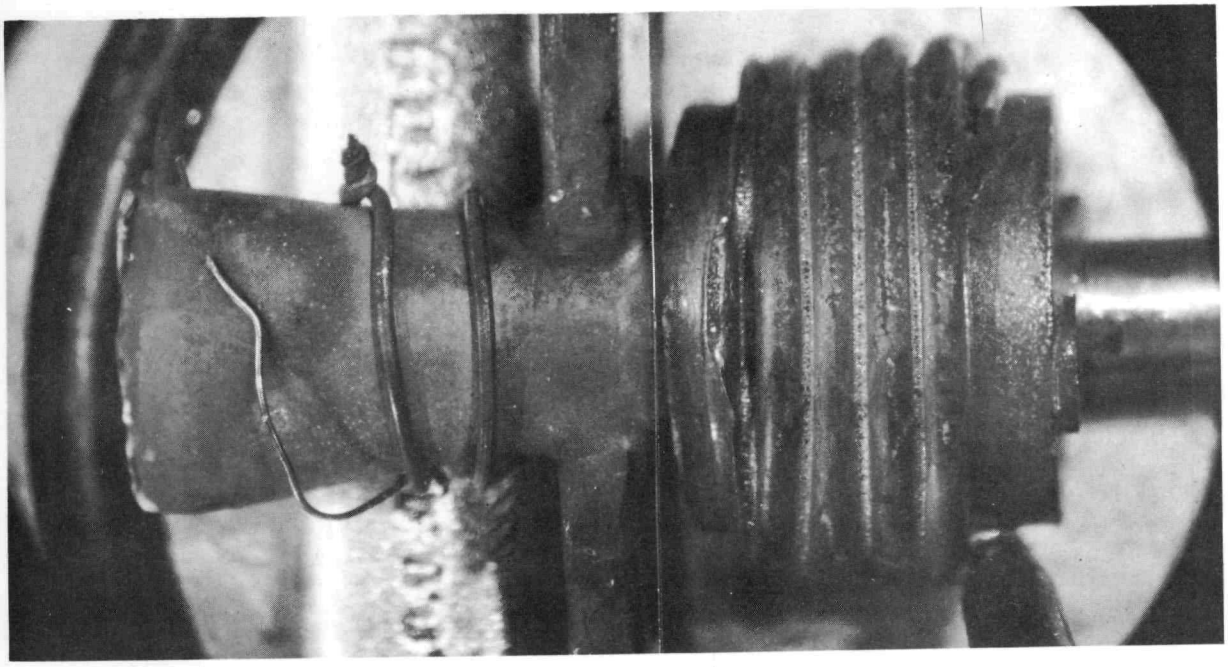

4X

P1319, P1320

FIGURE 15. CESIUM RESERVOIR FOR SD-4

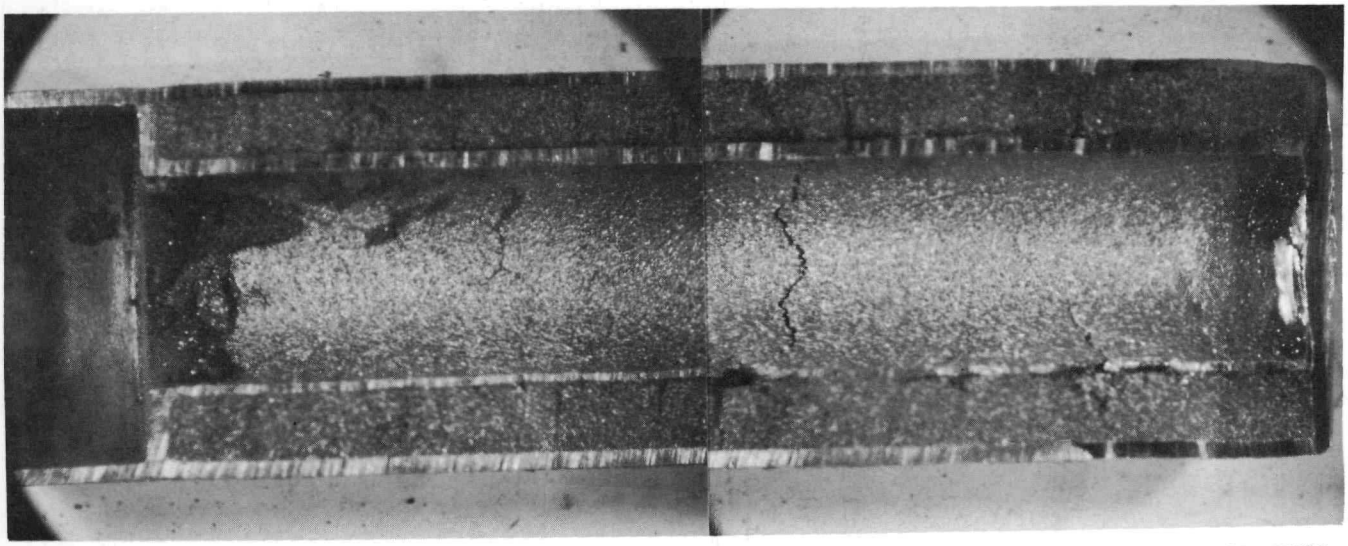

4X

P1327, P1328

FIGURE 16. INSIDE SURFACE OF EMITTER CAVITY

In the SD-2 diode, operated 2500 hr out-of-pile, the microstructure of the fuel was considerably changed from that of the as-fabricated material (Figure 17a). Areas of fuel near the inner diameter or heat-input surface of SD-2 were almost completely devoid of tungsten matrix material (Figure 17b). Away from the liner-cermet interface, considerable void space developed at the fuel-matrix interfaces (Figures 17c and 17d). It is believed that these voids were the result of growth and recovery processes occurring during thermal cycling.

The same type of migration (Figure 18a) occurred in the irradiated material at the inner liner-cermet interface but to a much lesser degree than in the nonirradiated material. The thermal gradient in the irradiated material may have been smaller than in the nonirradiated material. In the nonirradiated material, the source of heat was a heater in the emitter cavity, whereas in the irradiated emitter the source of heat was the fission process which, because of the attenuation of the neutrons, was greatest at the outer diameter surface. Some heat was being generated throughout the fuel, however. There was a much larger amount of porosity and cracking in the irradiated fuel (Figure 19) than in the nonirradiated fuel. Some of the voids may have developed, as in SD-2, during the initial 100-hr out-of-pile electrically heated test, but the increase in size and number of voids and cracks in the irradiated material is believed to be due primarily to the accumulation of fission products generated during the irradiation. It is doubtful that the thermal cycling was more severe in the irradiated material than in the nonirradiated material.

As noted during the visual examination, there appeared to be UO_2 deposited at both the top and the bottom of the emitter cavity. These areas are illustrated in Figures 20 and 21. The UO_2 deposited in these areas by vapor transport was significantly different from the UO_2 inside the cladding in that it appeared to have a columnar structure radiating away from the surface to which it was attached. Also, most of it was relatively free of the tungsten matrix material.

Composite photomicrographs of the emitter samples were obtained and are presented in Figures 22, 23, and 24. Each composite has higher magnification inserts included to show the condition of the fuel at different locations along the length of the emitter. Figure 23 is a transverse cross section of half of the emitter at about the axial center of the emitter. There seems to have been less movement of UO_2 and/or tungsten matrix near the top of the emitter than in the middle or at the bottom. The fact that the inner tungsten cladding is considerably thinner on one side than on the other is believed to be the result of fabrication procedures and not of movement of tungsten into the fuel. Figure 25 is a highly magnified view of the area shown in the circled area labeled "A" in Figure 23. This area shows that the UO_2 has taken on a columnar grain structure and must have operated at considerably higher temperatures than the surrounding UO_2 particles. The identity of the white-looking pieces of material shown in this area was not established. It was believed that they could be either tungsten or the fission-product alloy often found in irradiated UO_2. However, autoradiography, discussed later, indicated that this material is not the fission-product alloy. It was concluded that these areas resulted from localized variations in chemistry (stoichiometry) which may have nucleated during the out-of-pile electrically heated testing.

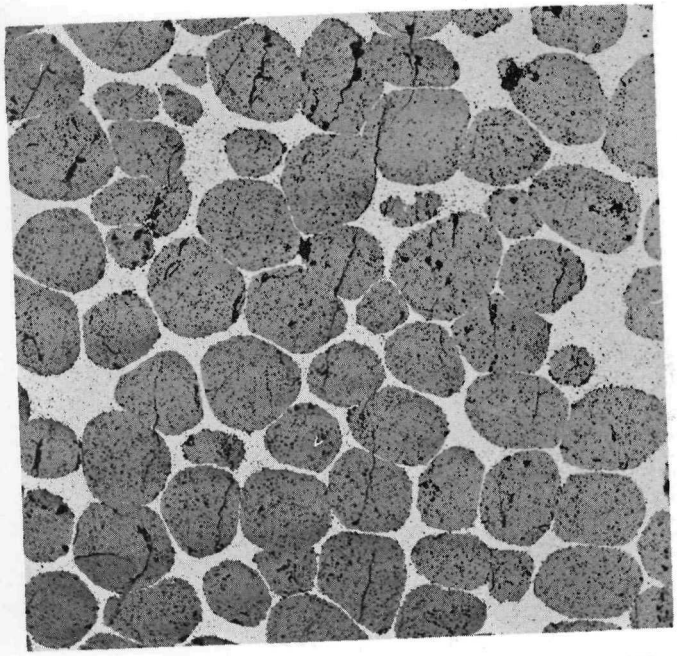

100X RM41652

a. As-Fabricated Fuel

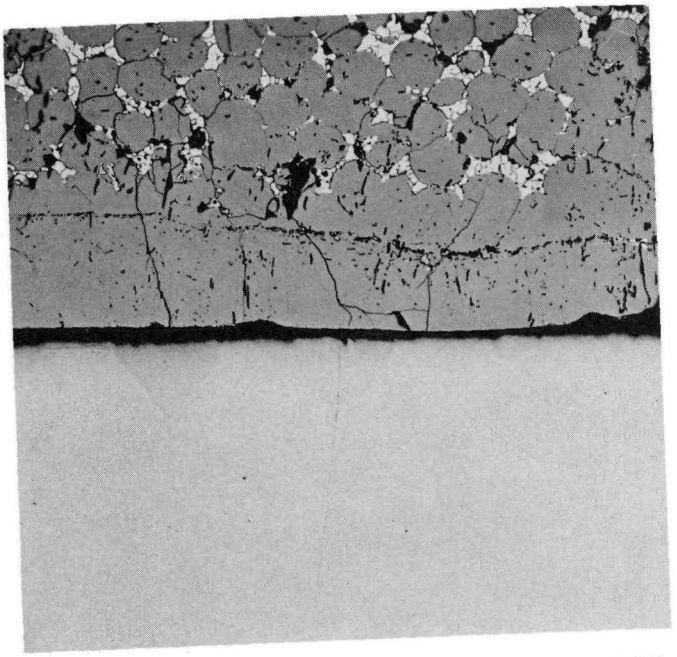

50X OD739

b. Inside Clad-Fuel Interface

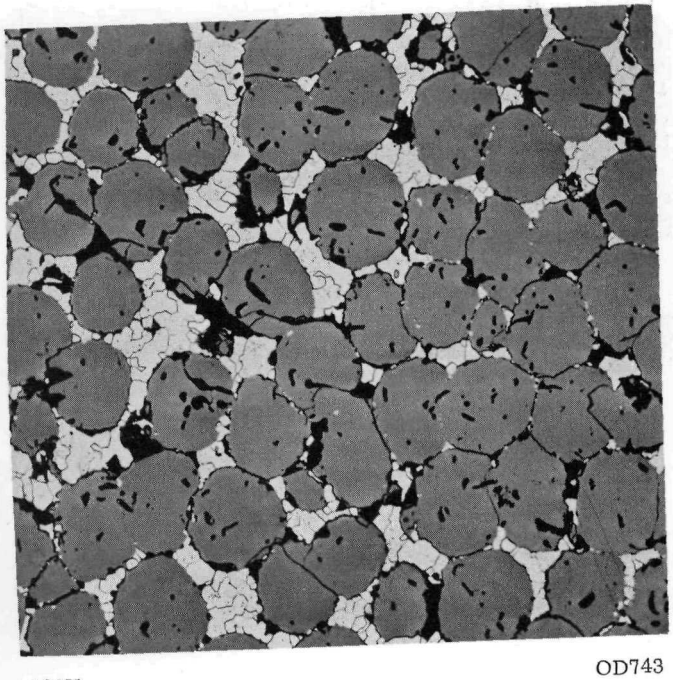

100X OD743

c. Typical Area Near Fuel

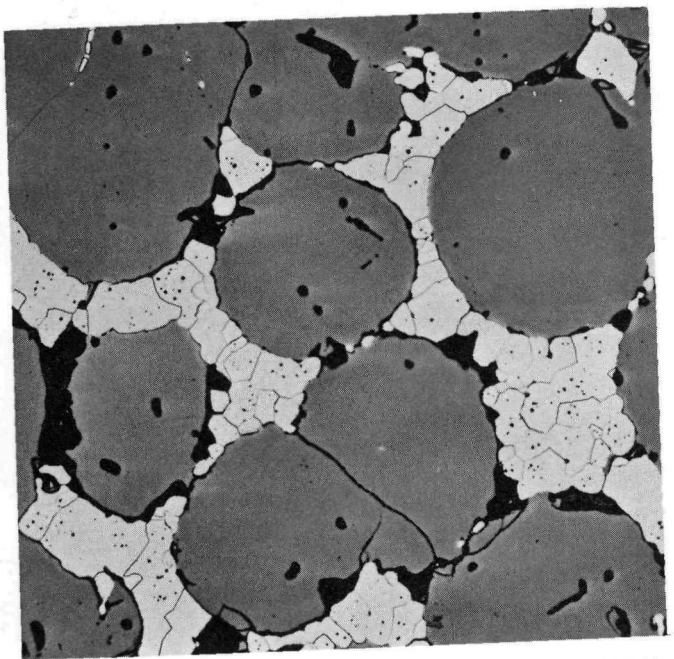

250X OD744

d. Typical Area Near Center of Fuel

FIGURE 17. MICROSTRUCTURE OF THE FUEL FROM SD-2 WHICH WAS OPERATED OUT-OF-PILE

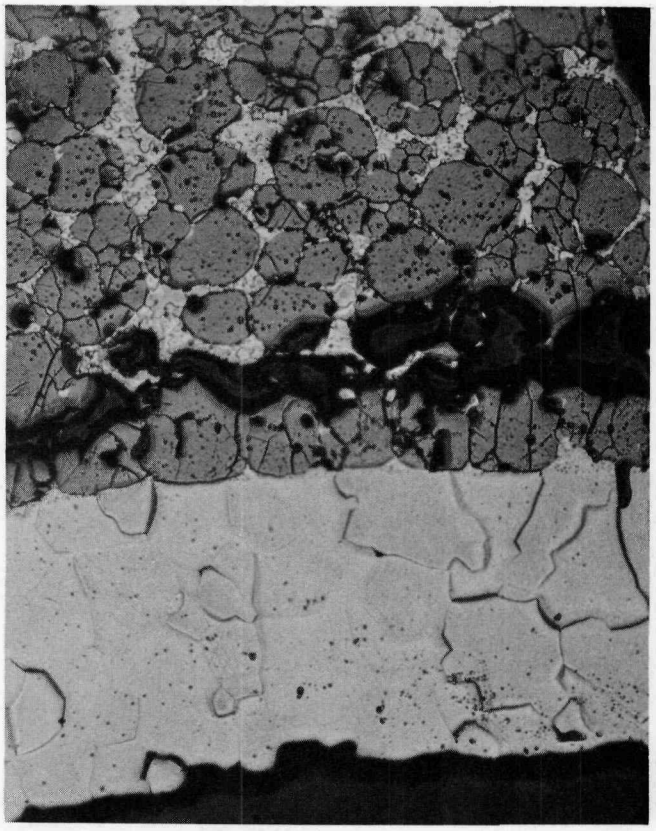

100X HC21570

a. Tungsten (Inner Cladding)-Core Interface

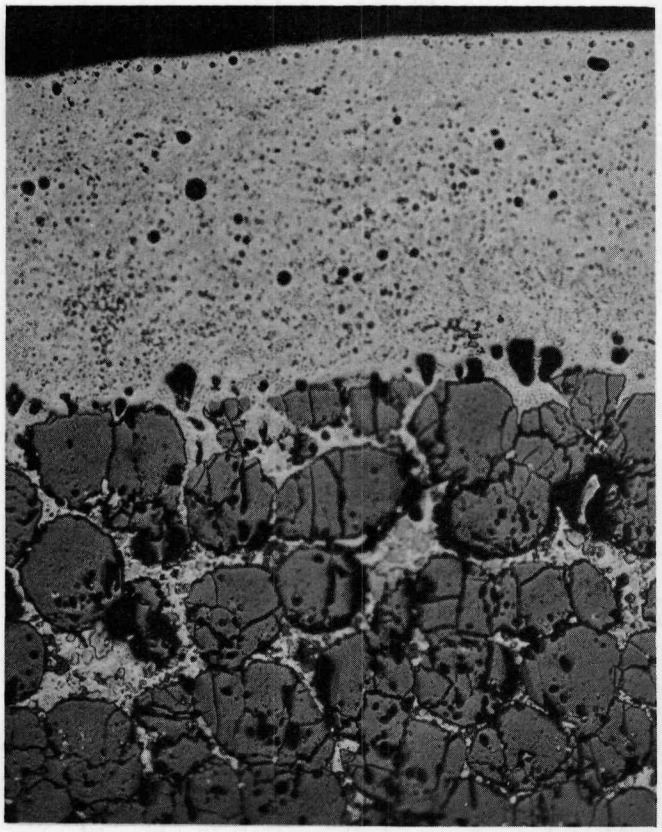

100X HC21571

b. Rhenium (Emitter Surface)-Core Interface

FIGURE 18. MICROSTRUCTURE OF IRRADIATED FUEL AT CLADDING-CORE INTERFACES

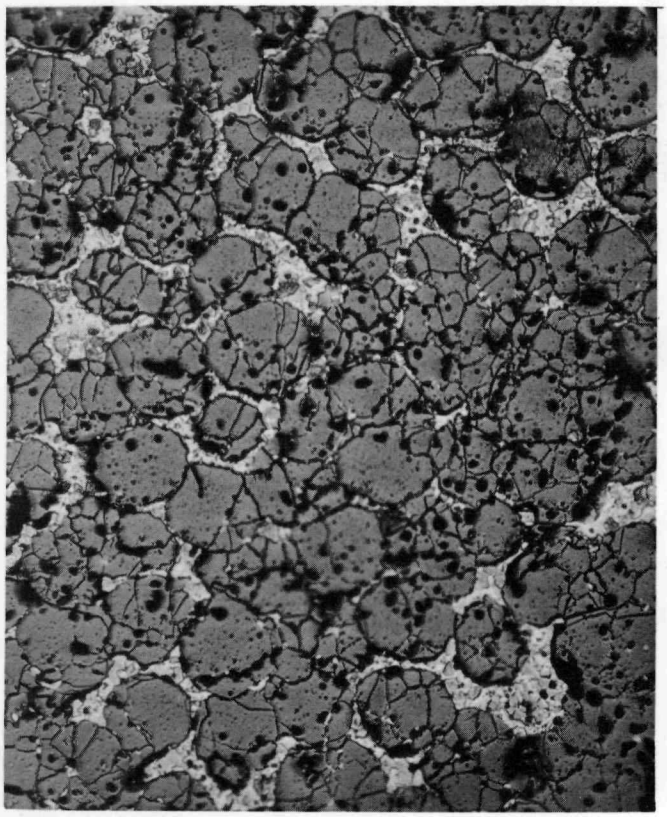

100X HC21572

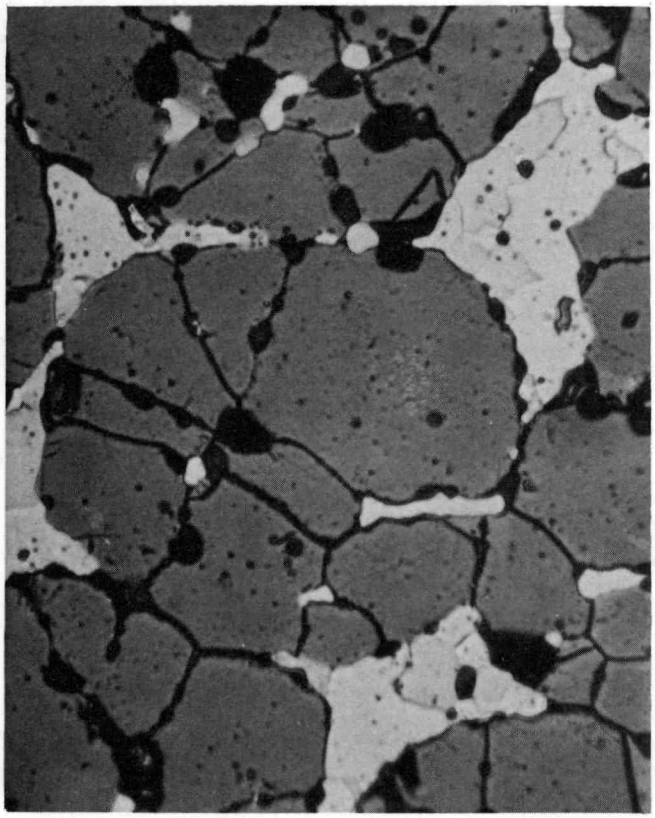

500X HC21581

FIGURE 19. TYPICAL MICROSTRUCTURES OF IRRADIATED FUEL

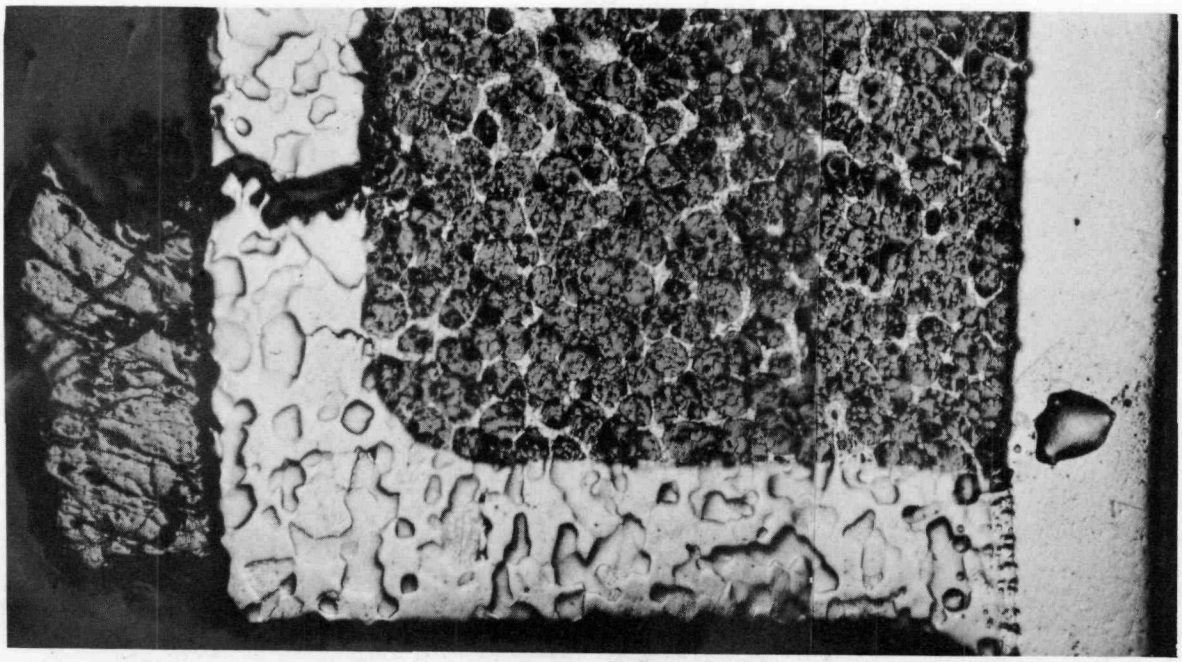

40X HC21551, HC21552

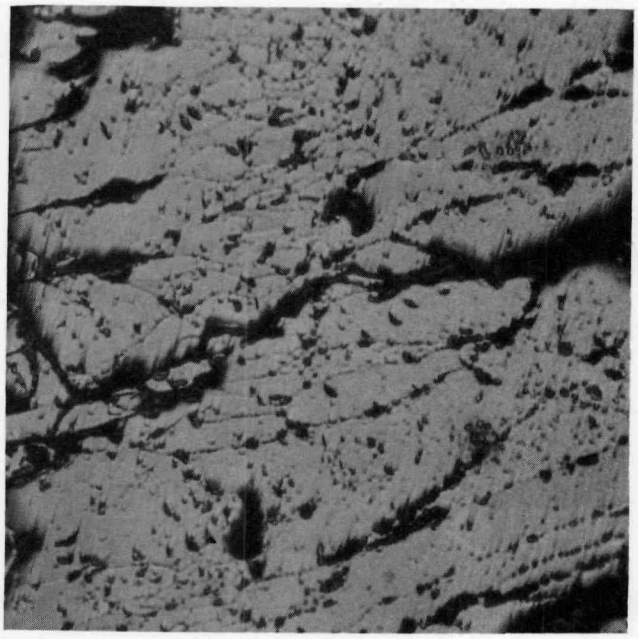

250X HC21616

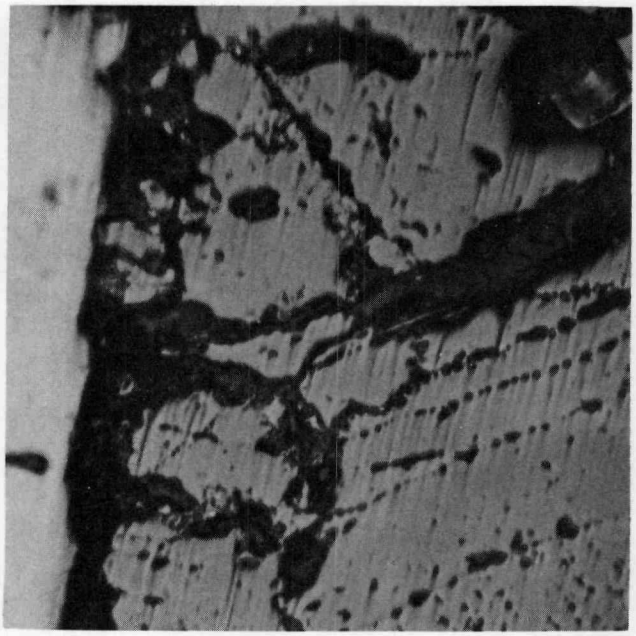

500X HC21611

FIGURE 20. UO_2 DEPOSITED NEAR THE TOP OF THE EMITTER CAVITY BY VAPOR DEPOSITION

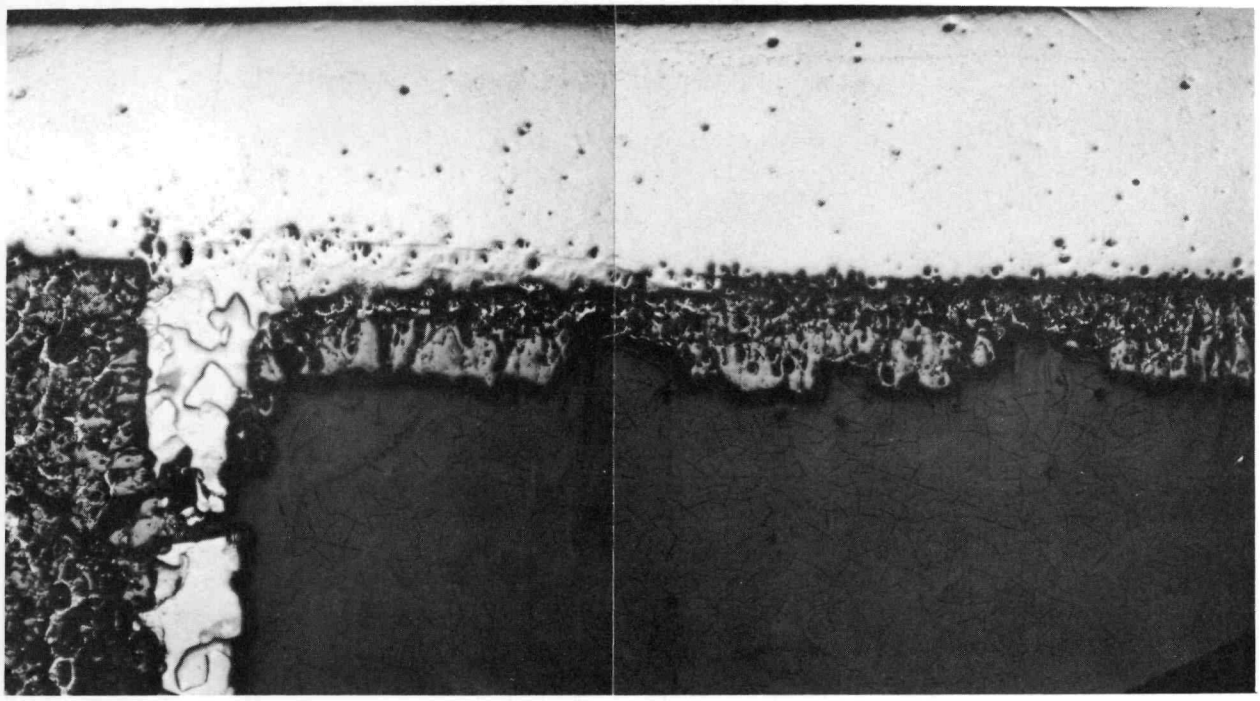

40X HC21565, HC21566

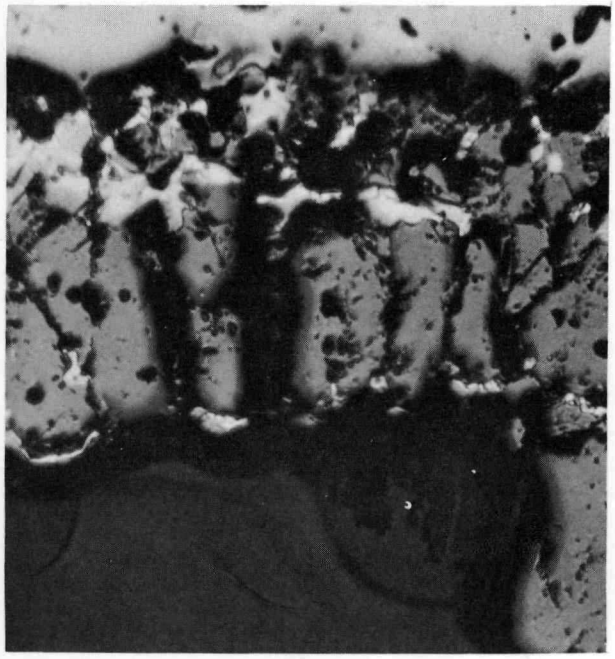

250X HC21621

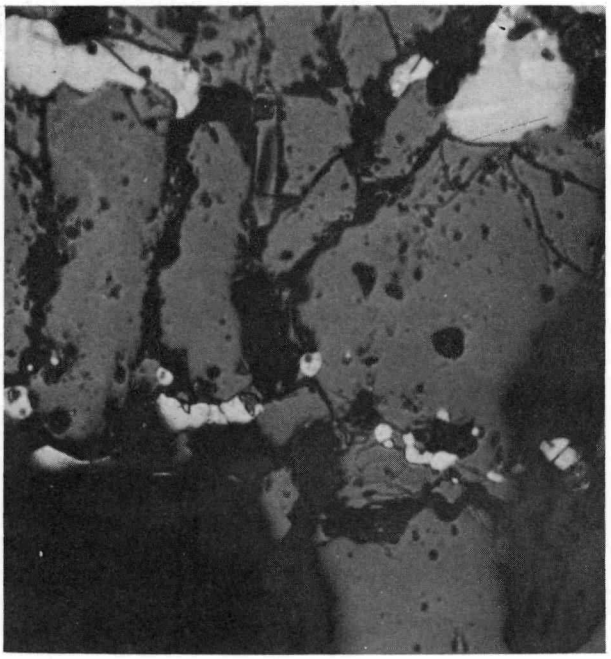

500X HC21616

FIGURE 21. UO_2 DEPOSITED AT THE BOTTOM OF THE EMITTER CAVITY BY VAPOR DEPOSITION

CONFIDENTIAL

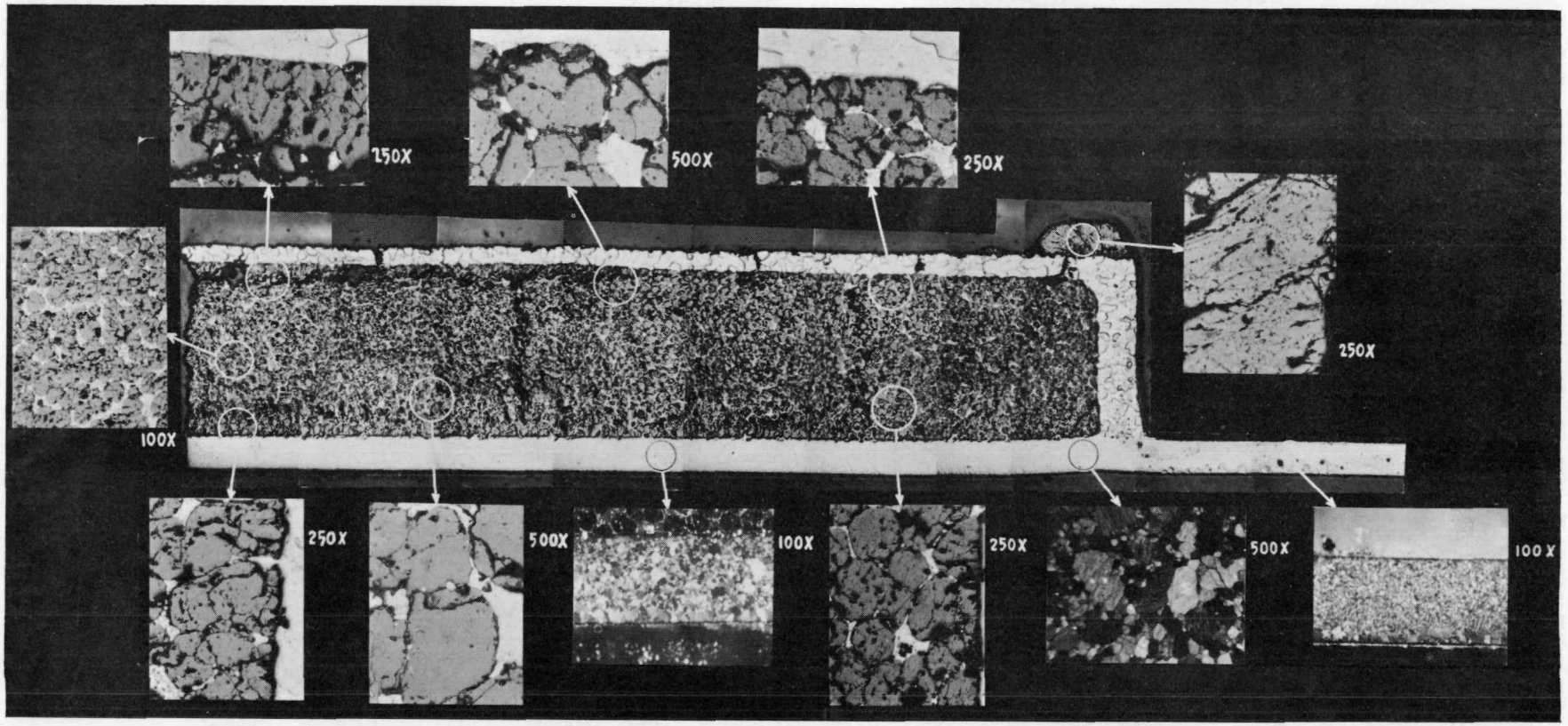

~8X

P1700

FIGURE 22. COMPOSITE OF TOP HALF OF EMITTER

CONFIDENTIAL

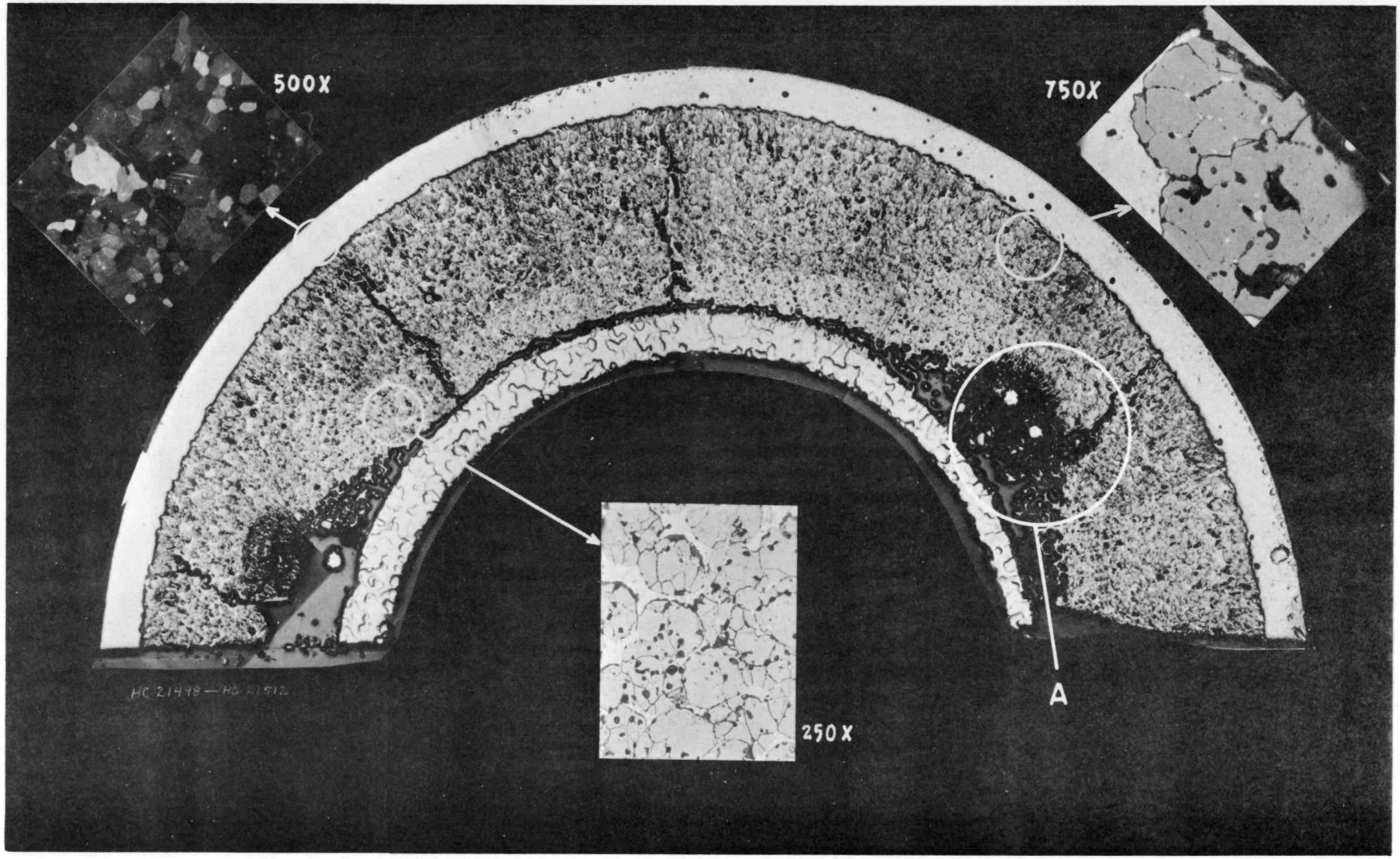

~16X P1702

FIGURE 23. COMPOSITE OF TRANSVERSE CROSS SECTION OF FUEL NEAR AXIAL CENTER OF EMITTER

CONFIDENTIAL
CONFIDENTIAL

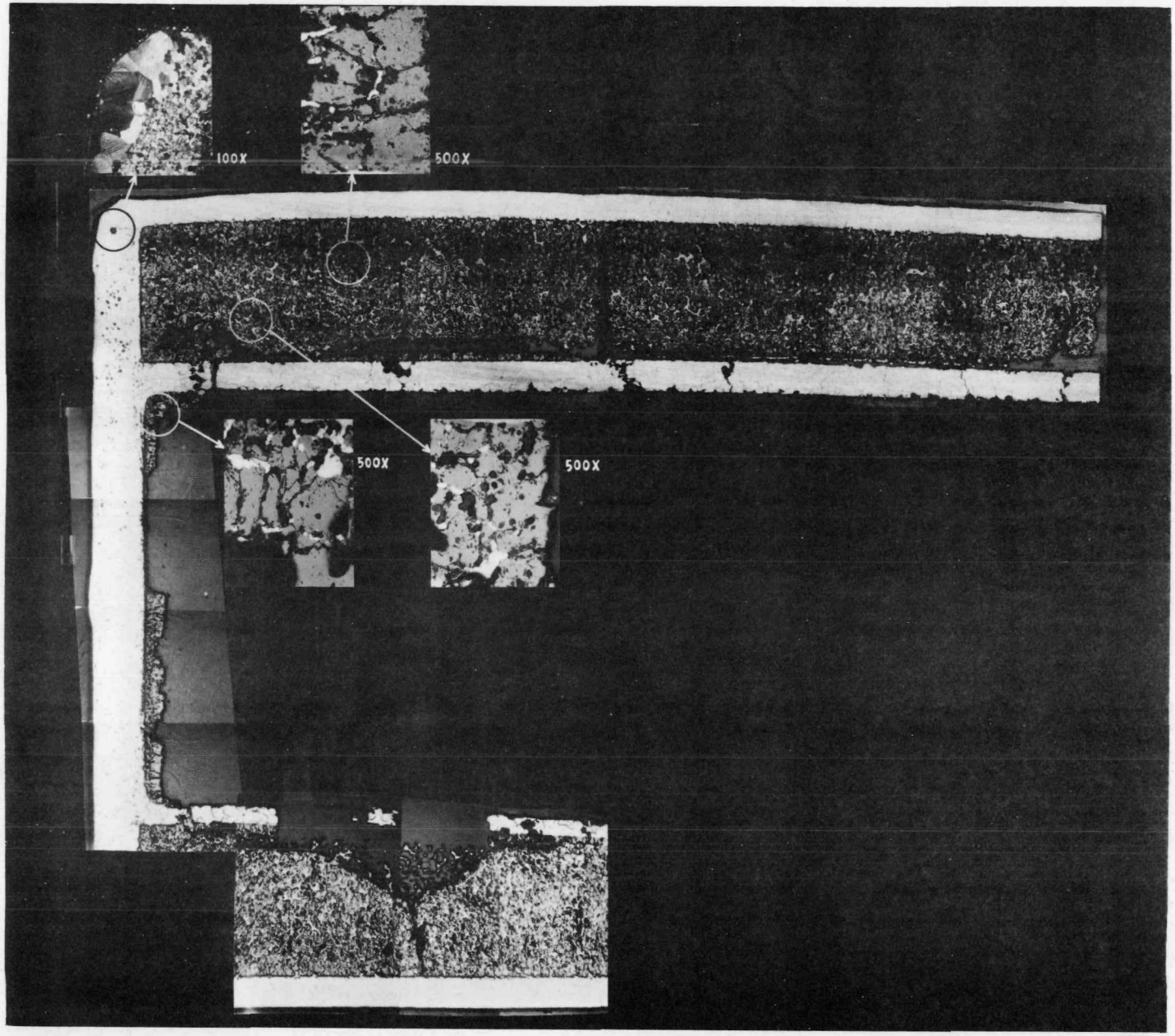

10X P1701

FIGURE 24. COMPOSITE OF BOTTOM HALF OF EMITTER

CONFIDENTIAL
CONFIDENTIAL

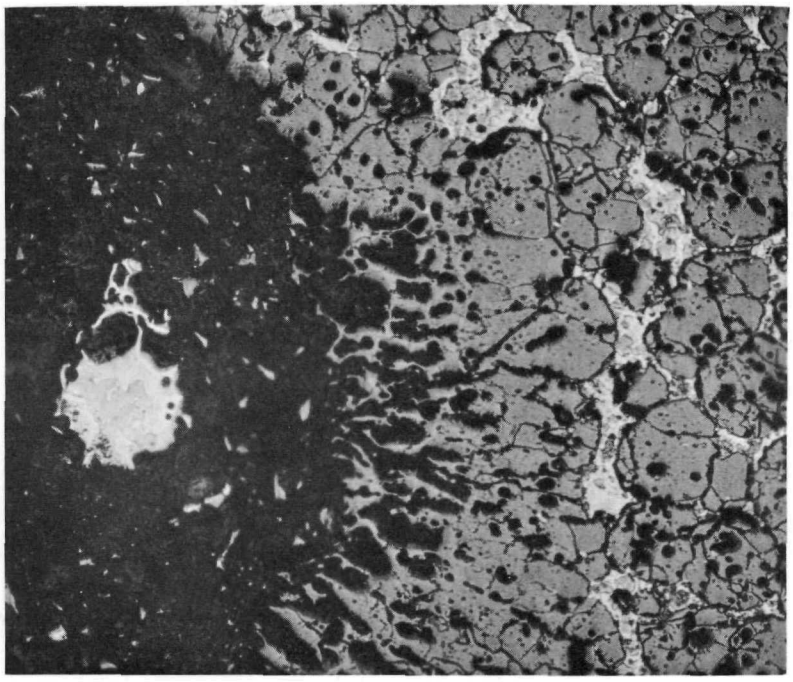

100X HC21569

FIGURE 25. APPARENT HOT SPOT IN FUEL NEAR INNER CLADDING-CORE INTERFACE

The microstructure of the rhenium cladding (emitter surface) revealed that the grains at the emitting surface were, in general, much larger than the grains in the interior of the cladding and at the cladding-fuel interface. Also, the grain size in the interior of the cladding and at the cladding-fuel interface was much larger in the fueled area of the emitter than it was in the nonfueled areas. The grain size at the emitting surface, however, did not appear significantly different in the fueled area as compared to the nonfueled areas. Figure 26 shows representative microstructures of the rhenium cladding above the fuel, at the top of the fuel, near the center of the fuel, and near the bottom of the fuel. Figure 27 shows, at higher magnification, the structures at the top and near the center of the fueled region of the emitter. There is little or no change in grain size at the emitting surface in the fueled areas as compared to the nonfueled area, but there is a great difference in the grain sizes at the two locations a small distance in from the emitting surface. Machining of the rhenium resulted in cold working of the outer layer of metal, providing a driving force for recrystallization and grain growth. Grain growth also occurred in the unworked interior rhenium opposite the fuel but to a lesser extent. Little or no grain growth occurred in the unworked interior rhenium in the nonfueled area of the emitter.

The metallographic study of the collector and heat exchanger consisted of examination of the collector surface for evidence of any kind of reaction or attack and an examination of the heaters and weld areas attaching the heat exchanger to the collector. A thin layer of molybdenum had been vapor deposited on the niobium collector surface prior to irradiation. It appeared that the molybdenum layer was still very uniform and about 0.4 mil (10 μ) thick. There was no evidence of any reaction or corrosive attack on this

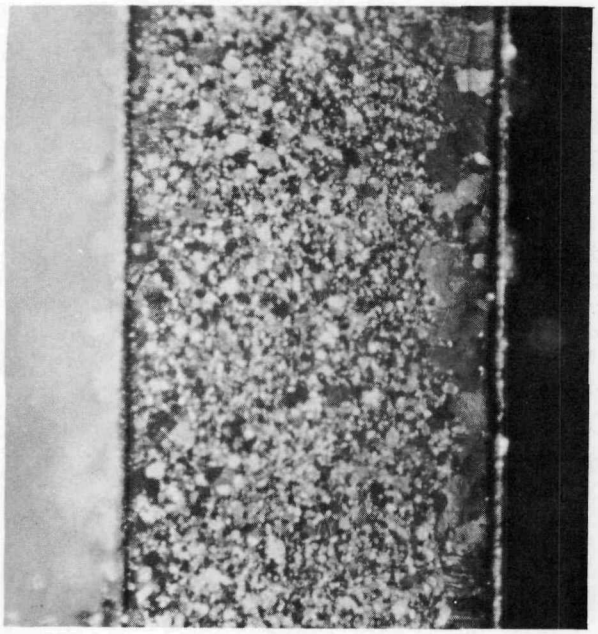

100X HC21594

a. Above the Fueled Area

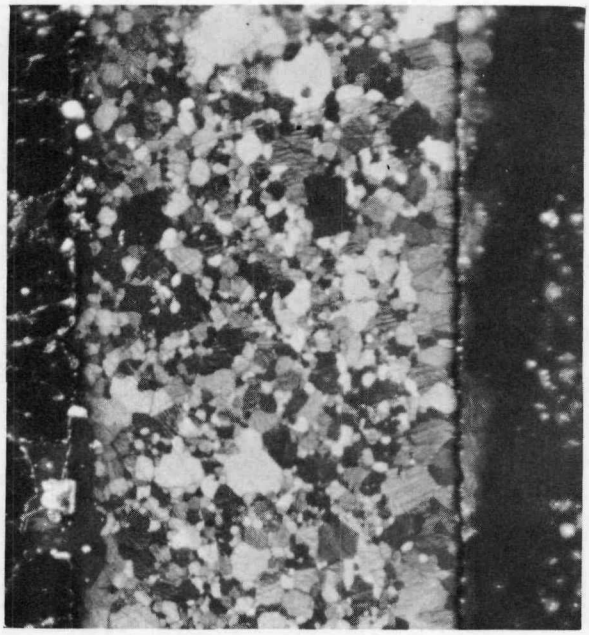

100X HC21592

b. Near the Top of the Fueled Area

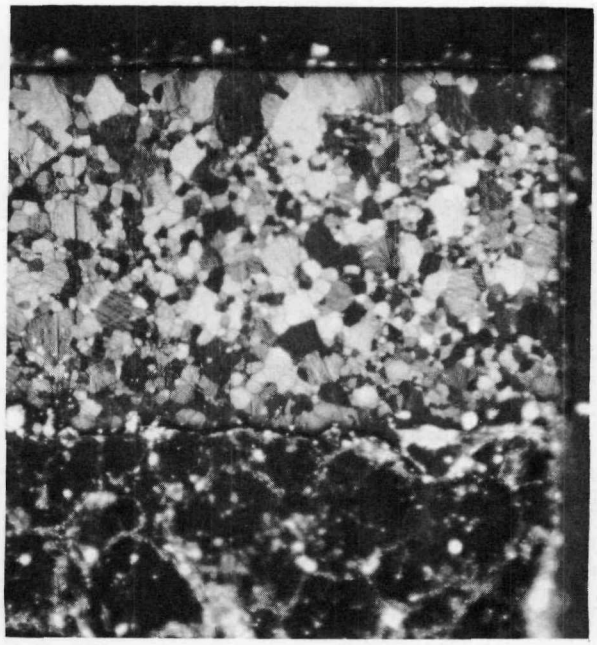

100X HC21599

c. Near the Center of the Fueled Area

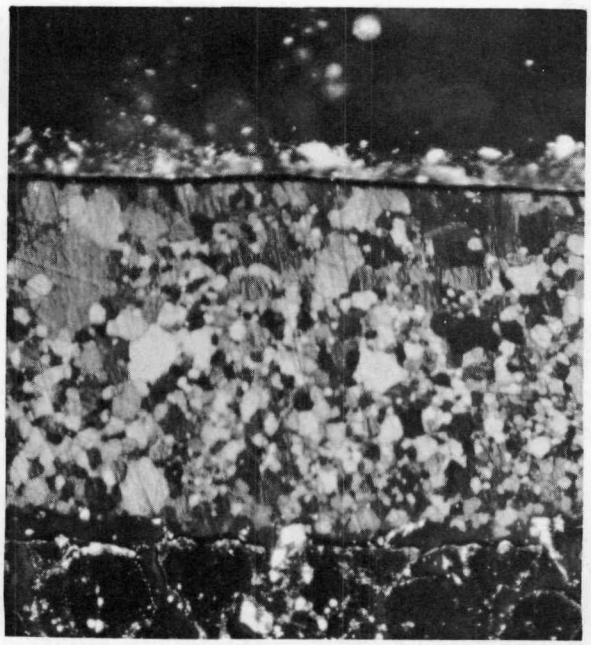

100X HC21600

d. Near the Bottom of the Fueled Area

FIGURE 26. REPRESENTATIVE MICROSTRUCTURES OF THE RHENIUM CLADDING (EMITTER) POLARIZED LIGHT

500X HC21595

a. Near the Top of the Fuel

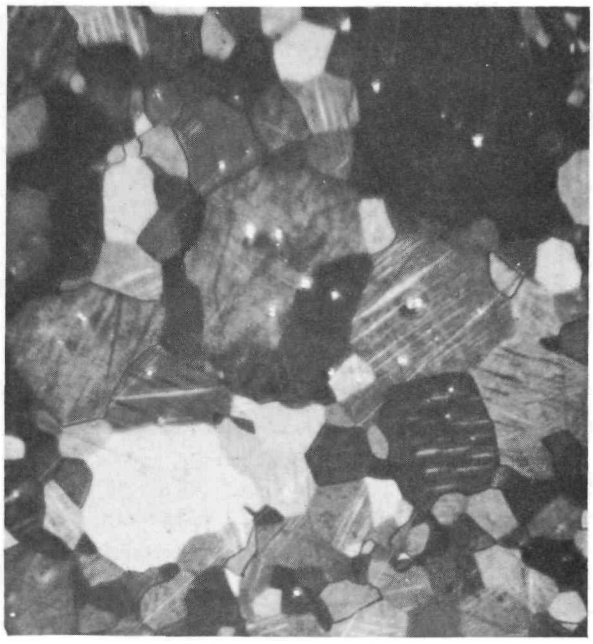

500X HC21604

b. Near the Center of the Fuel

FIGURE 27. REPRESENTATIVE MICROSTRUCTURE OF THE RHENIUM CLADDING (EMITTER MATERIAL) AT HIGH MAGNIFICATIONS

surface (Figure 28). There were some depressions in the surface of the collector but the fact that there was such a uniform coating of molybdenum indicated that these depressions were there after machining of the collector.

The examination of the heaters and the heat exchanger did not reveal anything unusual (Figure 29). Most of the brazes appeared to be excellent, although in one case (Figure 29d) where the heat-choke fin was brazed to the niobium collector, there appeared to be incomplete penetration of the braze metal. In general, this area of the diode appeared to be in excellent condition, however.

The area of most concern in the emitter support ring was the area of transition from the rhenium emitter to the molybdenum emitter support ring. Figure 30 presents representative views of this area in the as-polished condition and under polarized light. No significant deterioration was evident in this area. A second area of concern was the niobium-to-nickel transition area in the tube connecting the cesium reservoir to the collector. A photomicrograph of this transition area is presented in Figure 31. This area also appeared to be in excellent condition. There was some evidence of a slight corrosive attack on the nickel surface which was exposed to the cesium vapor, but it did not appear to be enough to cause concern.

In the metallographic examination of the upper ceramic insulator and the niobium support flanges in both the SD-2 out-of-pile diode and the SD-4 irradiated diode the Al_2O_3 appeared porous. Photomicrographs are shown in Figure 32. The photomicrographs also apparently show a gap between the niobium flange and the Al_2O_3 in both the out-of-pile and the irradiated samples. In both cases, the metallizing layer appeared to be bonded to the Al_2O_3, but in neither case did the braze material appear to be bonded to the metallizing layer, and only in the SD-4 diode did the braze material appear to be bonded to the niobium. These observations could be artifacts, however, in view of the difficulty in polishing metallized-layer interfaces. Helium leak checking of the interelectrode space indicated, however, that there were no leaks in this area, thus suggesting that the ceramic and ceramic-to-metal brazes were not permeable to helium, at least within the sensitivity of the helium leak detector, which is about 10^{-7} cm^3 per sec.

Microhardness measurements on both the nonirradiated and the irradiated ceramic insulators showed very little difference in the hardness. The data are presented in Table 5 as Knoop hardness numbers at a 100-g loading and a 5-kg loading. The 5-kg loading gives a lower hardness number because of the much larger indentation, which overlaps porosity. In general, the irradiated material appeared to be slightly harder than the unirradiated material but not significantly so.

TABLE 5. KNOOP MICROHARDNESS MEASUREMENTS ON THE CERAMIC INSULATORS FROM SD-2 AND SD-4

Sample Condition	Sample	Knoop Hardness Number	
		100-G Load	5-Kg Load
Nonirradiated (SD-2)	1	1098	908
	2	1390	1176
	3	1162	870
	Average	1217	985
Irradiated (SD-4)	1	1186	931
	2	1266	898
	3	1288	1217
	Average	1247	1015

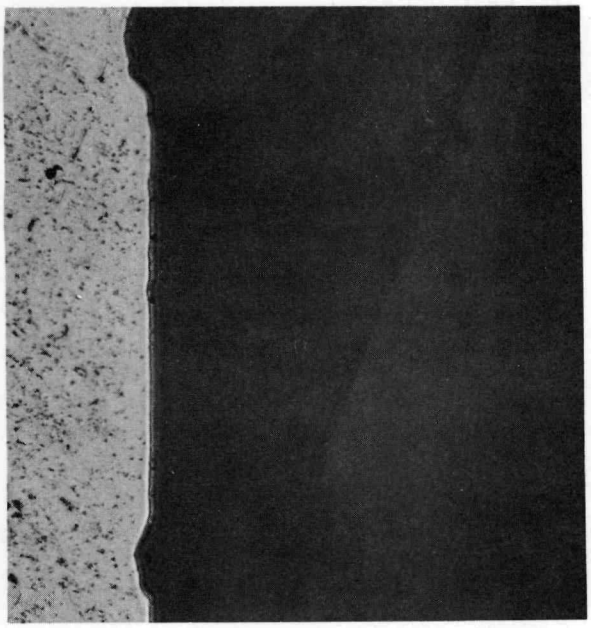

100X HC21631

a. As Polished with Oblique Lighting

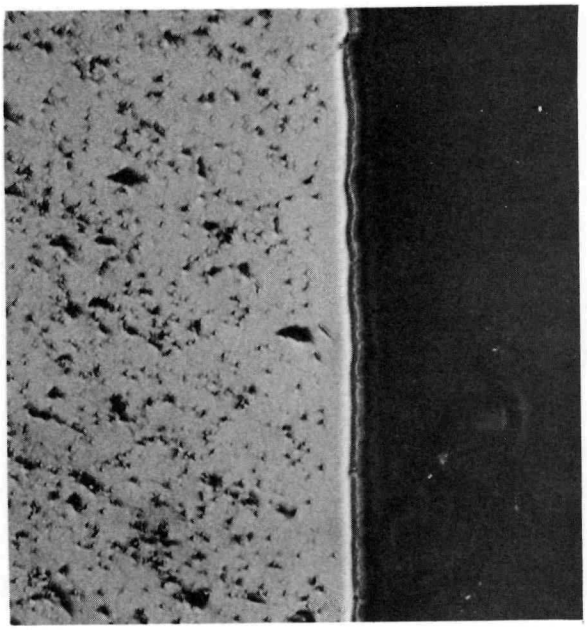

250X HC21635

b. As Polished with Oblique Lighting (Cut Surface at Right)

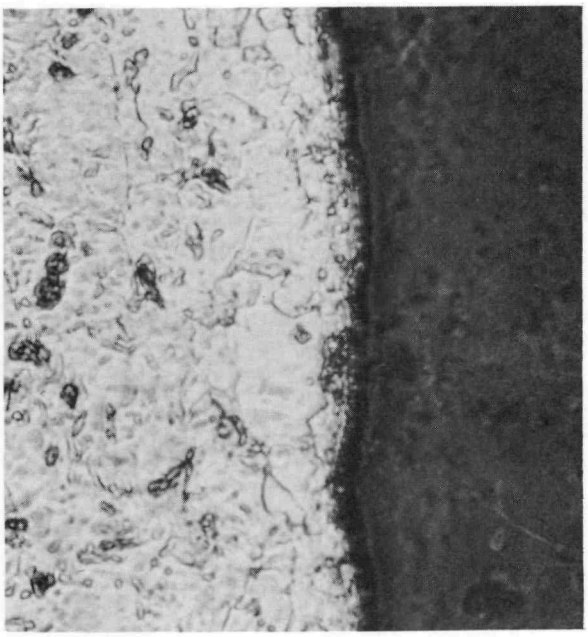

500X HC21661

c. Etched

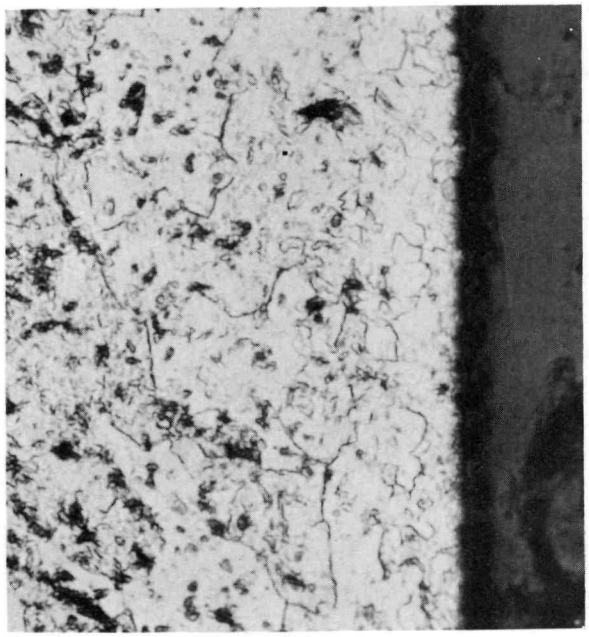

1000X HC21663

d. Etched

FIGURE 28. VAPOR-DEPOSITED LAYER OF MOLYBDENUM ON THE NIOBIUM COLLECTOR SURFACE

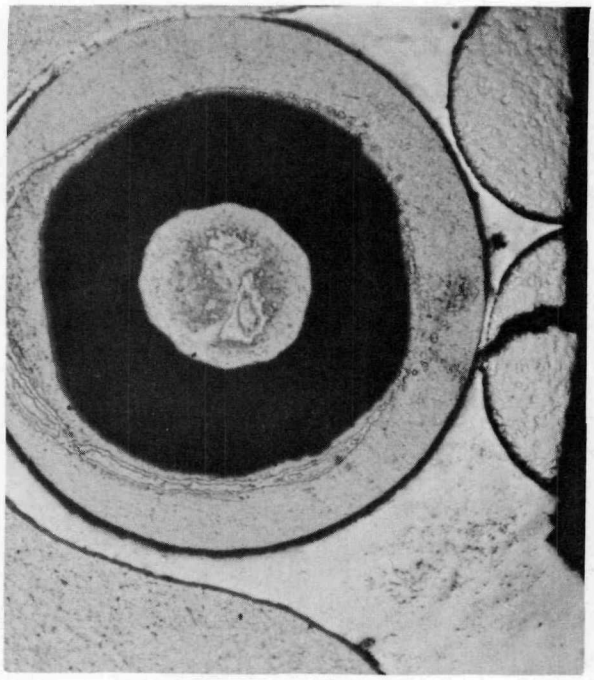

40X HC21624

a. Heaters and Braze Area

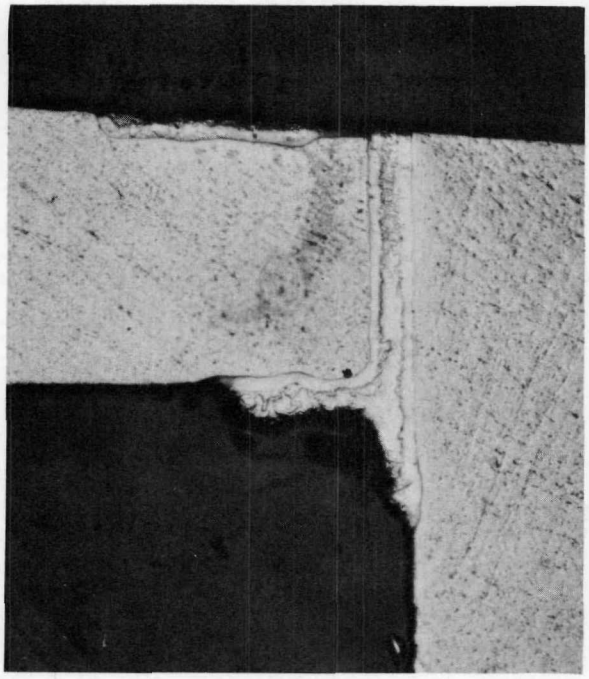

40X HC21622

b. Heat-Choke Fin Braze to Heat Exchanger

100X HC21589

c. Heat-Choke Fin Braze to Heat Exchanger

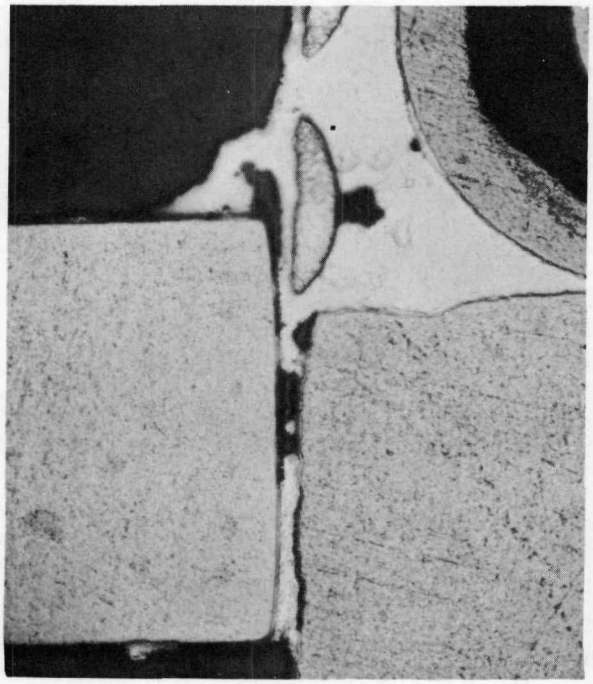

40X HC21623

d. Heat-Choke Fin Braze to Collector

FIGURE 29. MICROSTRUCTURES OF REPRESENTATIVE AREAS OF THE HEAT EXCHANGER

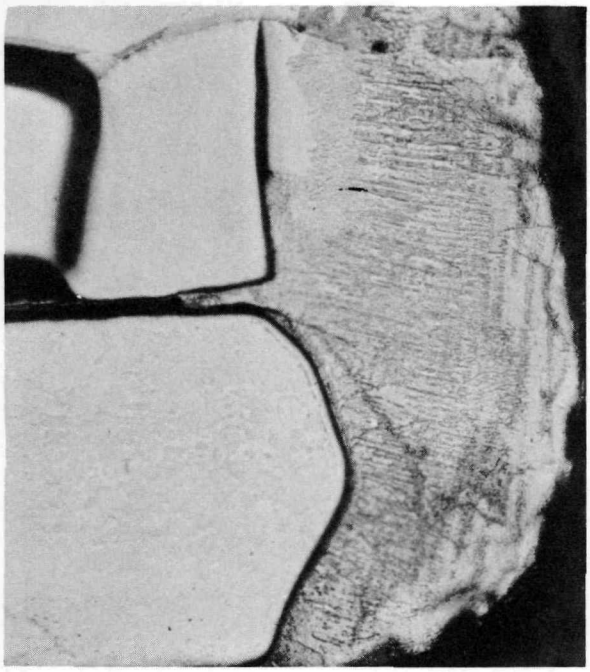

100X HC21659

a. As Polished Under Normal Light

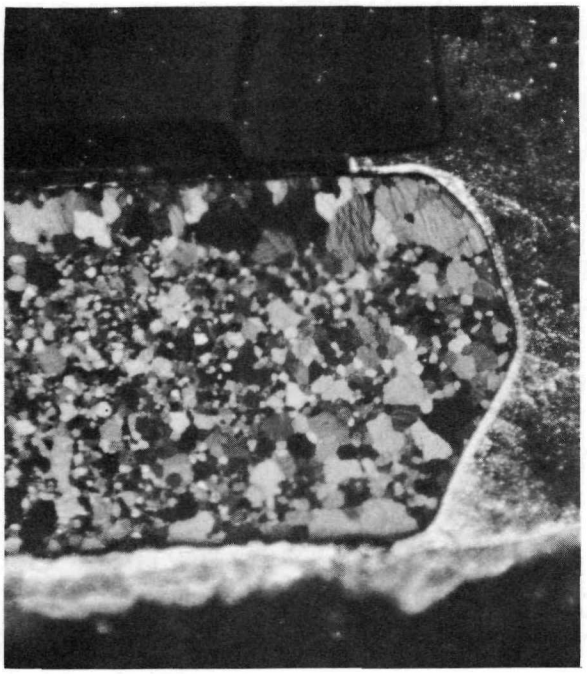

100X HC21658

b. As Polished Under Polarized Light

FIGURE 30. AREA OF THE WELD BETWEEN THE RHENIUM EMITTER AND THE MOLYBDENUM SUPPORT PLUG

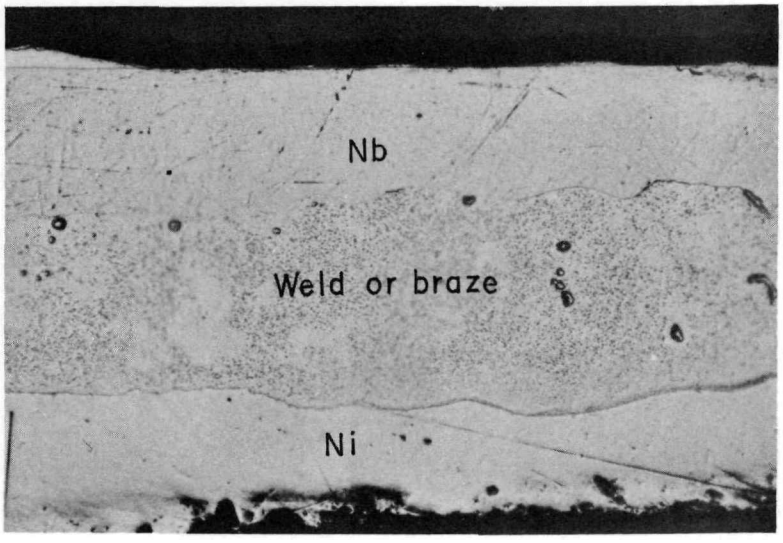

40X HC21638

FIGURE 31. NIOBIUM-TO-NICKEL WELD IN THE TUBE CONNECTING THE INTERELECTRODE SPACE TO THE CESIUM RESERVOIR

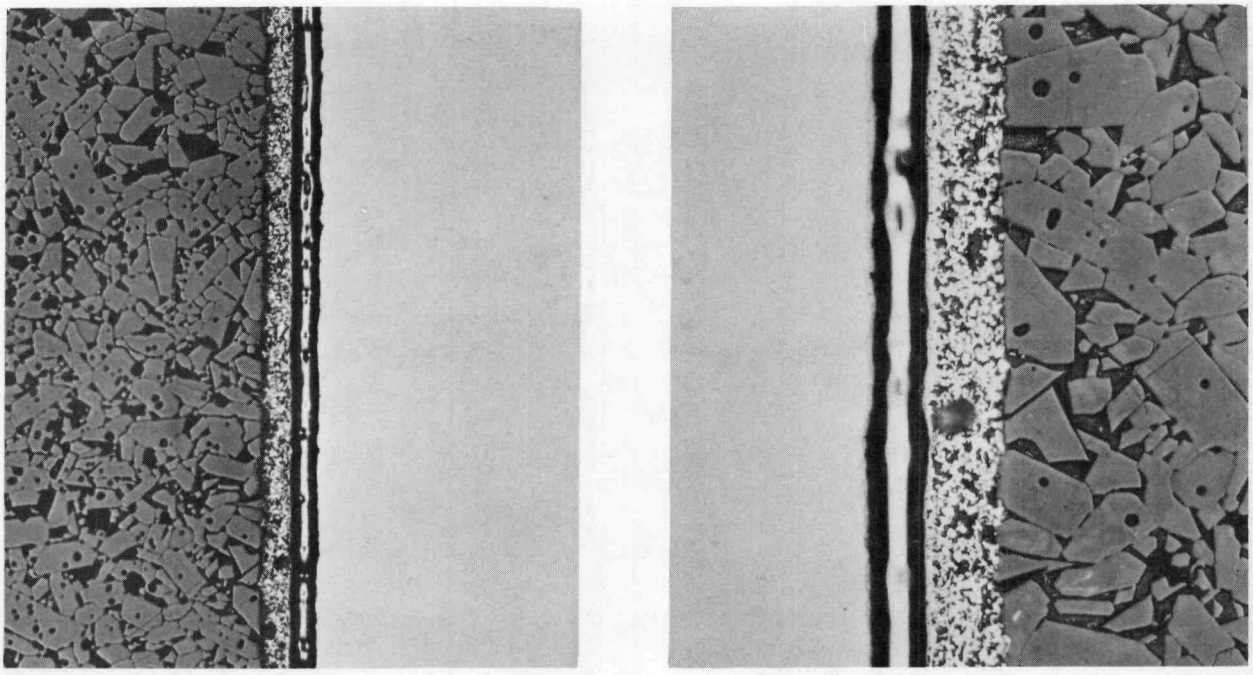

100X OD747 250X OD748

a. Out-of-Pile Diode (SD-2)

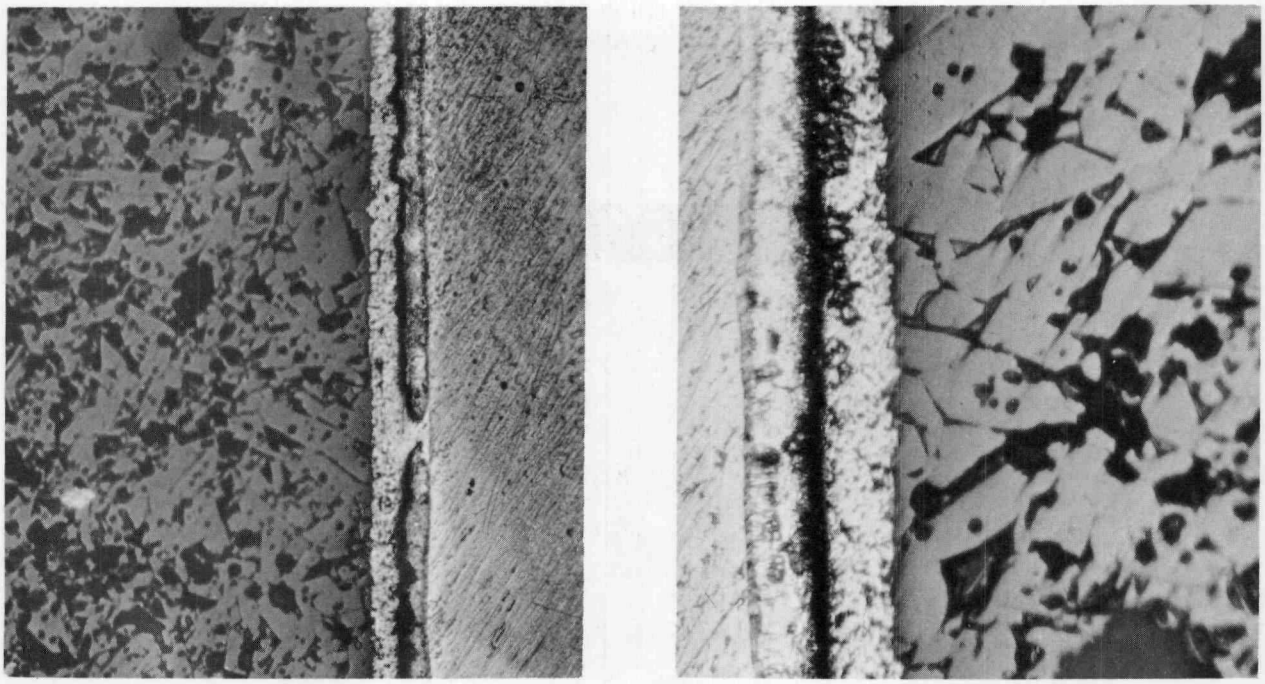

125X HC21889 250X HC21887

b. In-Pile Diode (SD-4)

FIGURE 32. COMPARISON OF CERAMIC INSULATORS USED IN OUT-OF-PILE AND IN-PILE DIODES

Determination of Fission-Product Distribution

Autoradiography

Autoradiographs were obtained of the polished surfaces of the fueled samples prepared for metallographic examination. Both beta and alpha autoradiographs were obtained in order to obtain the fission-product distribution and the uranium distribution in the samples. These, along with photomacrographs of the samples, are presented in Figures 33 through 41. The beta autoradiographs[1]* were obtained with high-resolution, low-sensitivity photographic plates. The alpha autoradiographs[2] were obtained by placing the surface against a thin film of cellulose nitrate. The cellulose nitrate was etched with NaOH to bring out the alpha tracks. The density of the tracks is a direct function of the amount of alpha-emitting material.

The beta radiographs showed that the concentration of fission products in the fuel, as was expected, was considerably greater near the outer diameter than at the inner diameter. The concentration should diminish uniformly with distance from the outer surface because the number of fissions per unit volume decreases with distance from the outer surface. Also, because the ends see more neutrons than the center, the concentration of fission products should be greater near the ends. There was no evidence of migration of the fission products, however, and the alpha autoradiography showed no variation in intensity. In general, the autoradiography of the fuel did not indicate the occurrence of anything unusual.

Gamma Scanning

A study of the axial and radial distribution of fission products in the diode was conducted by measuring the gamma energy spectrum at increments along the length of the diode and at increments along the radius of the fuel. The axial distribution was studied both before and after the emitter was separated from the rest of the diode. The radial distribution was determined after the emitter was sectioned longitudinally. In each case the sample was traversed past a shielded collimating slit 0.5 in. wide by 0.002 in. high by 12 in. long. The gamma energy spectrum was recorded using a multichannel analyzer and a 1.5 by 1.5 in. NaI (Tl) crystal at each increment along the length (radius) of the fuel. Standard sources of Cs^{127} and Ra^{226} having photopeaks of known energies were run to establish the energy levels of the fission-product spectrum. No attempt was made to identify any of the photopeaks by half-life studies. Four distinguishable photopeaks were chosen for determination of the activity versus the length and breadth of the fuel. These peaks are believed to be due to either one or a combination of the isotopes listed in Figures 42 through 49, which illustrate how the activity of these fission products varies both axially and radially. It appears from these graphs that the fission products did not migrate appreciably. The curves in Figures 44 and 48, which include the activity of the fission product Cs^{137} do appear to be slightly more erratic than the others, indicating the possibility of some redistribution of the isotopes involved. This is not surprising in the case of cesium, which has a boiling point of 690 C, well below the irradiation temperature.

*References at end.

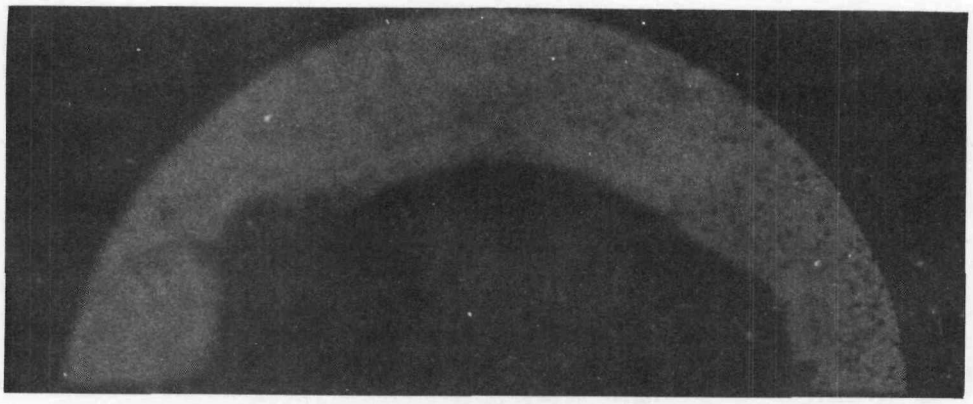

~8.5X AR153

FIGURE 33. ALPHA AUTORADIOGRAPH OF TRANSVERSE CROSS SECTION NEAR AXIAL CENTER OF EMITTER

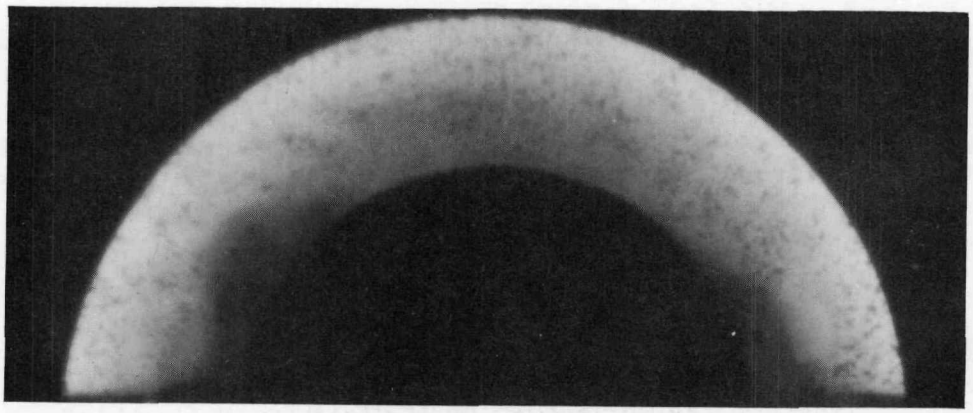

~8.5X AR154

FIGURE 34. BETA AUTORADIOGRAPH OF TRANSVERSE CROSS SECTION NEAR AXIAL CENTER OF EMITTER

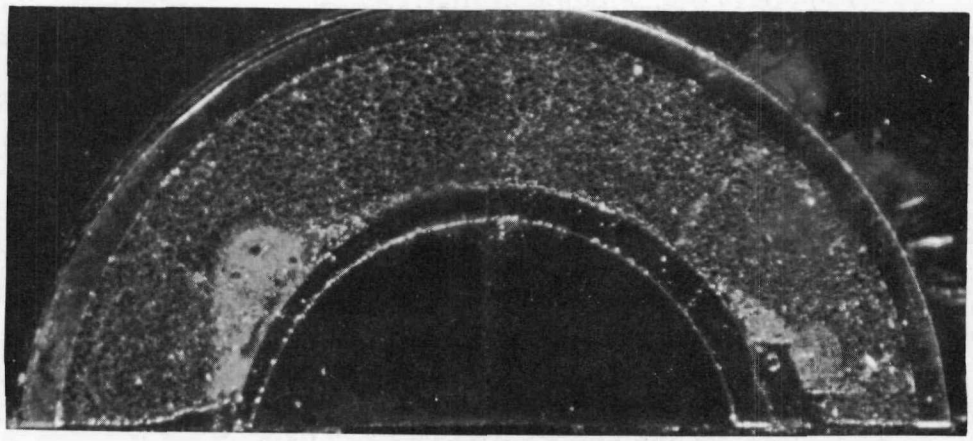

~8.5X P1429

FIGURE 35. PHOTOMACROGRAPH OF TRANSVERSE CROSS SECTION NEAR AXIAL CENTER OF EMITTER

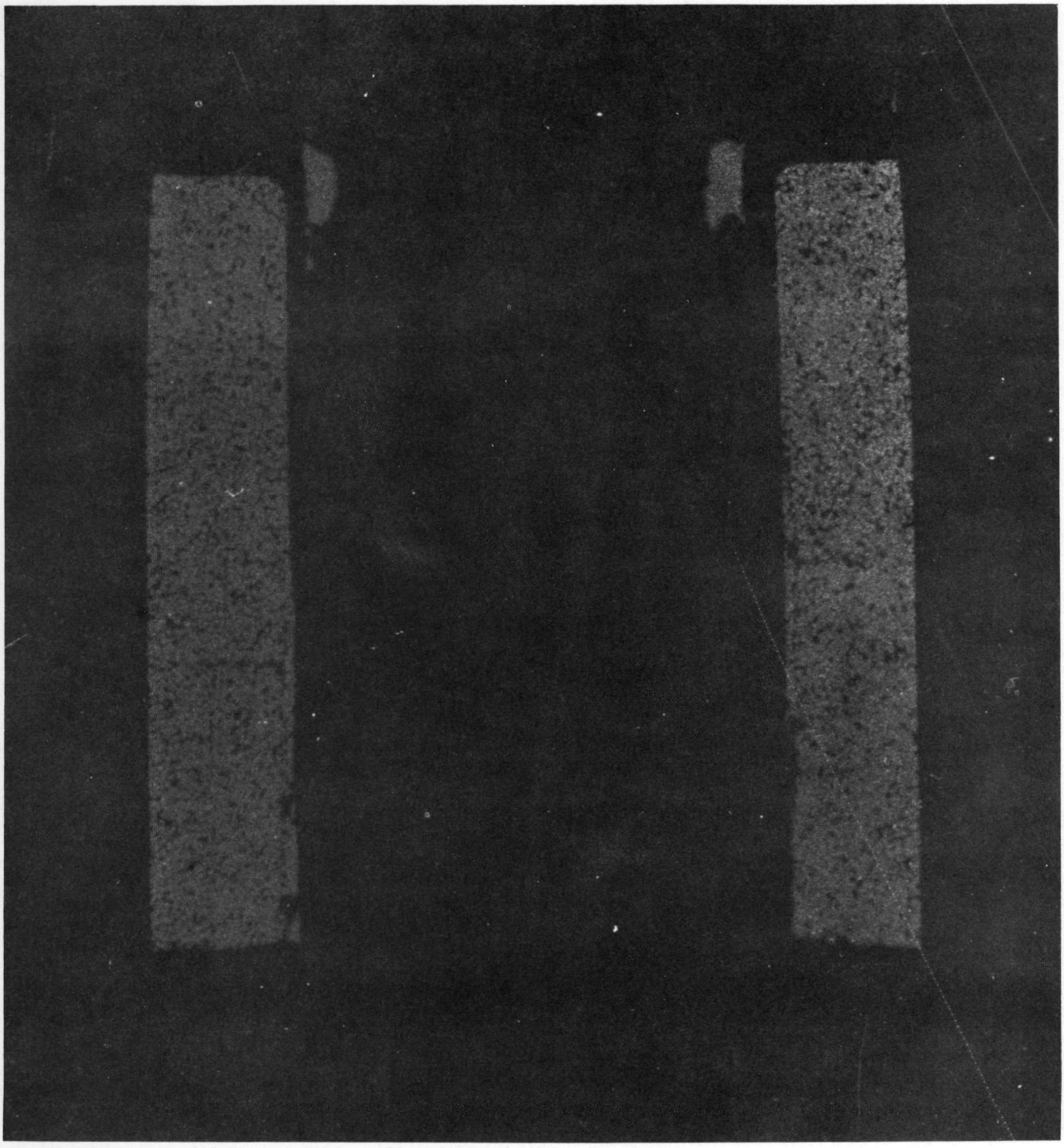

10X AR155

FIGURE 36. ALPHA AUTORADIOGRAPH OF TOP HALF OF EMITTER

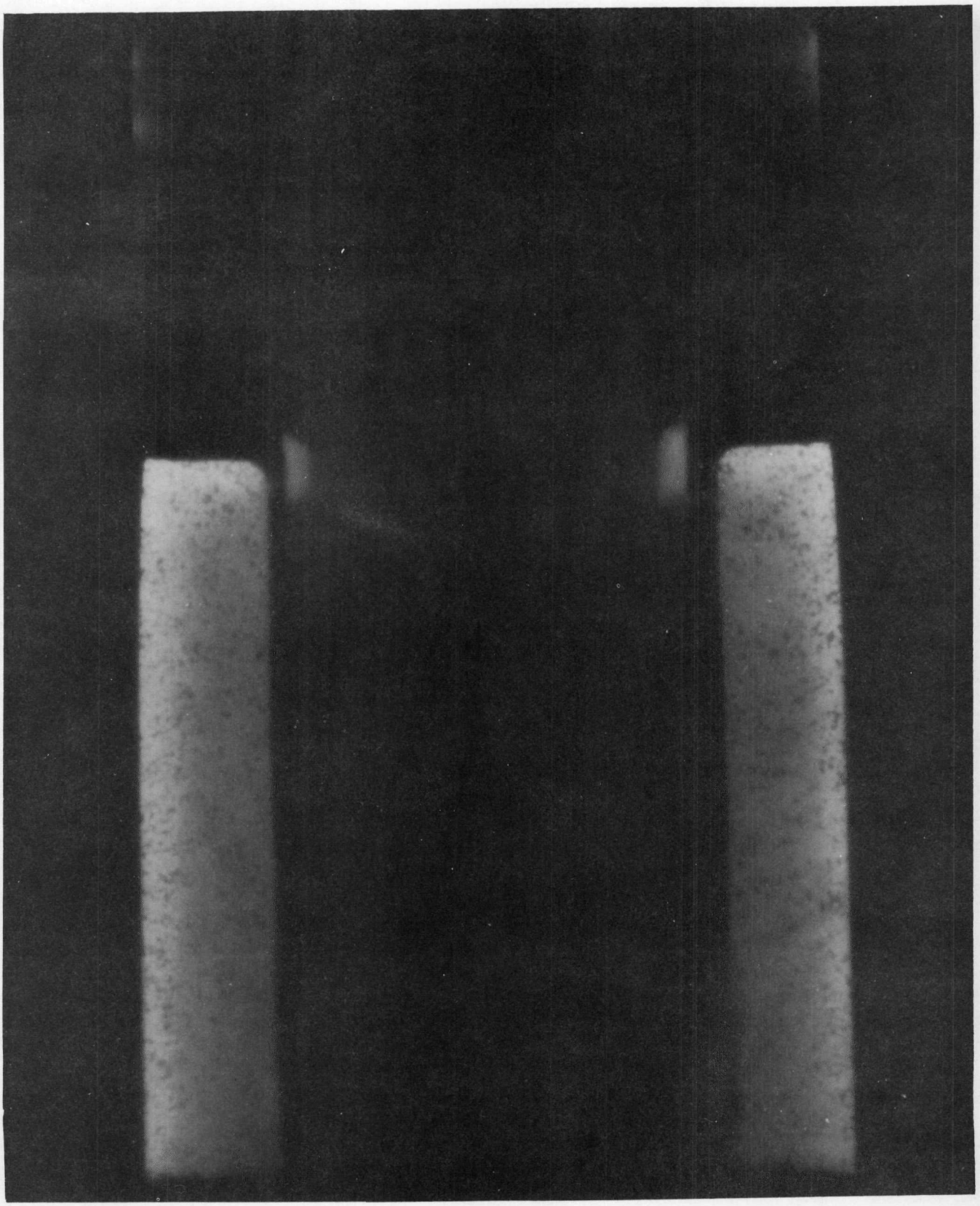

10X AR156

FIGURE 37. BETA AUTORADIOGRAPH OF TOP HALF OF EMITTER

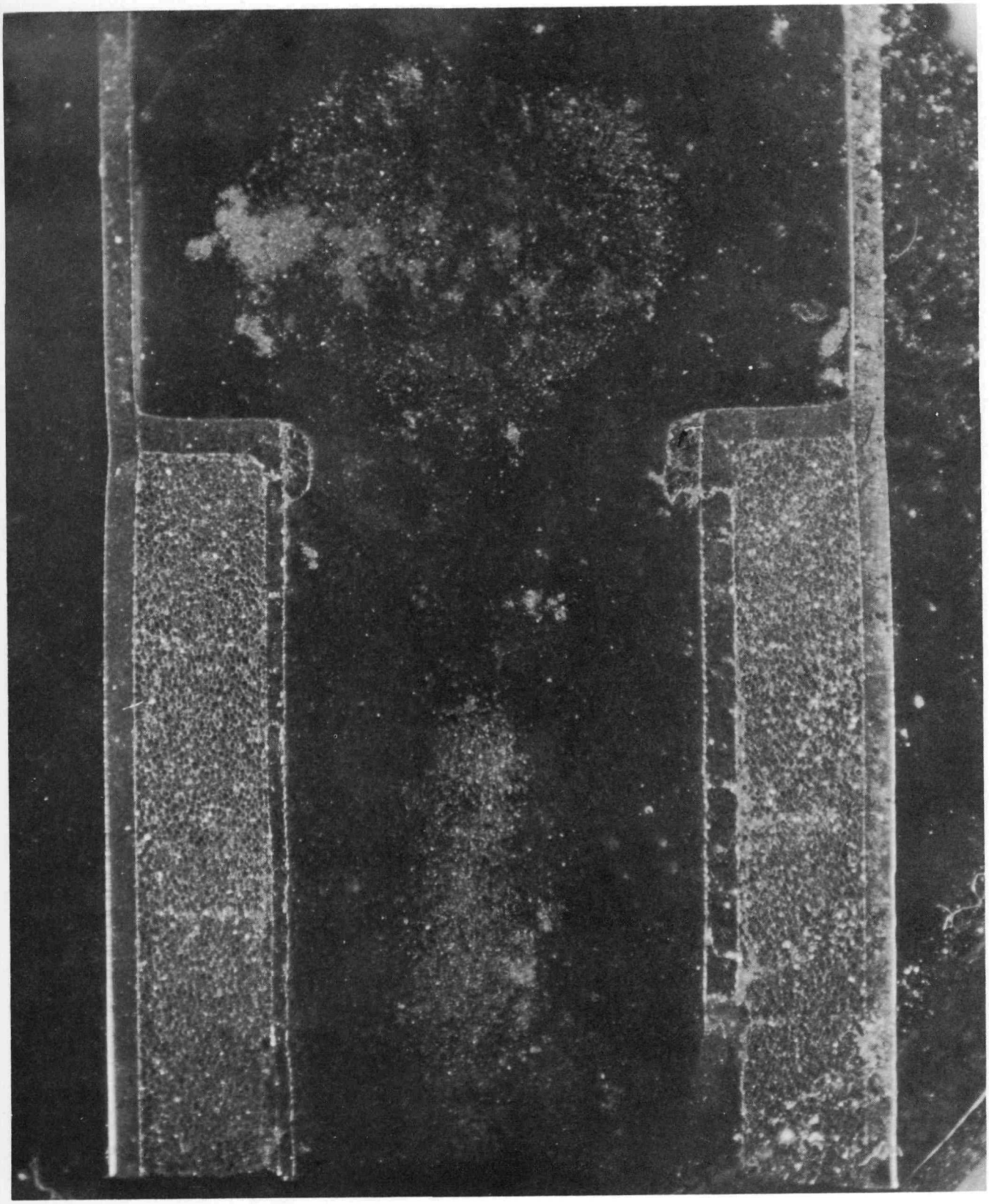

10X

P1431

FIGURE 38. PHOTOMACROGRAPH OF TOP HALF OF EMITTER

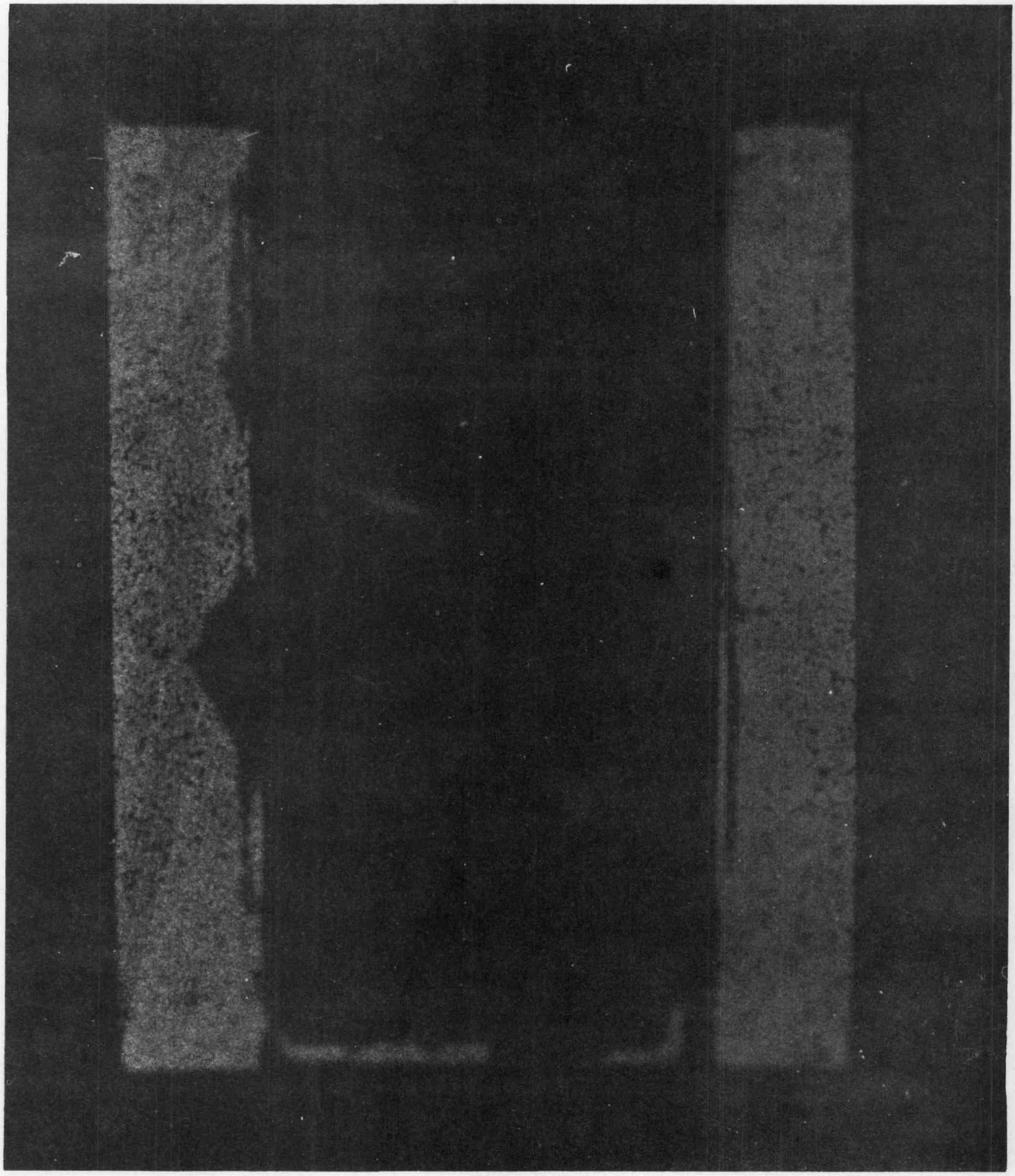

10X AR157

FIGURE 39. ALPHA AUTORADIOGRAPH OF BOTTOM HALF OF EMITTER

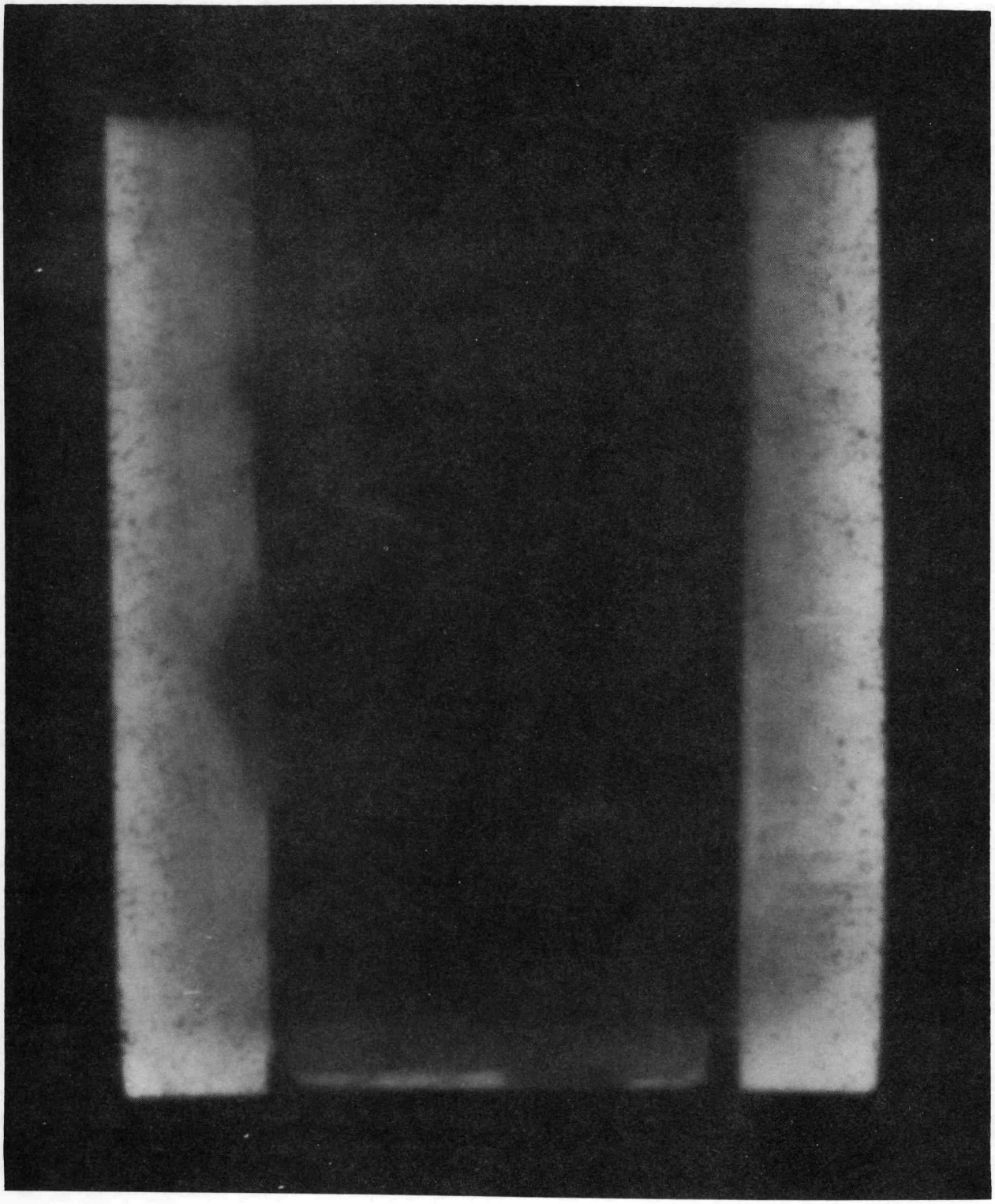

10X AR158

FIGURE 40. BETA AUTORADIOGRAPH OF BOTTOM HALF OF EMITTER

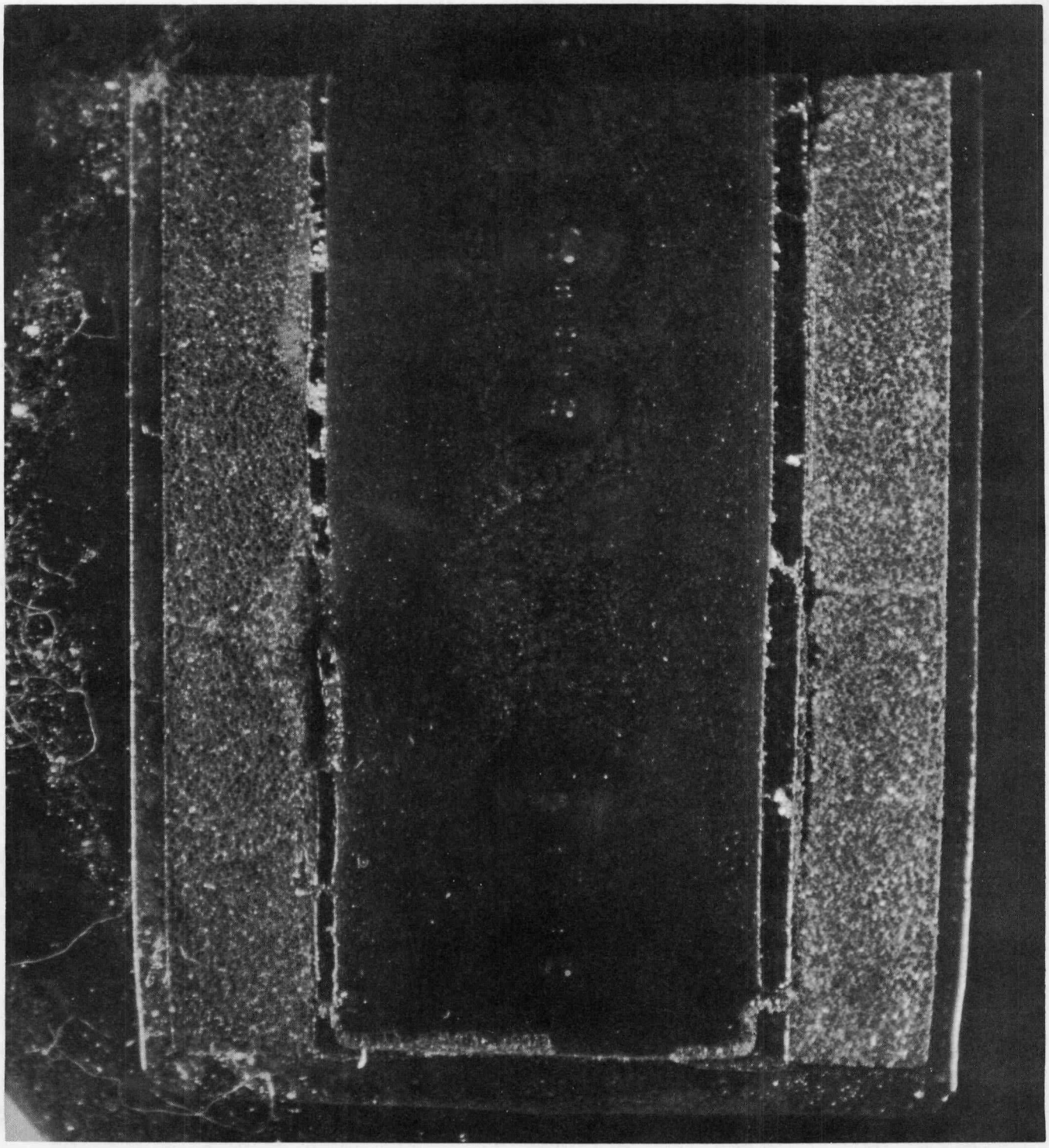

10X P1430

FIGURE 41. PHOTOMACROGRAPH OF BOTTOM HALF OF EMITTER

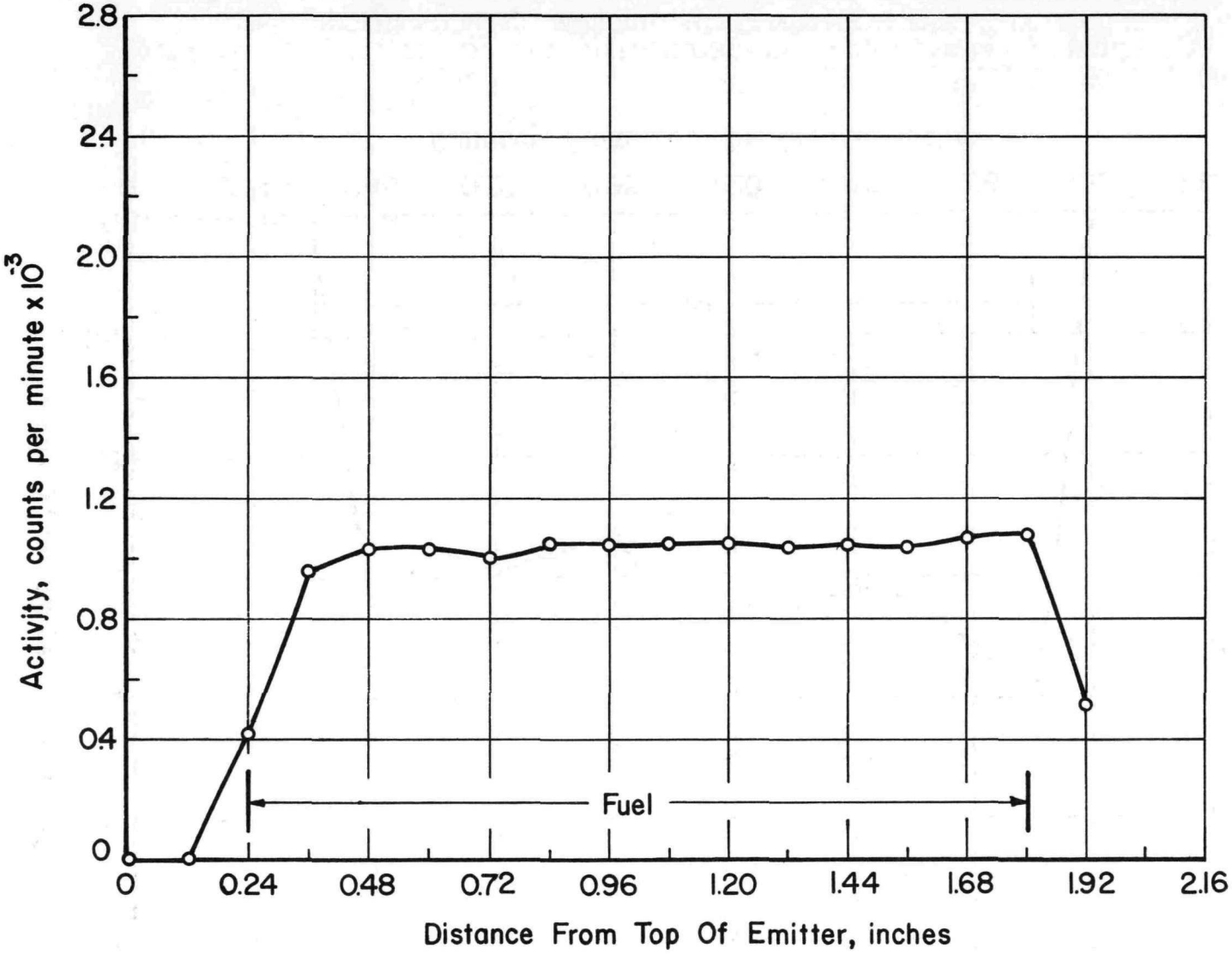

FIGURE 42. ACTIVITY OF THE FISSION PRODUCTS BARIUM-140, CERIUM-141, AND/OR CERIUM-144 VERSUS THE LENGTH OF THE EMITTER

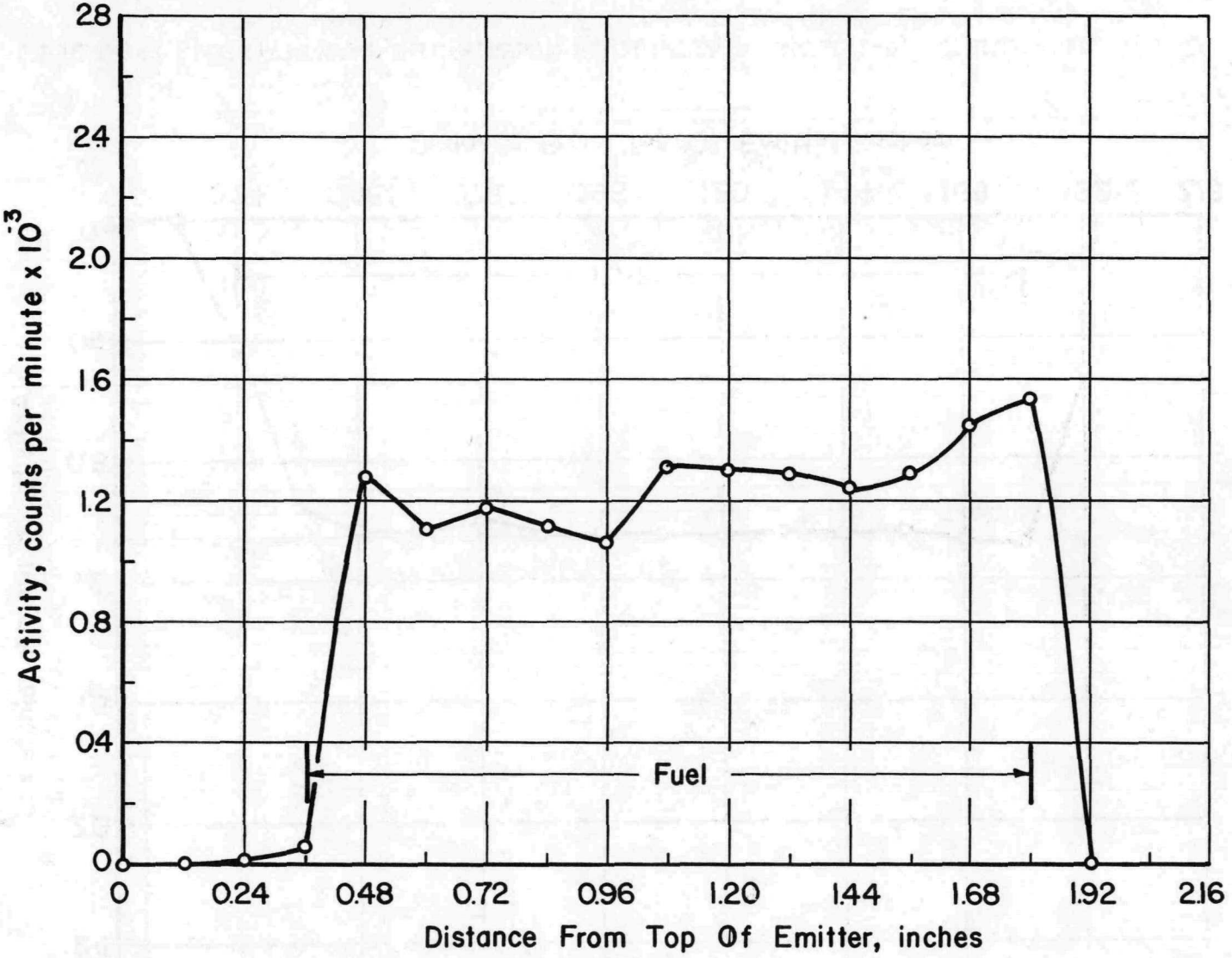

FIGURE 43. ACTIVITY OF THE FISSION PRODUCTS BARIUM-140 AND/OR RUTHENIUM-103 VERSUS THE LENGTH OF THE EMITTER

CONFIDENTIAL

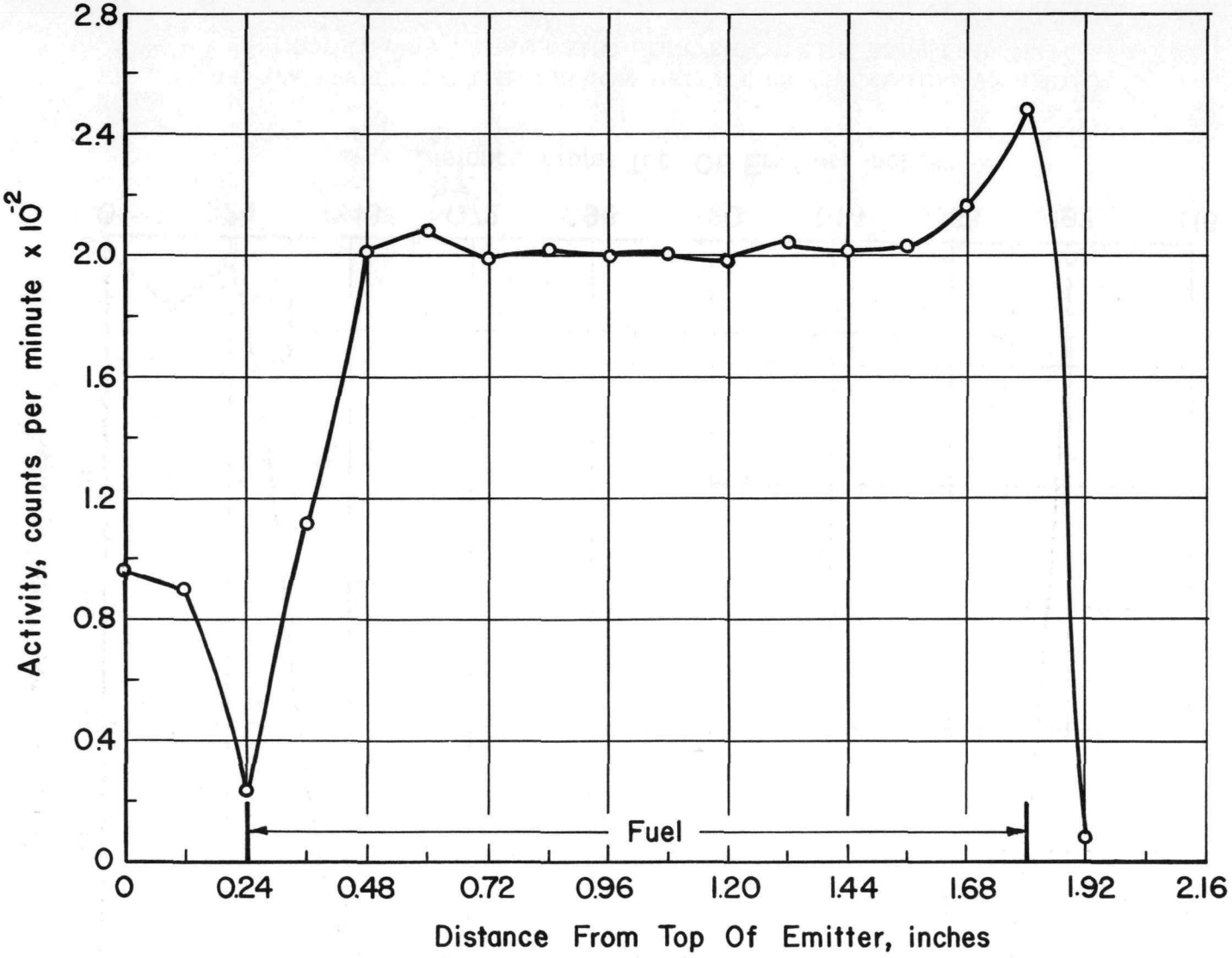

FIGURE 44. ACTIVITY OF THE FISSION PRODUCTS CESIUM-137 AND/OR BARIUM-140 VERSUS THE LENGTH OF THE EMITTER

CONFIDENTIAL

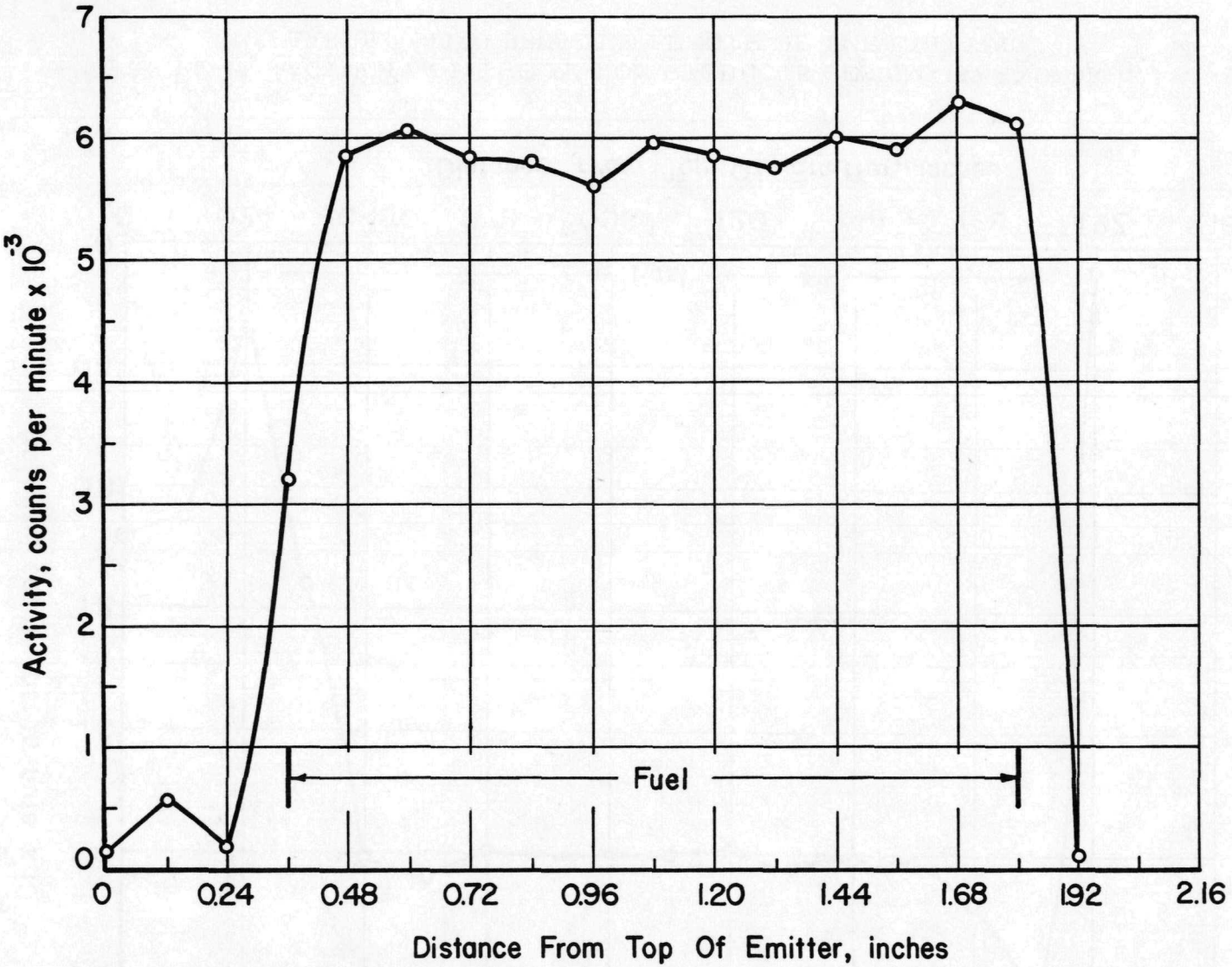

FIGURE 45. ACTIVITY OF THE FISSION PRODUCTS ZIRCONIUM-95 AND/OR NIOBIUM-95 VERSUS THE LENGTH OF THE EMITTER

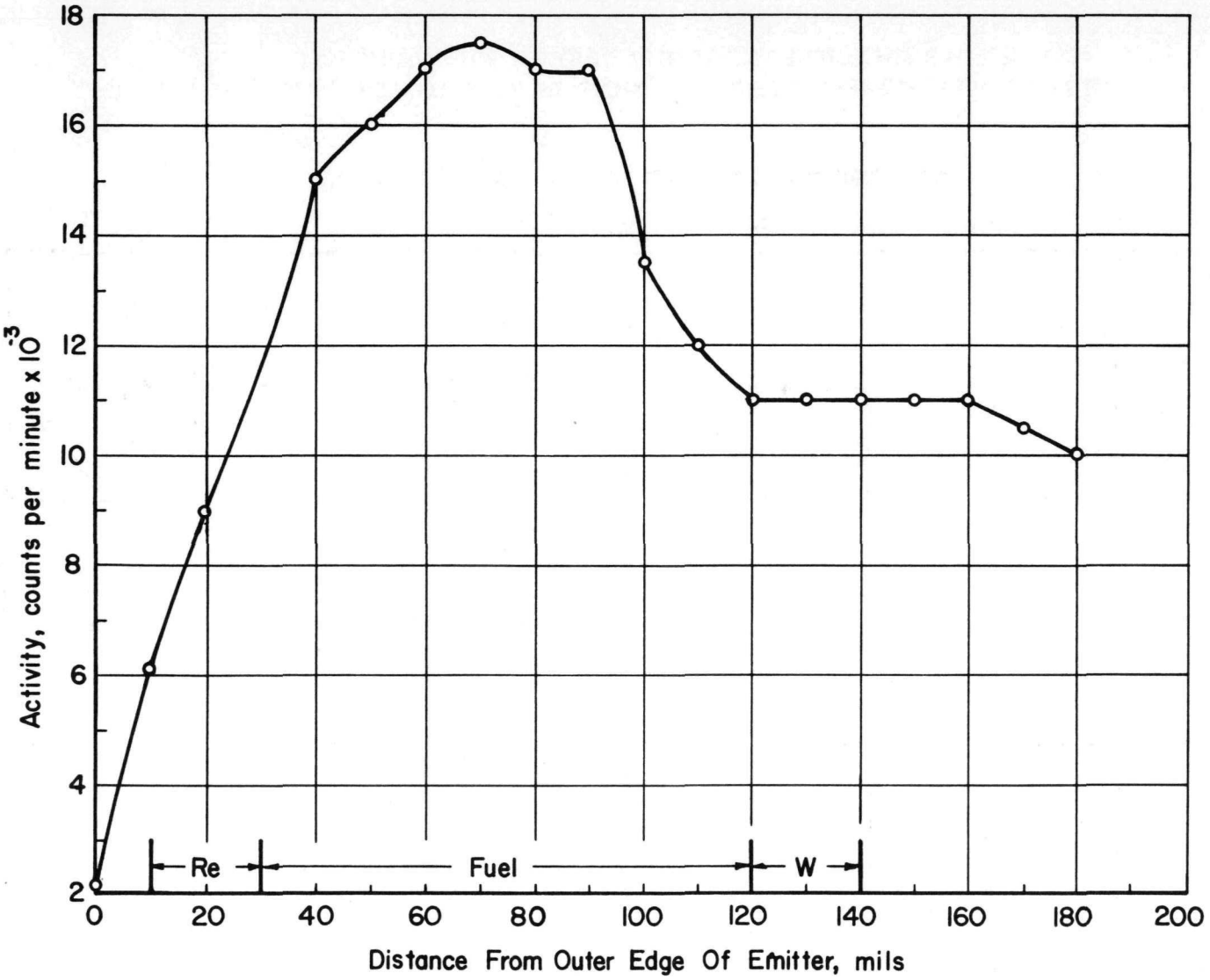

FIGURE 46. ACTIVITY OF THE FISSION PRODUCTS BARIUM-140, CERIUM-141, AND/OR CERIUM-144 VERSUS THE RADIUS OF THE EMITTER

CONFIDENTIAL

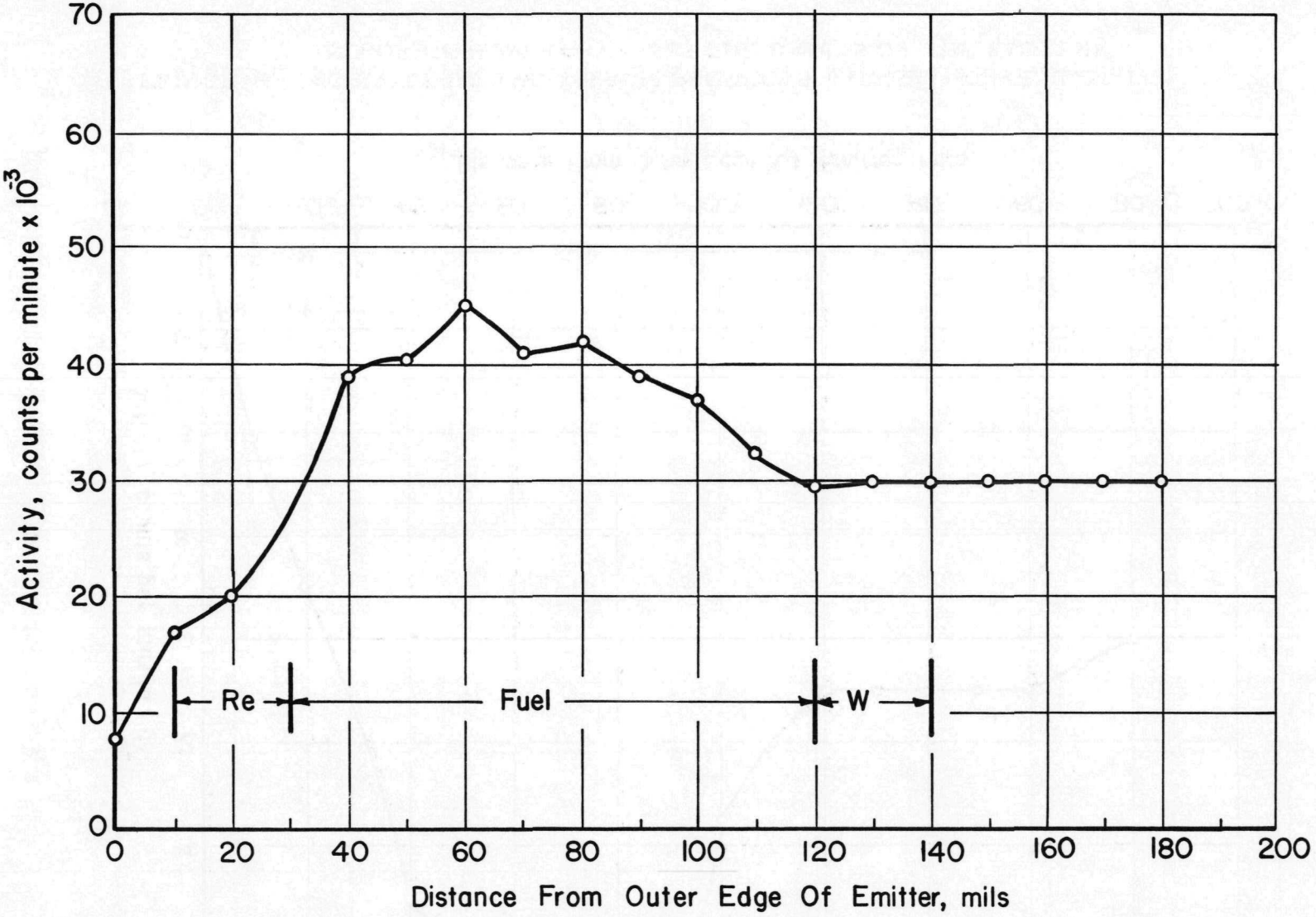

FIGURE 47. ACTIVITY OF THE FISSION PRODUCTS BARIUM-140 AND/OR RUTHENIUM-103 VERSUS THE RADIUS OF THE EMITTER

CONFIDENTIAL

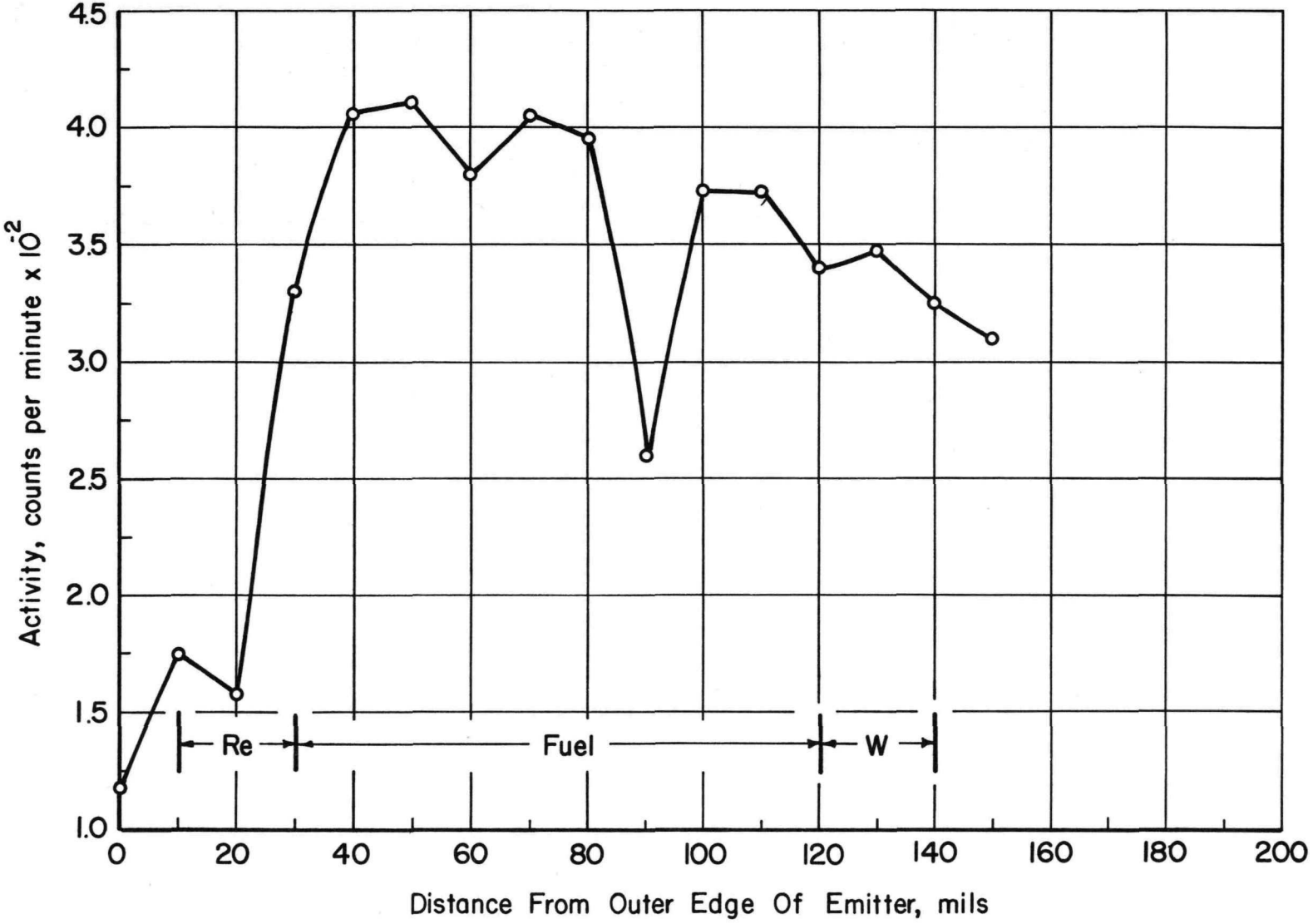

FIGURE 48. ACTIVITY OF THE FISSION PRODUCTS CESIUM-137 AND/OR BARIUM-140 VERSUS THE RADIUS OF THE EMITTER

CONFIDENTIAL

CONFIDENTIAL

CONFIDENTIAL

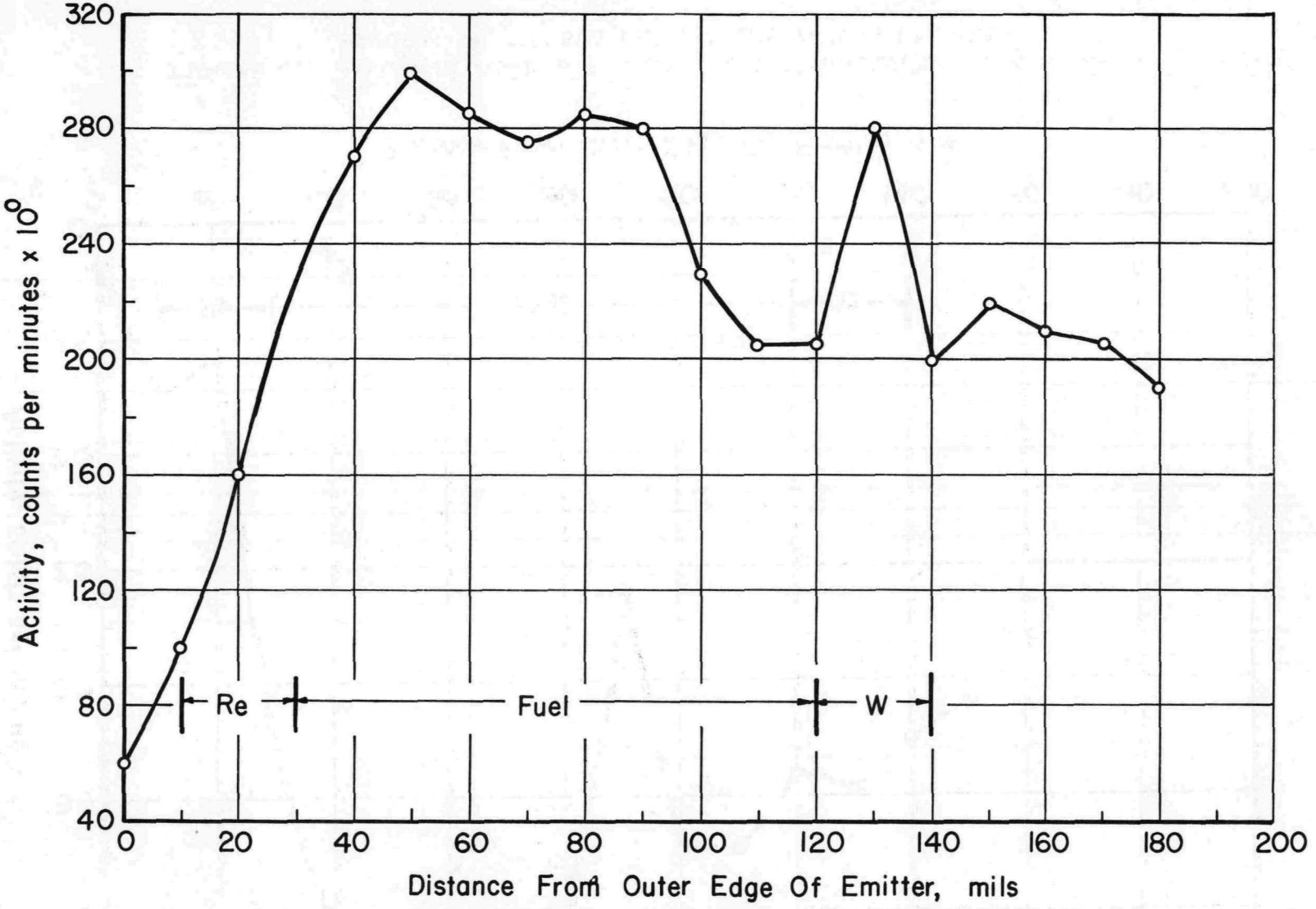

FIGURE 49. ACTIVITY OF THE FISSION PRODUCTS ZIRCONIUM-195 AND/OR NIOBIUM-95 VERSUS THE RADIUS OF THE EMITTER

CONFIDENTIAL

Chemical and Vacuum-Fusion Analyses

Several samples were taken from various locations in the diode and semiquantitative analyses by X-ray emission were obtained. The results of these analyses are presented in Table 6 along with the location from which each sample was taken. In all cases, the sample was obtained by scraping the desired surface with a sharp-edged tool or a fine-tooth rotary file. It is believed that the UO_2 and tungsten found in the sample removed from the emitter surface were dislodged from the emitter cavity at the time the sample was taken and contaminated the surface sample.

TABLE 6. SEMIQUANTITATIVE ANALYSES OF SAMPLES FROM THE SD-4 DIODE BY X-RAY EMISSION[a]

Sample Location	Element, w/o						
	U	W	Re	Mo	Nb	Cs	Cu
Bottom of heat shield at top of emitter	Major[b]	--	--	--	--	--	--
Emitter surface	36.	14.	14.	14.	21.	≤0.3	≤0.3
Collector surface	≤0.1	≤0.1	≤0.1	1.5	98.	≤0.1	≤0.1
Top surface of bottom ceramic insulator bushing	≤0.1	≤0.1	≤0.1	1.5	9.8	≤0.3	≤0.1

(a) Estimated accuracy of analyses is ±50 percent.
(b) Background due to high radiation level of sample masked all lines except those for uranium.

There is no readily apparent explanation as to why molybdenum and niobium were present in the samples of the emitter surface and the bottom ceramic insulator bushing. Work performed at LRL[3] indicates that vaporization of molybdenum or niobium should not be appreciable at temperatures below 1500 C. Calculations of the amount of molybdenum that would have vaporized in a hard vacuum at a temperature of 900 C (maximum collector temperature) were orders of magnitude less than that found on the emitter surface alone. Sampling procedures were monitored carefully, and it is believed that there was no cross contamination of samples either during the sampling or the analyses.

It was expected that an appreciable quantity of osmium would be present in the emitter sample as a result of neutron activation and decay of rhenium. The sample removed from the emitter surface was thus specifically analyzed for osmium, but no osmium was detected. However, the molybdenum, rhenium, and copper in the samples have X-ray lines which interfere with the major lines of osmium. This interference, coupled with the fact that osmium exhibits weak lines under the best conditions, made its detection very unlikely. Similar problems are encountered with the detection of osmium by atomic absorption and by mass spectroscopy, so no further attempts to determine the amount of osmium present were made.

Both the diode and the cesium reservoir were heated in a vacuum furnace in order to drive off and collect any volatile material. Heat treatments were conducted at

650 and 750 C and some material or materials were removed as evidenced by the deposition of a white powder on the surface of the bell jar of the system. A sample of this material was removed and, because of its high activity, was analyzed by gamma-ray spectroscopy. Prior to chemical separations only Cs^{134} could be observed, but following the removal of cesium by silicotungstate precipitations, Zn^{65} was detected. The presence of Zn^{65} nuclide was confirmed by a radiochemical separation for zinc. The specific activity of the Zn^{65} nuclide in the powder was about 10 microcuries per mg of powder. The Cs^{134} in the sample was the result of neutron activation of the Cs^{133} in the the diode. The Zn^{65} resulted from the neutron activation of Cu^{63} to Cu^{64} and its subsequent decay to Zn^{64} which, in turn, experienced neutron activation to Zn^{65}.

In order to determine the effectiveness of the zirconium getter, vacuum-fusion analyses were performed on duplicate samples from the getter and from the copper cooling straps connecting the heat exchanger to the cesium reservoir. The results of these analyses (Table 7) indicated that most of the available oxygen and hydrogen was gettered by the zirconium. It is interesting to note that both of the copper samples contained small quantities of helium, whereas the zirconium samples did not.

TABLE 7. VACUUM-FUSION ANALYSES OF SELECTED SAMPLES FROM SD-4

Sample	Amount of Element Present, cm^3 per g of material		
	O_2	H_2	He
Zirconium getter	1.63	1.35×10^{-3}	--
	1.56	2.39×10^{-2}	--
Copper cooling strap	0.105	2.66×10^{-4}	2.66×10^{-4}
	0.065	9.32×10^{-4}	1.42×10^{-4}

CONCLUSIONS

The major significant conclusions made from the postirradiation examination of the SD-4 are as follows:

(1) Apparently, about 80 percent of the fission gas generated was released from the fuel. The fission gas escaped from the diode through a leak in the gas-sampling tube.

(2) There was some redistribution of UO_2 through cracks in the tungsten inner liner. The liner, and the tungsten matrix, evidently retarded gross redistribution and loss of fuel.

(3) A 2 to 3 percent increase in the outer diameter of the rhenium emitter did not significantly affect its performance at the approximately 1600 C operating temperature.

(4) There was no significant difference in the outer surface grain structure of the rhenium emitter over the fueled zone as compared to the unfueled zone, indicating that the surface obtained by preirradiation treatments was stable and not affected by the irradiation.

(5) The vacuum-deposited molybdenum surface layer applied to the niobium collector was apparently not affected by the irradiation.

(6) The diode structural welds and brazes were apparently not affected by the irradiation.

(7) The alumina insulator was not significantly affected by the irradiation.

ACKNOWLEDGMENTS

The authors wish to acknowledge the assistance of Messrs. M. Berchtold and E. Sands for the hot-cell examination and the remote metallography.

REFERENCES

(1) Boyle, R. F., Ketron, W. V., Nelson, R. C., and Smith, R. E., "Autoradiography: A Useful Tool for Examining Irradiated UO_2", Nucleonics, 22 (4), 76-78 (1964).

(2) Davies, J. H., and Darmitzel, R. W., "Alpha Autoradiograph Technique for Irradiated Fuel", Nucleonics, 23 (7), 86-87 (1965).

(3) Dayton, R. W., Simons, E. M., et al., "Reactor Materials: A Quarterly Technical Progress Review", 9 (2), 124-125 (Summer, 1966).

JHS/EOS/VWS:pa

Blank Page